Chemical ubiquitylation of linker histone H1.2 by combining unnatural amino acids with click chemistry

Dissertation

submitted for the degree of
Doctor of Natural Sciences (Dr. rer. nat.)

Presented by

Daniel Rösner

at the

Faculty of Sciences
Department of Chemistry

Konstanz, 2016

Date of the oral examination: 24th of March 2016

First referee: Prof. Dr. Andreas Marx

Second referee: Prof. Dr. Martin Scheffner

Third referee: Prof. Dr. Heiko M. Möller

Parts of this thesis are published in:

D. Schneider*, T. Schneider*, D. Rösner*, M. Scheffner and A. Marx,
Improving bioorthogonal protein ubiquitylation by click reaction.
Bioorg Med Chem, 2013. **21**(12): p. 3430-3435.

D. Rösner*, T. Schneider*, D. Schneider*, M. Scheffner and A. Marx,
Click chemistry for targeted protein ubiquitylation and ubiquitin chain formation.
Nat Protoc, 2015. **10**(10): p. 1594-611.

* These authors contributed equally to this work.

Danksagung

Die vorliegende Arbeit entstand von Januar 2011 bis November 2015 an der Universität Konstanz in der Arbeitsgruppe für Organische und Zelluläre Chemie von Prof. Dr. Andreas Marx im Fachbereich Chemie.

An erster Stelle möchte ich mich bei Prof. Dr. Andreas Marx für die Aufnahme in seine Arbeitsgruppe, sowie die Bereitstellung des interessanten Themas bedanken. Für viele wissenschaftliche Diskussionen, seine ständige Unterstützung und sein Vertrauen im Rahmen einer exzellenten Betreuung bin ich ihm ebenfalls dankbar.

Herrn Prof. Dr. Martin Scheffner danke ich für die Übernahme des Zweitgutachtens, für die Unterstützung in erfolgreichen Kooperationen und inspirierende, fachliche Diskussionen in meinem Thesis Committee. Prof. Dr. Heiko Möller danke ich für die Übernahme des Drittgutachtens. Außerdem danke ich Prof. Dr. Valentin Wittmann für die Übernahme des Prüfungsvorsitzes.

Besonders möchte ich mich bei Tatjana Schneider und Dr. Daniel Schneider für die Hilfsbereitschaft im Labor und die großartige Zusammenarbeit im *Team Ubiquitin* bedanken.

Weiterhin danke ich Dr. Marina Rubini als Ansprechpartnerin beim Einbau von unnatürlichen Aminosäuren, sowie Dr. Andreas Marquardt für die Unterstüzung bei der Massenspektrometrie. Außerdem danke ich der Arbeitsgruppe Mayer für die Hilfestellung bei den Kinase Assays und der Bereitstellung von Laborressourcen.

Simon Geigges, Ho-Wah Siu und Emilia Luise Amrou danke ich für helfende Hände im Labor während ihrer Master- bzw. Bachelorarbeit.

Der Konstanz Research School Chemical Biology danke ich für die wissenschaftliche Weiterbildung.

Allen ehemaligen und aktuellen Mitarbeitern der Arbeitsgruppe Marx danke ich für das tolle Arbeitsklima, die abenteuerlichen Ausflüge und die ausgelassenen Feste.

Besonders danken möchte ich meiner Freundin und all meinen (Sports-)Freunden, die meine Zeit in Konstanz zu einer unvergesslichen, wunderbaren Erfahrung gemacht haben und für besten Ausgleich sorgten, wenn es im Labor eher suboptimal lief.

Mein größter Dank gilt meiner Familie, besonders meinen Eltern, die mich während meiner gesamten Ausbildung bedingungslos unterstützt und immer an mich geglaubt haben.

Zusammenfassung

In eukaryotischen Zellen liegt die DNA komprimiert als Nucleoprotein-Komplex, auch bekannt als Chromatin, vor. Dabei ist die DNA in der untersten Organisationsstufe, dem Nukleosom, um ein Oktamer aus Kernhistonen gewickelt.[1] Höher geordnete Strukturen werden durch Angliederung von Linker Histone gebildet.[2, 3] Die Mitglieder der Linker Histon Familie sind wie alle Histone hoch basische Proteine und bestehen aus einer gefalteten globulären Domäne (GD), die für die Erkennung und die Interaktion mit dem Nukleosom zuständig ist, sowie einer langen, unstrukturierten C-terminalen Region und einem kurzen N-terminalen Abschnitt.[4, 5] Die genaue Funktionsweise der Linker Histone bei der Ausbildung höher geordneter Chromatinstrukturen ist noch nicht vollständig aufgeklärt. Ein Aspekt der Regulation der Chromatinstruktur und damit vieler DNA basierender Prozesse, wird durch Histonmodifikationen wie z. B. Methylierung, Acetylierung und Ubiquitylierung gesteuert.[6] Die Diversität dieser posttranslationalen Modifikationen (PTMs) und der daraus resultierenden Funktionen führte zur Formulierung der Histone Code Hypothese.[7] Unter der Vielzahl verschiedener PTMs gehört die Mono-Ubiquitylierung zu einer der am wenigsten verstandenen epigenetischen Markierungen. Insbesondere über die Mono-Ubiquitylierung von Linker Histonen ist sehr wenig bekannt. Eine Ursache dafür liegt in der Unzugänglichkeit von homogen modifizierten Linker Histonen, welche für genauere Untersuchungen unabdingbar sind. Ziel dieser Arbeit war daher die Herstellung von definierten, mono-ubiquitylierten linker Histonen mittels Click Reaktion, sowie deren funktionelle Charakterisierung.

Um die mono-ubiquitylierten Linker Histone der Variante H1.2 mittels Click Reaktionen herzustellen, wurden unnatürliche Aminosäuren, die über eine Alkin- bzw. Azidgruppe verfügen, an verschiedenen Positionen in die jeweiligen Proteine eingebaut. Nach Optimierung der Expression sowie der Reinigung von H1.2 gelang es, das propargyl-derivatisierte Lysine Plk mittels *Amber Codon Suppression* (ACS) gezielt in vier verschiedenen Positionen innerhalb der GD einzubauen und die modifizierten Proteine erfolgreich zu isolieren. Die C-terminale Azid-Modifikation von Ubiquitin (Ub) wurde durch den Einbau von Azidohomoalanin (Aha) mittels *Selecitve Pressure Incorporation* (SPI) erreicht. Nach intensiver Optimierung der Click Reaktionsbedingungen, konnte H1.2 an allen vier gewünschten Positionen mit Ub kovalent modifiziert werden. Die erfolgreiche Konjugation wurde mittels Massenspektrometrie (MS) bestätigt. Weiterhin zeigten alle H1.2-Ub Konjugate in CD spektroskopischen Studien eine korrekte, dem unmodifizierten Wildtyp entsprechende Faltung.

Anschließend wurde die Fähigkeit der H1.2-Ub Konjugate zur Binding an Nukleosomen und zur Assemblierung von Chromatosomen untersucht. Dazu wurden definierte Nukleosomen aufgebaut und die Bildung von Chromatosomen sowie deren Eigenschaften untersucht. Hier zeigte sich, dass alle Konjugate, unabhängig von der Position der Mono-Ubiquitylierung, in der Lage sind, die nukleosomale Struktur zu erkennen und Chromatosomen aufzubauen. Dies weist auf variable Bindungsformen von H1 am Nukleosom hin, welche bereits zuvor beschrieben wurden.[8]

Um die mono-ubiquitylierten Konjugate als putative Vorlagen für weitere PTMs genauer zu beleuchten, wurde ihre Eignung als Substrat für Linker Histone-modifizierende Enzyme untersucht. Hier konnte gezeigt werden, dass H1.2-Ub Konjugate trotz Mono-Ubiquitylierung Akzeptoren für die Phosphorylierung durch den Kinasekomplex cdk1/cyclin B darstellen. Diese Ergebnisse wurden sowohl in *in vitro* als auch in *ex vivo* Experimenten erhalten und demonstrieren, dass die mittels Click Reaktion hergestellten H1.2-Ub Konjugate auch in komplexen, biologischen Systemen einsetzbar sind.

Abschließende Studien mit Poly(ADP-ribose)-Polymerase 1 (PARP-1) deuteten an, dass die Mono-Ubiquitylierung der globulären Domäne in H1.2 keinen wesentlichen Einfluss auf die Umgestaltung der Chromatosomen durch PARP-1 hat, obwohl die H1.2-Ub Konjugate als Akzeptoren für poly(ADP-ribos)ylierung fungieren und aus H1.2-Ub bestehende Chromatosomen mit PARP-1 interagieren.

Abstract

In eukaryotic cells, the DNA is compacted in a nucleoprotein complex, also known as chromatin. On the basic level of organization termed nucleosome, the DNA is wrapped around an octamer of core histones.[1] Higher order structures are formed upon incorporation of linker histones.[2, 3] Members of the linker histone family - like all histones - are highly basic proteins and consist of a folded globular domain (GD) that is responsible for the recognition and interaction with the nucleosome, as well as a long, unstructured C-terminal region and a short N-terminal tail.[4, 5] The exact functionality of linker histones in higher order chromatin structures is not completely clarified yet. One aspect of regulating the chromatin structure and thereby many DNA-based processes is controlled by histone modifications such as methylation, acetylation and ubiquitylation.[6] The diversity of posttranslational modifications (PTMs) and the resulting functions brought up the histone code hypothesis.[7] Among the variety of PTMs mono-ubiquitylation remains one of the least understood epigenetic modifications. In particular, very little is known about linker histone mono-ubiquitylation. One reason is the inaccessibility of homogeneously modified linker histones, which are crucial for distinct studies. Therefore, the aim of this thesis was the generation of defined mono-ubiquitylated linker histones by click reaction as well as their functional characterization.

In order to generate mono-ubiquitylated linker histones of the H1.2 variant by click reaction, unnatural amino acids, equipped with an alkyne- or azide group were incorporated into the respective protein at different sites. After optimizing the expression as well as the purification of H1.2, site-specific incorporation of propargyl-derivatized lysine Plk by amber codon suppression (ACS) was accomplished at four different positions within the globular domain and the modified proteins were successfully isolated. The C-terminal modification of Ubiquitin (Ub) with an azide was achieved by the incorporation of Azidohomoalanine (Aha) via selective pressure incorporation (SPI). After optimization of the click reaction conditions, covalent modification of all four desired positions in H1.2 with Ub was achieved. Successful conjugation was verified by mass spectroscopy (MS). Furthermore, in CD-spectroscopic studies, all H1.2-Ub conjugates exhibited a correct folding in comparison to the unmodified wild-type.

Afterwards, the ability of H1.2-Ub conjugates to bind to nucleosomes and to reconstitute chromatosomes was investigated. For this purpose, defined nucleosomes were assembled and the formation of chromatosomes, as well as their properties were studied. Here, all conjugates were able to recognize the structure of the nucleosome and to reconstitute chromatosomes, independently of the position of mono-ubiquitylation. The results indicate variable binding modes of H1 on nucleosomes, which had been already described before.[8]

To elucidate the role of mono-ubiquitylated conjugates as putative templates for additional PTMs, they were accessed as substrates for linker histone-modifying enzymes. Here, it was demonstrated that H1.2-Ub conjugates are acceptors for phosphorylation by the kinase complex cdk1/cyclin B despite their mono-ubiquitylation. These results were obtained in *in vitro* as well as in *ex vivo* experiments,

demonstrating that H1.2-Ub generated by click reaction conjugates are applicable in complex biological systems.

Finally, studies with poly(ADP-ribose)polymerase 1 (PARP-1) suggested that mono-ubiquitylation of the globular domain of H1.2 might not have a major influence on the chromatosome remodeling by PAPR-1, although the H1.2-Ub conjugates serve as acceptors for poly(ADP-ribos)ylation and PARP-1 interacts with chromatosomes consisting of H1.2-Ub.

Table of contents

1 Introduction

1.1 Chromatin

In eukaryotic cells the genetic information is organized in a nucleoprotein complex, termed chromatin. In relation to its transcriptional potential two types of chromatin can be distinguished. The actively transcribed euchromatin is less condensed and encodes most of the protein coding sequences whereas the transcriptionally inactive heterochromatin is highly compacted.[9] Whereas constitutive heterochromatin is enriched in gene poor repetitive DNA sequences and always compact, facultative heterochromatin undergoes transition from a compact, transcriptionally inactive state to a more open, transcriptionally competent state. Condensation and decondensation of the chromatin is critically important, since it facilitates regulation of most DNA based processes like transcription, replication and DNA repair.[6] Several levels of chromatin condensation are required to achieve a high degree of compaction, in order to fit about two meters of DNA into the nucleus with a diameter of less than 10 micrometer (Figure 1.1).

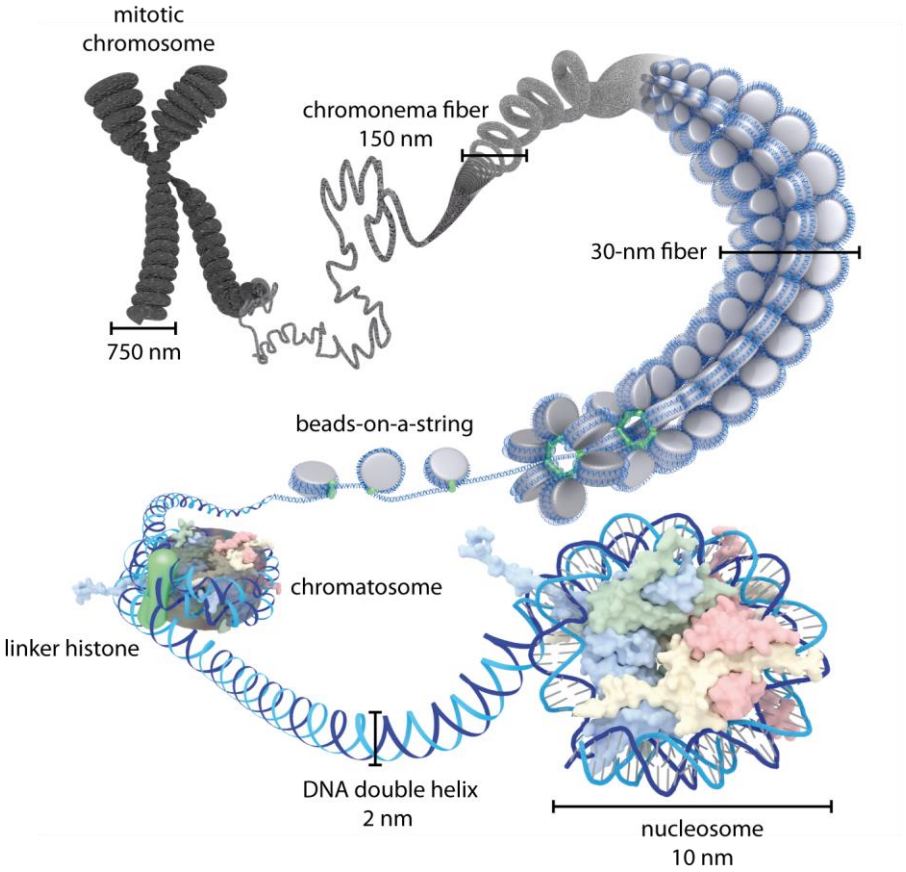

Figure 1.1 Schematic representation of chromatin organization. Kindly provided by Dr. Samra Ludmann.

The highest level of condensation is achieved in metaphase chromosomes during mitosis with a 10,000–20,000 fold compaction of the DNA. The folding of this 500–750 nm chromatin fiber is promoted by condensin, located in the central axis.[10] Many details about the folding geometry of the underlying chromatin structure remain unclear.[11] Multivalent cations, fiber-fiber interactions and chromatin associated proteins contribute to the chromatin structure at this organization level.[12, 13] Besides electron microscopy (EM) studies reporting cylindrical fibers with diameters ranging from 120–170 nm[14], different irregularly folded fiber-like structures with a variety in length and diameter have been described[15]. These so called chromonema fibers finally give rise to chromosome condensation by supercoiling. Throughout all levels of chromatin organization structural support and regulatory communication is provided by chromatin loops.[16] Such loops were first observed in metaphase chromosomes upon controlled reduction in ionic strength.[17] Under these conditions chromatin revealed a sub-chromosomal structure with a condensed 30-nm fiber.[17] Two major models were proposed for the arrangement of nucleosomes within the 30-nm fiber (Figure 1.2). The one-start solenoid-type helix is characterized by a bent linker DNA and linearly arranged nucleosomes[18-20] whereas the zigzag structure exhibits a straight DNA linker and a two-start stack of nucleosomes[21]. Different orientation angles between the fiber axis and the linker DNA further divide the zigzag model into the twisted cross-linked model[22] and the helical ribbon model[23].

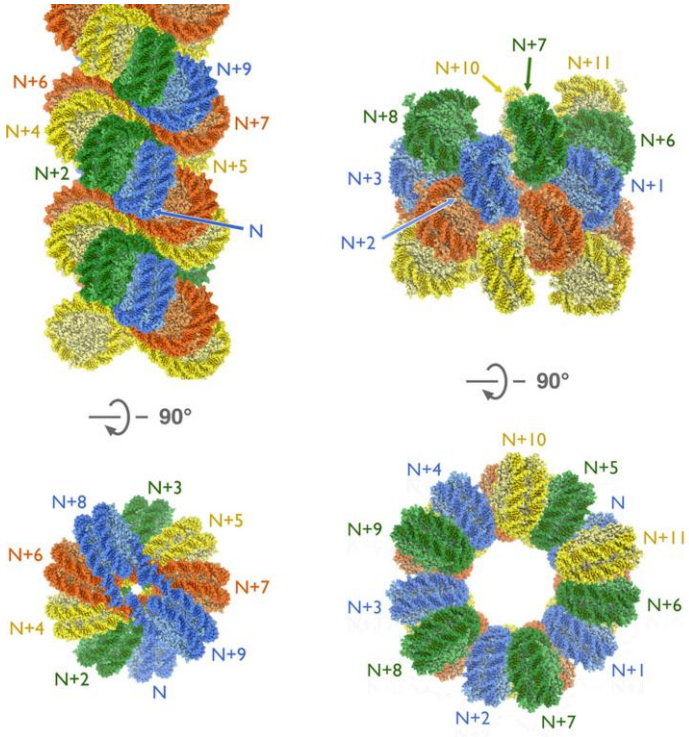

Figure 1.2 Proposed models of the 30-nm fiber with the two-start zigzag structure (left) and the one-start solenoid structure (right). In both models, the positions of the nucleosomes in the linear DNA sequence are indicated with N, N+1, N+2, etc. Reprinted from [24]. Copyright © 2014 American Chemical Society.

Although extensively studied, the relevance and structure of the 30-nm fiber remains controversial. Furthermore, the structure of the 30-nm fiber was found to depend on the ionic strength, the length of

linker DNA and the density of linker histones,[25] suggesting a highly dynamic structure and leading to the hypothesis of a heteromorphic compact fiber comprising both major models[26]. However, there is general agreement that the compaction of chromatin into the 30-nm fiber emerges from polynucleosome arrays. This structure is also known as beads-on-a-string with nucleosomes as beads interconnected by DNA as string (Figure 1.1). It represents the first level of chromosomal compaction, leading to an approximately five fold compaction of DNA.[27] In the hierarchical packing of DNA the nucleosome with a diameter of 10 nm serves as the basic repeating unit, comprising 180–200 base pairs (bp) of DNA.[28] Within this structure, 145–147 bp of DNA are wrapped around an octamer of core histones in 1.65 left-handed superhelical turns forming the nucleosome core particle (NCP) (Figure 1.3).[1, 29-33] The core histones are small proteins consisting of 100–130 amino acids and are highly conserved in eukaryotes [34]. Due to their positive charge, all core histones have a strong affinity to the negatively charged DNA. Structurally, each core histone exhibits a folded globular domain and a long unstructured N-terminal tail. The helix-strand-helix structure of the globular domain comprises three *α*-helices forming the histone-fold motif.[29] Crystal structures revealed an interaction of the core histone surface with the phosphate backbone of the DNA and the interaction of core histones by the histone-fold motifs holding together the NCP.[1, 31] In this arrangement, two core histone monomers with complementary histone-folds pair in a head-to-tail conformation to assemble a histone-fold heterodimer called handshake motif.[29, 35-37] Heterodimers are formed by pairing of H3 with H4 and H2A with H2B, thus exhibiting a convex surface for DNA binding. H3/H4 heterodimers further associate in a head to head arrangement to form tetramers. Together with two H2A/H2B heterodimers, which bind to each half of the tetramer by forming a four helix bundle, the histone octamer is formed. The DNA entry and exit site of the NCP is located in direct contact with the H3/H4 tetramer.[1] Several flexible and unstructured N-terminal tails from the core histones extend beyond the NCP and bind intranucleosomal or neighboring nucleosomes.[38, 39] Moreover, these tails are sites of numerous combinatorial post-translational modifications (see 1.3), which have important roles in replication, transcription and DNA repair.[40]

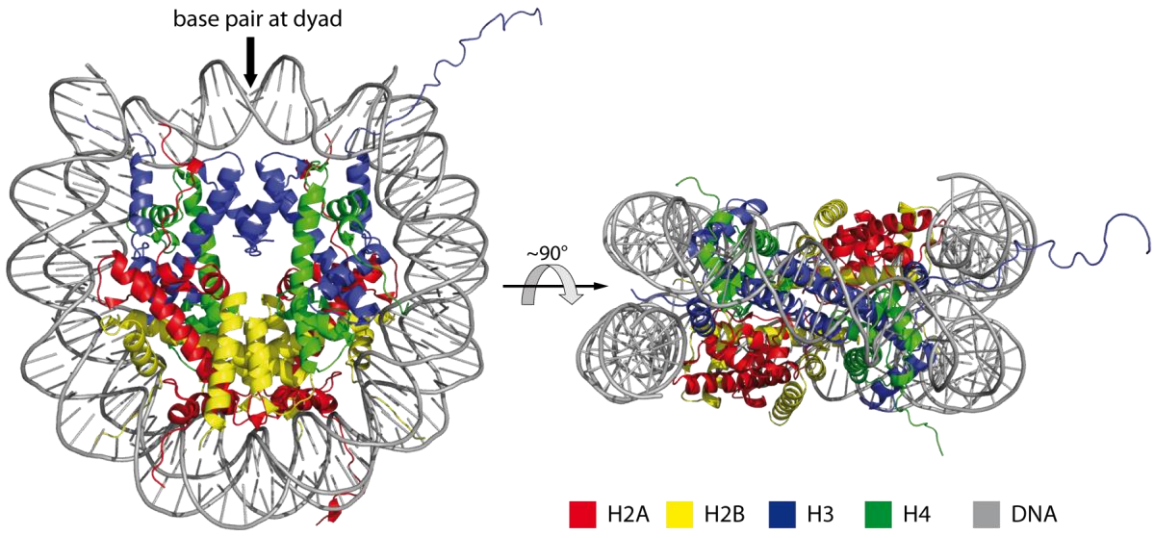

Figure 1.3 Structure of the nucleosome core particle (PDB: 1AOI) with DNA and core histones colored as indicated.

1.2 Linker histones

Higher order structures formed by nucleosomal arrays at physiological ionic strength require other proteins for stabilization.[12] Among these architectural proteins[41] the most abundant protein family in eukaryotes are linker histones (H1 and H5). Initially it was presumed, that in living cells one linker histone is present per nucleosome[42]. Further studies revealed a stoichiometry over a range of about 0.8–1.4, depending on the tissue and the nucleosome repeat length.[42-44] In nucleosomal arrays the nucleosomes are separated by histone free, extranucleosomal linker DNA. In contrast to nucleosomal DNA the linker DNA is not constrained in the superhelix by core histones and is sensitive for digestion by nucleases.[45] Binding of linker histone to the nucleosome dyad[46, 47] (see Figure 1.3) near the DNA entry/exit site[4, 48, 49] forms higher order chromatin structures[2, 3, 18] and protects 20 bp of linker DNA from micrococcal nuclease digestion[3, 30]. This complex is referred to as chromatosome [32] (see Figure 1.1). However, the exact localization of the linker histone in chromatin and positions of linker DNA interactions are controversial.[50]

1.2.1 Structure and positioning

The influence of H1 on chromatin folding is dependent on its unique structural characteristics. Linker histones consist of around 200 amino acids (aa) with a high content of basic aa and exhibit a tripartite structure. The central globular domain (GD) comprising 70–80 aa is flanked by a short N-terminal tail (~30 aa) and a long C-terminal domain (CTD) (~100 aa).[5] Swapping[51] and deletion[52] experiments indicated that the N terminus is not important for nucleosome binding.[4, 53] In contrast, the GD interacts with the nucleosome by structure specific recognition[4, 54] and is responsible for micrococcal nuclease (MNase) protection[4, 30]. The secondary structure of the GD from two chicken linker histone homologs (cH5 and cH1) was resolved at atomic resolution by X-ray[5] and 2D NMR[55] respectively, with both, the N and C terminus lacking high resolution indicating an unstructured nature of the tails (Figure 1.4). Comparison of the two 3D structures revealed striking similarity of the characteristic secondary structure elements in the GD.[56] Three α-helices and a C-terminal β-hairpin assemble to form a winged helix domain (WHD).[5, 55] Additionally, a cluster of conserved basic residues with potential for DNA binding is located at the opposite site of the GD.[5] Thus, at least two separated DNA binding sites within the GD enable the linker histone to interact with different DNA regions in the nucleosome and elucidate the favored binding of linker histones to DNA crossovers[57]. Hence, the GD directs structure-specific recognition and binding to the nucleosome.[4, 58]

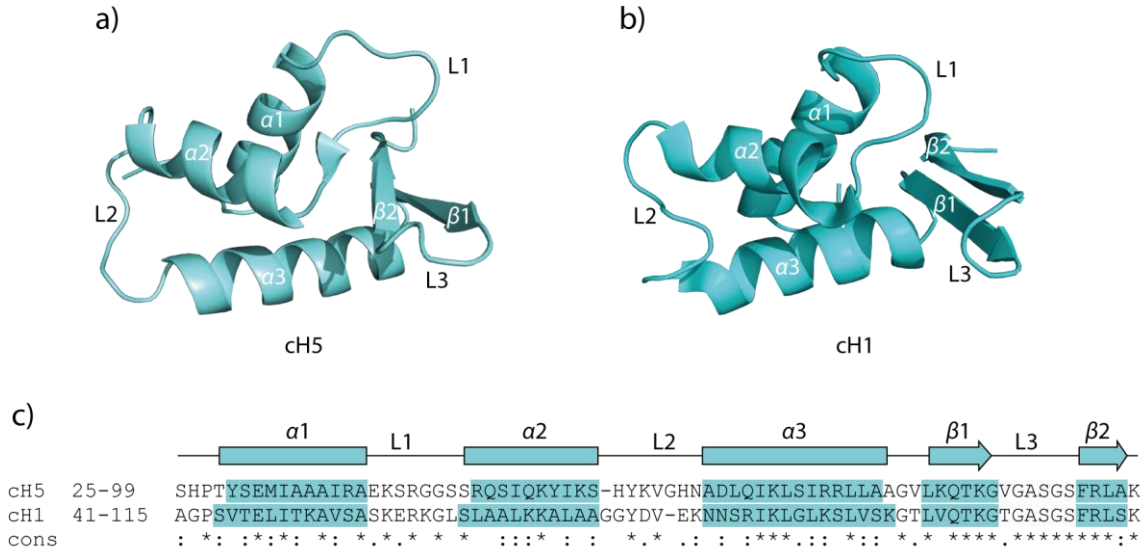

Figure 1.4 WHD of linker histones. a) X-ray structure of linker histone cH5 (PDB: 1HST). b) Tertiary structure of linker histone cH1 (PDB: 1GHC) obtained from 2D NMR. c) Amino acid sequence alignment of GDs of cH5 and cH1 with indicated secondary structure elements; loops (L1–3), *α*-helices (*α*1–3) and *β*-hairpins (*β*1 and *β*2). The degree of amino acid conservation (cons) is displayed: high (*), medium (:) and low (.).

The CTD is required for the association of H1 to chromatin *in vivo*[59, 60] and was found to facilitate the formation of the 30-nm fiber[52]. The long CTD comprises approximately half of the H1 sequence and is highly basic due to high content (40 %) of lysine (see Figure 1.6), allowing higher order chromatin structure regulation through neutralization of the DNA backbone.[61] Along these lines, two distinct functional regions for DNA binding in the CTD were suggested by mutational studies.[58, 62] Upon DNA binding, the intrinsically disordered C terminus folds from random coil into *α*-helices, *β*-sheets, loops and turns[63, 64] and facilitates the formation of the nucleosome stem structure by settling into the helices of the linker DNA[65]. Inter-nucleosomal stem-to-stem interactions are hypothesized to stabilize the folding in higher order chromatin structures [48]. Moreover, the CTD domain is also involved in protein-protein interactions.[66]

In the light of accumulating evidence that linker histones play an important role in the formation and stabilization of the 30-nm chromatin fiber[20, 53] and numerous studies indicating the binding of the linker histones around the dyad region of the nucleosome[32, 46] a variety of experimental methods was applied to reveal the precise localization and function of linker histones and its GD within the 30-nm fiber. Hence, two major classes of competing structural models for the binding mode of linker histones at the nucleosome were proposed (Figure 1.5). In the symmetrical model, the GD is centrally located on the dyad axis of the nucleosome (“on-dyad”), interacting with both entry/exit sites of linker DNA (Figure 1.5a).[4, 32, 48, 53, 67, 68] MNase digestion and DNase footprint analysis resulted in the protection of 20 bp linker DNA[69] with 10 bp at each site[4, 53]. The recently resolved crystal structure of the GD of cH5 in complex with the nucleosome revealed three DNA binding sites, with the L1 loop and *α*3 helix interacting with both linker DNA and L3 loop binding to the minor groove of the dyad

DNA (Figure 1.4a, Figure 1.5a)[68]. These results support previous data obtained by cryo-electron microscopy (cryo-EM) and hydroxyl radical footprint analysis[53] and are consistent with computational models suggesting three DNA binding sites for the linker histone in a chromatosomal context[67]. A different position of the GD is described in the asymmetrical model based on DNA crosslinking studies,[70] indicating a localization of the GD on the nucleosome off the dyad axis ("off-dyad") with binding to only one site of the linker DNA (Figure 1.5b), interacting with 10 bp[8, 49] or 20 bp[59, 71].

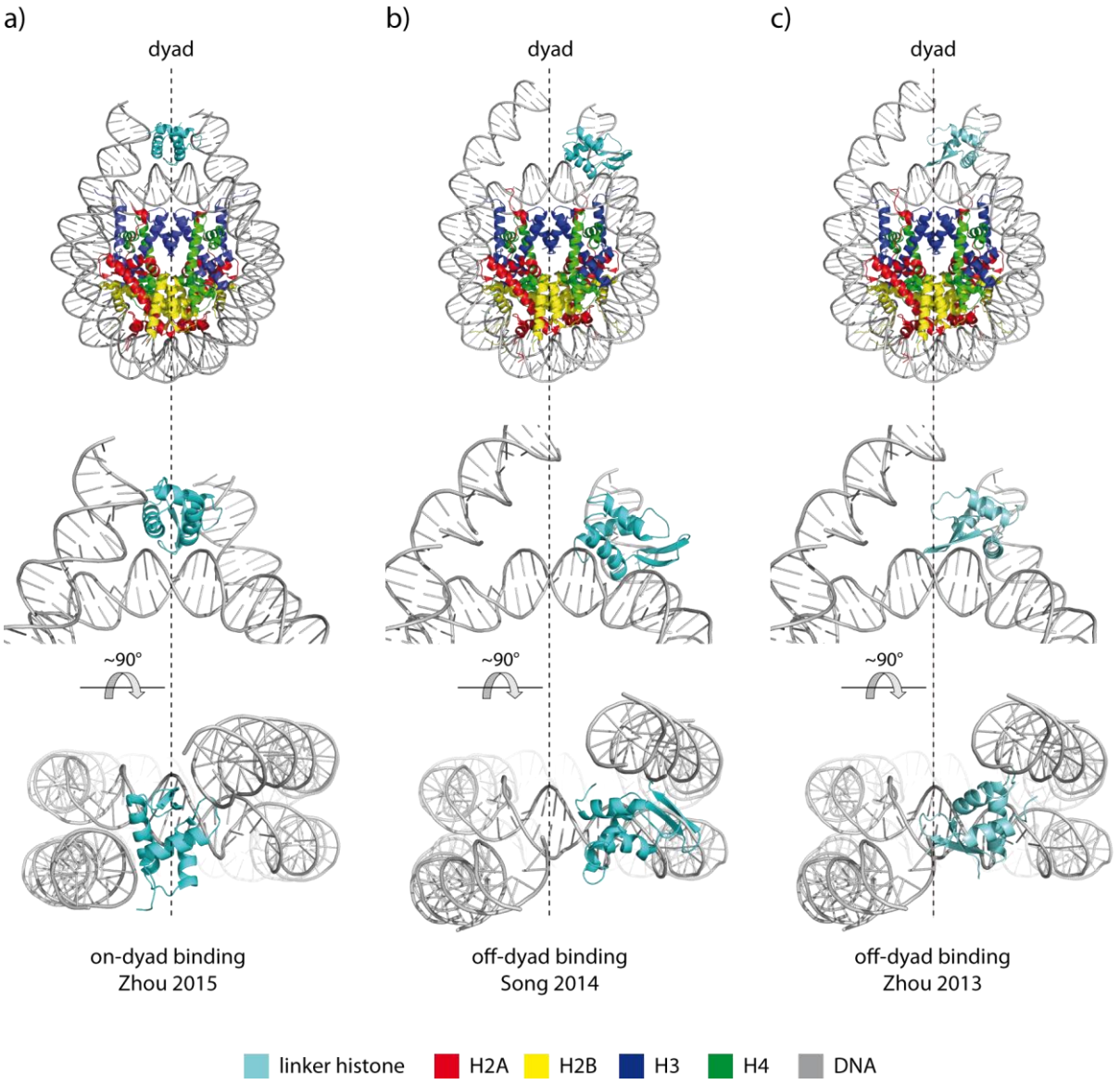

Figure 1.5 Binding models of linker histones on the nucleosome. a) Symmetric on-dyad binding of the GD of cH5 on the nucleosome obtained from X-ray crystallography (PDB: 4QLC).[68] b) Asymmetric off-dyad localization of the GD of human (h)H1.4 kindly provided by Song *et al*.[21] Here, based on cryo-EM studies with hH1.4, the sequence of hH1.4 was fitted into cH5 (PDB: 1HST) and modeled into a nucleosome derived from the tetranucleosome structure (PDB: 1ZBB). c) Asymmetric off-dyad binding of the GD of drosophila (d)H1. According to the structure presented by Zhou *et al*.[58] cH5 (PDB: 1HST) was manually placed into the structure of the nucleosome, provided by Song *et al*.. Position of the nucleosome dyad is indication by a dashed line. Linker histones, core histones and DNA are colored as annotated.

Results from *in vivo* photobleaching microscopy supported the existence of two DNA binding sites (Figure 1.4b) in the asymmetrically positioned GD, which interacts in this model with one site of the linker DNA and the major groove 10 bp away from the dyad.[59] Recent cryo-EM studies of 30-nm fibers condensed by human H1.4 showed an asymmetric off-dyad localization (Figure 1.5b)[21] and revealed a different binding orientation compared to drosophila H1 investigated by NMR and mutational studies, which demonstrated an off-dyad binding mode as well (Figure 1.5c)[58]. Mapping the corresponding residues of hH1.4 into the crystal structure of cH5 bound to the nucleosome (PDB: 4QLC), showed interactions with only one linker DNA and the dyad, supporting the off-dyad binding mode of hH1.4.[68] Consequently, the on- and off-dyad binding modes of different linker histones are assumed to play an important role in defining the higher order chromatin structure. Along these lines, linker histone variants might use diverse binding modes to regulate the function and stability of chromatin fibers.[68]

1.2.2 H1.2 and H1 variants

In comparison to core histones, the linker histone family is evolutionary less conserved and many organisms possess multiple H1 variants characterized by a high sequence homology. In humans, the linker histone family comprises eleven members with their own genes[72] with H1.1 to H1.5 sharing 89 % sequence identity. Generally, the GD is evolutionarily conserved whereas the N- and the C-terminal tails are both more variable in their sequence. Two types of H1 genes were distinguished. Whereas the replication dependent genes are mainly expressed in dividing cells and transcribed during S-phase representing the major variants H1.1 to H1.5, the replication independent H1 genes encode for replacement histones, expressed in resting cells, for example H1.0 and H1.x.[73] Among the seven somatic variants (H1.1 to H1.5, H1.0 and H1x)[72, 74] (see Figure 1.6), H1.1 to H1.5 are expressed ubiquitously [75-77] with H1.2 and H1.4 predominant in most cell types[78] and H1.0 in terminally differentiated cells exclusively[79]. Besides the somatic variants, germ-line specific variants comprising three testis specific variants (H1.1t, H1T2 and HILS1)[80-82] and one oocyte specific variant (H1oo)[83] were identified.[72] The somatic variants H1.1 to H1.5 are characterized by micro heterogeneity in their N- and C-terminal tails[84] (Figure 1.6) and differ from the rest of the H1 family exhibiting a high sequence and size variability in their tails compared to the WHD[85].

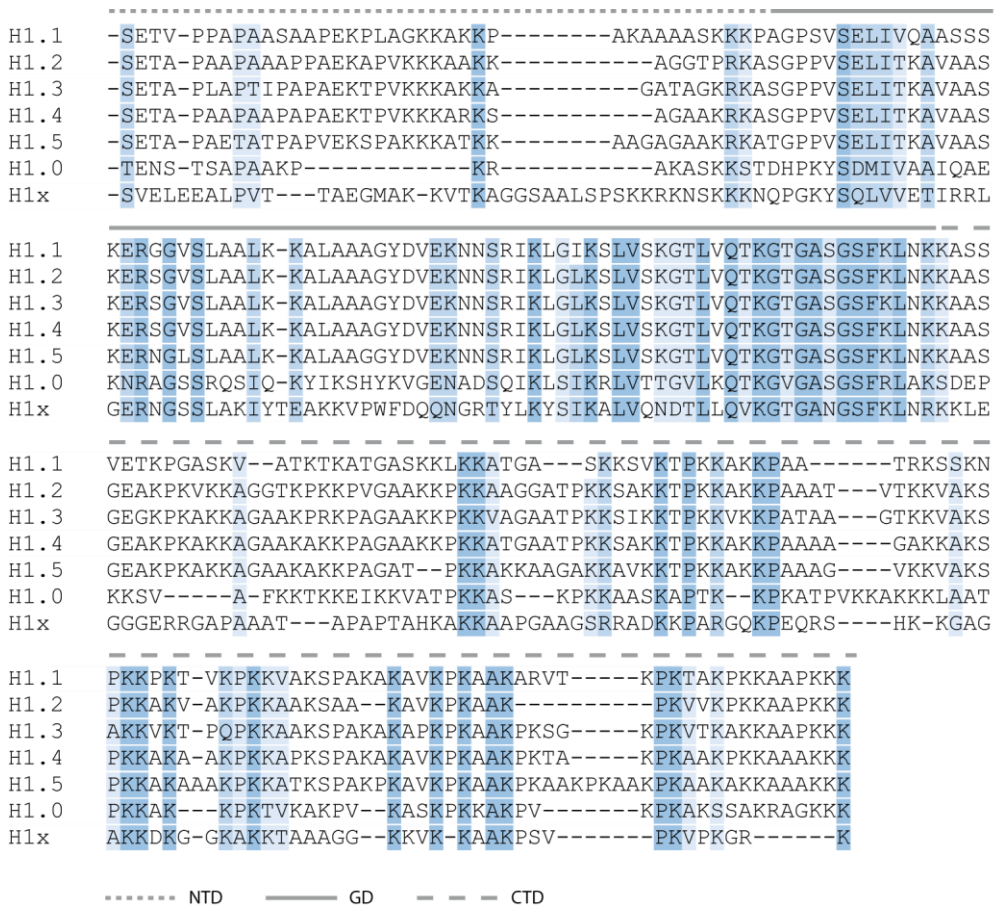

Figure 1.6 Amino acid sequence alignment of human somatic linker histone variants. The degree of amino acid conservation corresponds to the coloring. The N-terminal domain (NTD), globular domain (GD) and C-terminal domain (CTD) are indicated by dashed and solid lines. Alignment was performed with T-Coffee[86].

To investigate distinct functions of different H1 variants, knockout experiments were performed. Initially, single or double knockout of H1.2, H1.3 and H1.4 orthologs in mice were investigated, resulting in no phenotypical changes. This lack of alteration was attributed to a compensatory effect of the variants and a redundancy between the variants was hypothesized.[87] Only when a triple knockout study was conducted, a 50 % reduction in nucleosome repeat length and in the ratio of H1 : nucleosome was observed resulting in embryonic lethality[43]. Further *in vitro* studies with H1 triple knockout in embryonic stem cells revealed alterations in the chromatin structure and in gene expression at DNA methylation sites.[44] In contrast, overexpression of H1.0 analogue in mouse cell lines lead to an increase in nucleosome repeat length and a decline in cell cycle progression.[88] Interestingly, H1.2 overexpression had no effect on cell cycle progression[89], demonstrating functional differences between the variants. Despite the micro heterogeneity, further experimental data supported non redundant functions of H1 variants. *In vitro* studies with extracted H1 variants from rats revealed the following chromatin binding affinities: H1.3 and H1.4 > H1.2 and H1.5 > H1.1[90]. Differences in binding dynamics, residence time and localization in the nuclei were also observed *in vivo* by fluorescence recovery after photobleaching (FRAP) utilizing eGFP-H1 fusion proteins in human cells, suggesting a stop-and-go model for the dynamical binding of linker histones to chromatin.[66, 91] Furthermore, individual variants exhibit diverse effects on gene regulation.[88, 92, 93] Mapping their genomic distri-

bution displayed depletion of H1.2 to H1.5 from active regulatory and CpG-dense regions, while binding to regions with methylated DNA depends on the context, indicating a three-dimensional genome organization[94]. Notably, usage of variant-specific antibodies demonstrated strongest correlation with low gene expression for H1.2, being less abundant at regulatory regions of inactive genes and enriched at domains with low GC content[95] – implying a distinct functional role of H1.2[96]. A particular role of H1.2 as transcriptional repressor was revealed by its association with p53 leading to a block in chromatin acetylation[97]. Remarkably, H1.2 displays also distinct extra nuclear functions. Upon DNA strand breaks H1.2 translocates to the mitochondria in the cytoplasm and triggers the release of apoptotic factors by binding to Bak, a pro-apoptotic member of the Bcl-2 family.[98-100] Subsequently, a recent study identified the C-terminal domain of H1.2 for apoptogenic activity.[101] Although micro heterogeneity in H1 variants is sparsely elucidated, in combination with observed variant-specific PTM patterns individual variants may play distinct roles in the regulation of higher order chromatin structures. It is assumed that specificity of individual variants is partially caused by their sequence diversity, but mostly by PTMs[72].

1.3 Histone modifications

Gene expression is regulated by several epigenetic marks, including RNA silencing, DNA methylation, nucleosome positioning and posttranslational histone modification, playing fundamental roles in the control of chromatin structure, embryonic development and diseases.[40] With epigenetic marks interacting with each other, histones and their PTMs are key players in epigenetics and known to influence chromatin structure[6], DNA replication[102] and repair[103]. Predominantly, histones are dynamically modified at their N-terminal tails protruding beyond the nucleosome, thereby altering histone-DNA and histone-histone interactions. Besides direct biophysical effects on chromatin structure, PTMs of histones are recognized by proteins that interact with specific marks. Together with enzymes attaching and removing the PTMs these proteins are often called histone mark "readers", "writers" and "erasers" (Figure 1.7). The PTMs can occur simultaneously at selected residues, facilitating crosstalk between different marks at the same site[104], within the same tail[105, 106] or at different tails[107]. Hence, the distinct combination of modifications determines the chromatin state[108] and thus the biological outcome. The recruitment of cellular factors ("readers") by particular histone modification patterns inducing distinct downstream events is termed histone code (Figure 1.1).[7] Besides PTMs of core histones, which have been extensively studied, linker histones emerged to play an important role in epigenetics, based on numerous different PTMs identified including phosphorylation, acetylation, methylation, ubiquitylation and ADP-ribosylation.[109, 110] Furthermore, linker histone variants are particularly modified and these patterns determine their specific function and interaction with different factors.[111, 112] However, with exception of H1 phosphorylation the most extensively studied PTM on H1[113], the mechanism of action of other PTMs on linker histones is often poorly understood.

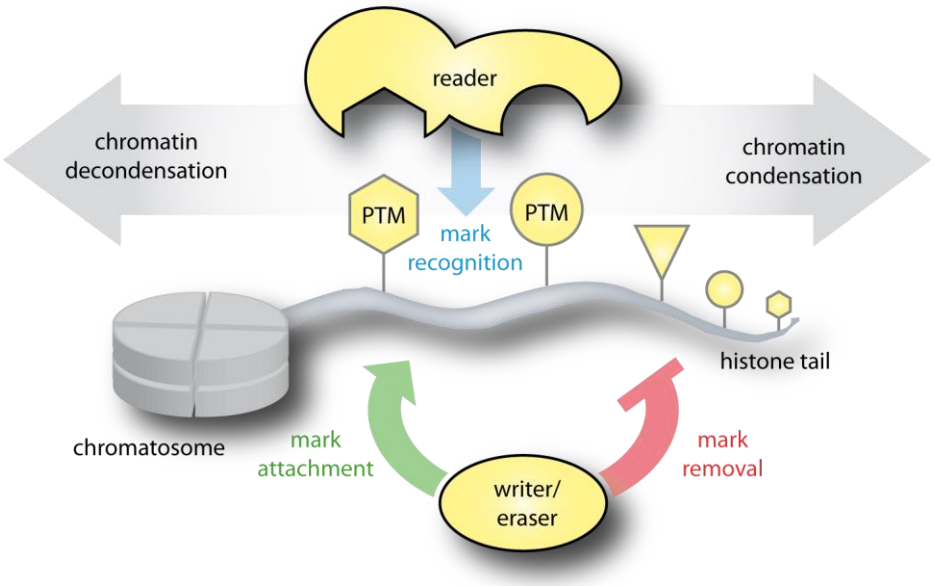

Figure 1.7 Histone code hypothesis. Distinct histone PTMs act in combination or sequentially to form a histone code, that is recognized by specific reader proteins facilitating specific downstream events. These histone marks are attached and removed by enzymes termed writers and erasers.

1.3.1 Phosphorylation

Phosphorylation of linker histones is connected to a variety of different functions like cell differentiation[114], cancer[115], apoptosis[116], DNA damage[117] and ligation[118]. Among these, cell cycle dependent phosphorylation[119, 120] represents the major field of research[121]. Several phosphorylation sites were mapped by MS (Figure 1.8a) but could not be linked to a specific function (Figure 1.8).[109, 122] Cell cycle dependent phosphorylation is mediated by cyclin dependent kinases (cdks) and regulates chromatin dynamics in interphase and chromatin condensation in mitosis[113, 123] in a two-step process[124] (Figure 1.8b). Although most of the kinases are well known and several phosphorylation sites in H1 variants were identified within a C-terminal consensus sequence (S/T)-P-X-(K/R), the phosphatases in this reversible process remain elusive. Whereas serine residues are phosphorylated in interphase and mitosis, phosphorylation of threonine residues occurs solely in mitosis.[125]. During cell cycle, phosphorylation levels of H1 variants change dramatically, starting from lowest level in G1 phase rising during S and G_2 to reach a maximum at metaphase.[120, 126, 127]. In this process, it was observed that alterations in phosphorylation prevents entry in mitosis[128]. During interphase (G_0-S) partial phosphorylation of H1, disrupting H1-DNA interaction, results in chromatin decondensation and allows transcriptional regulation by binding of nuclear proteins.[123, 129, 130]. In mitosis, all H1 variants are rapidly phosphorylated to a maximum level as a result of cdk activity at sites of S/T-P-X-K with H1.2 phosphorylation at T31, T146 and T154, as revealed by MS analysis (Figure 1.8b).[131] Highest overall phosphorylation levels were observed for H1.5 in mitosis as well as in interphase.[131] Hyper phosphorylation of H1 variants is required to retain chromatin in a compact structure during mitosis.[128]

Interestingly, site-specific modification of H1 variants was observed by MS analysis of mouse fibroblasts[120]. Highly phosphorylated H1.5 (residues S17, S172 and S188) and H1.4 (S172 and S183) were observed in S-phase.[131, 132] In contrast, the majority of H1.0, H1.1 and H1.2 were unphosphorylated or in case of H1.2 monophosphorylated at S173.[120, 131]. Immunofluorescence studies with phosphorylation site-specific antibodies revealed distinct localization of H1.2 S172p at active DNA transcription and replication sites.[132]

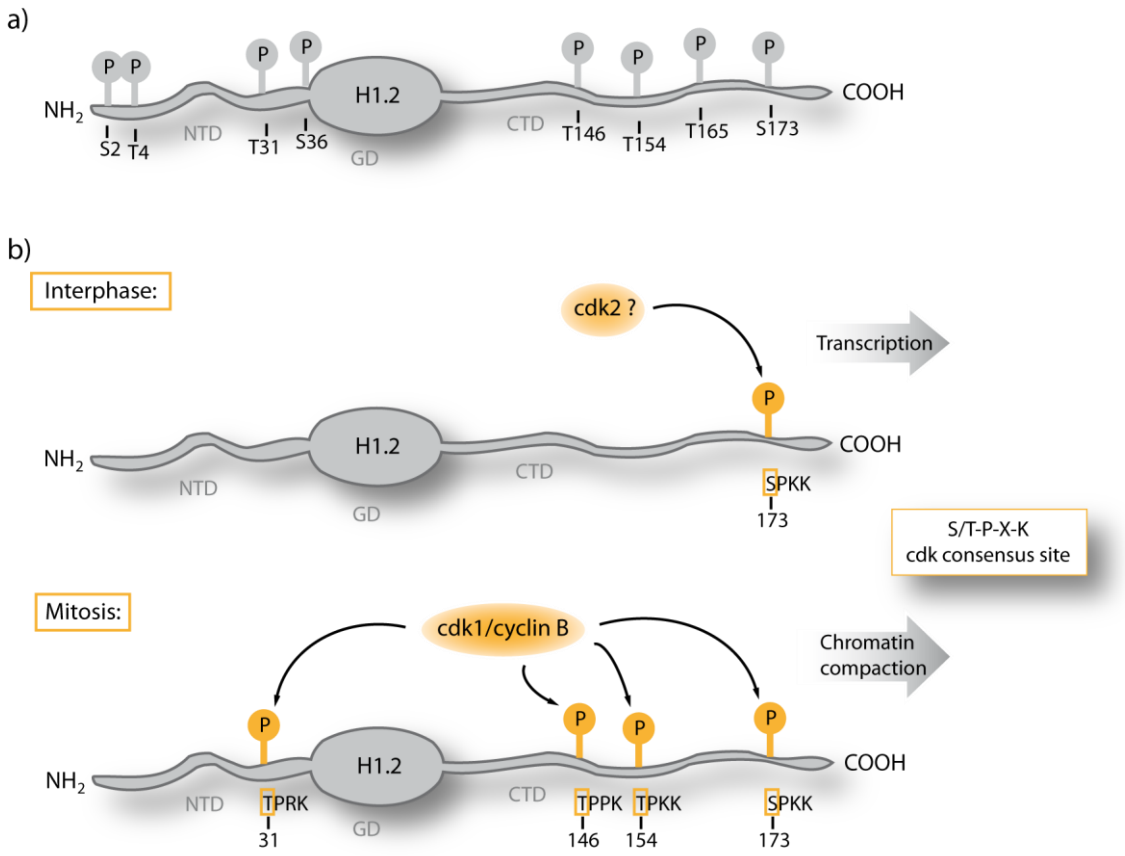

Figure 1.8 Phosphorylation of H1.2. a) Phosphorylation sites identified by MS.[121] b) Cell cycle-dependent phosphorylation. P: Phosphorylation, S/T-P-X-K cdk consensus site.

1.3.2 Ubiquitylation

Ubiquitin (Ub) is a small protein of ~8.5 kDa consisting of 76 aa. It is evolutionary highly conserved and essential in eukaryotes. Modification of substrate proteins with Ub is termed “ubiquitylation” and plays fundamental roles in various cellular processes like protein degradation[133], DNA repair[134] and transcriptional regulation[135]. In this process, an isopeptide bond is formed between the ε-amino group of a lysine residue of the substrate and the C-terminal glycine of Ub. Ubiquitylation is mediated in three steps comprising three classes of enzymes: Activation of Ub by ubiquitin-activating enzymes (E1), conjugation by ubiquitin conjugating enzymes (E2) and attachment to the substrate protein by ubiquitin ligases (E3) (Figure 1.9).[133, 136] Like other PTMs ubiquitylation is reversible and the removal of covalently attached Ub is carried out by a large family of de-ubiquitylating enzymes (DUBs).[137] Modification of a substrate protein with a single Ub moiety is termed mono-ubiquitylation and represents the simplest form.

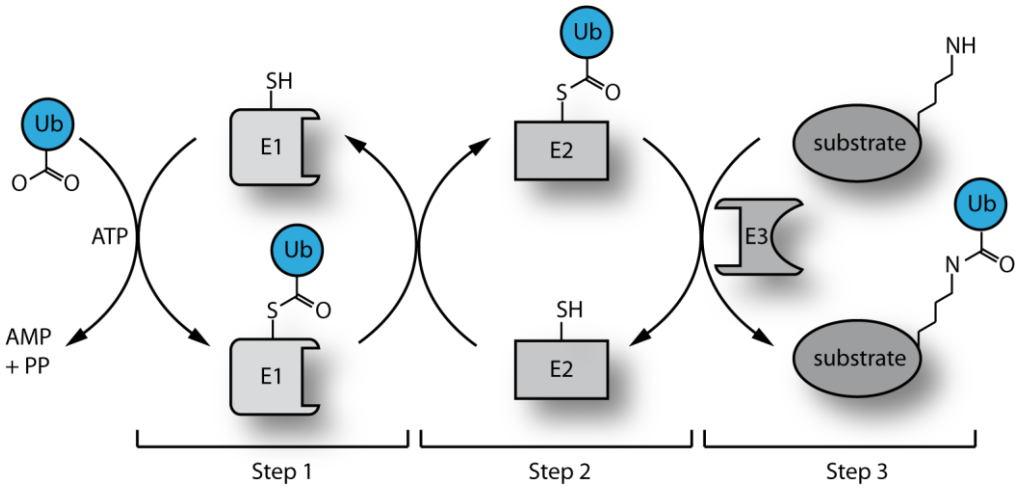

Figure 1.9 Ubiquitylation cascade. In the first step, the C terminus of Ub is activated in an ATP-dependent manner and covalently linked by a thioester bond to an active cysteine site on the E1 enzyme. In the second step, the activated Ub is transferred to the E2 enzyme via another thioester bond. Finally, the E2 enzyme transfers the activated Ub via an isopeptide bond to a lysine residue in the substrate protein bound to an E3 enzyme.

The attachment of multiple Ub moieties to different lysine residues of the substrate is referred to as multiple mono-ubiquitylation. Furthermore, the attached ubiquitin itself contains seven Lys and can serve as an ubiquitylation substrate as well, resulting in the formation of ubiquitin chains of various length and linkages (“poly-ubiquitylation”)[138]. Importantly, the actual type of ubiquitylation probably determines the fate of the modified substrate protein.[139] The best characterized function of poly-ubiquitylation is targeting proteins for proteasomal degradation by the 26S proteasome.[140] However, poly-ubiquitylation and mono-ubiquitylation have many other, non-proteolytic functions.[141, 142] In particular, mono-ubiquitylation is the major form of histone ubiquitylation and plays an important role in the regulation of gene expression.[135] Whereas mono-ubiquitylation at Lys120 of H2B[143] was observed at actively transcribed regions, ubiquitylation of H2A at Lys119[144] is associated with transcriptional repression[145]. Moreover, both ubiquitylated species play a role in double strand break repair.[134] Since the discovery of H2A ubiquitylation already 40 years ago[146], regulation of H2A and H2B mono-ubiquitylation were extensively studied, revealing several pathways and factors associated with mono-ubiquitylation of core histones[147]. In contrast, only very few studies were conducted targeting mono-ubiquitylation of linker histones. In *Drosophila melanogaster* H1 was identified to be mono-ubiquitylated by TAFII250, a component of the general transcriptions factor TFIID. Here, mono-ubiquitylated Ub was found to be important for the regulation of transcriptional activity in embryos.[148] Interestingly, TAFII250 exhibits both, Ub-activating (E1) and Ub conjugating (E2) activity and ubiquitylates H1 without the cooperation of an E3 ligase.[148] Moreover, an acyltransferase activity on core histones as well as kinase activity on the basal transcription factor TFIIA were identified in TAFII250.[149, 150] Hence, mono-ubiquitylation of H1 might play a role in controlling gene expression.[141] Beyond that, two other functions of mono-ubiquitylated H1 were proposed, indicating the functional diversity of this modification. In HIV-1 resistant T-cells mono-ubiquitylation of H1.5 is required for the antiviral protection[151]. In parallel, H1.2 was found to be mono-ubiquitylated *in vitro* and *in vivo* by the RING domain E3 ligase RNF168 in complex with Rad6 in

response to ionizing radiation-induced DNA damage.[152] Moreover, the E2 enzyme UBC13 together with RNF8 was found to selectively modify H1.2 and H1x with K63-linked poly-ubiquitin chains upon DNA double strand break recruiting RNF168 and DNA repair factors to the lesion site.[153] These observations point to a role of H1.2 ubiquitylation in DNA repair and maintenance of genomic stability as well as its participation in the histone code. To identify the acceptor sites and novel targets of mono-ubiquitylation, large-scale proteomics studies were performed. The first acceptor site identified by MS in human linker histones (H1.2 to H1.4) was lysine residue 46.[109] Subsequently, proteome-wide analysis of ubiquitylation by MS utilizing ectopically expressed *Strep*-tagged ubiquitin or immunoenrichment of a diglycine motive resulting from trypsin digestion revealed several additional ubiquitylation sites in H1.2 (Figure 1.10) and other variants.[154-156] However, none of these modification sites could be linked to a specific function so far.

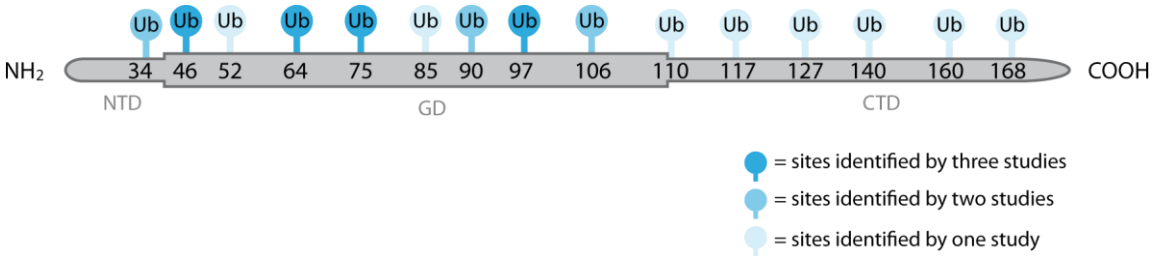

Figure 1.10 Ubiquitylation sites identified in H1.2 by MS.[154-156]

1.3.3 ADP-ribosylation

ADP-ribosylation is a reversible posttranslational modification, catalyzed by a family of enzymes termed ADP-ribosyltransferases (ARTs), with ADP-ribosyltransferase diphtheria toxin-like 1 (ARTD1, also known as poly(ADP-ribose) polymerase 1, PARP-1) as the best-studied member. PARP-1 is chromatin associated and highly abundant.[157] Besides DNA repair[158], PARP-1 plays important roles in a wide range of biological processes, including maintenance of genomic stability[159] and transcriptional regulation[160]. Mono(ADP-ribos)ylation comprises the transfer of one ADP-ribose moiety from the co-substrate NAD^+ to a specific amino acid residue of an acceptor protein. Further elongation and branching results in the formation of poly(ADP-ribose) (PAR) chains, termed poly(ADP-ribos)ylation (PARylation). ADP-ribosylation by PARP-1 is reported for H1 and all core histones *in vivo* and *in vitro*,[161] with PARP-1 itself as major acceptor[162]. Several acceptor sites on H1 were identified including E2, E15 and E114.[163] Nevertheless, the sites have not been confirmed by MS yet and the function of individual ADP-ribose marks is still unknown.

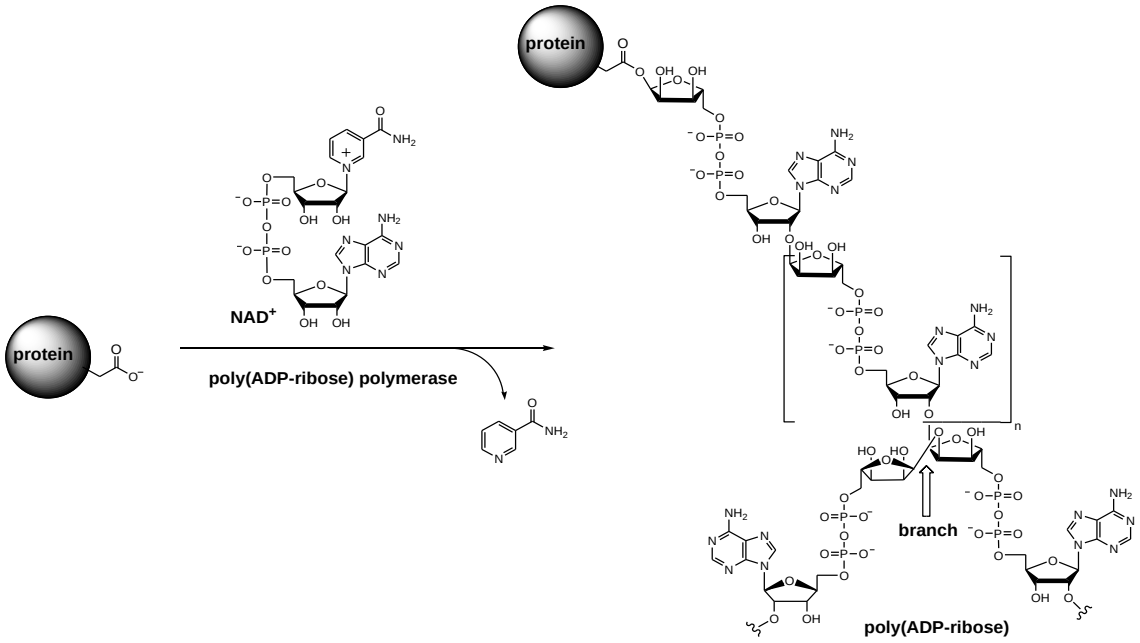

Figure 1.11 Poly(ADP-ribos)ylation. PARPs use NAD^+ as substrate to transfer a single or multiple ADP-ribose moieties on a target protein, leading to mono(ADP-ribos)ylation or poly(ADP-ribos)ylation with linear or branched chains of poly(ADP-ribose).

PARP-1-mediated ADP-ribosylation induces decondensation of higher order chromatin structures by reducing the interactions between nucleosomes and the integration of nucleosomes in chromatin.[164, 165] Based on its polyanionic character (see Figure 1.11), PAR can compete with DNA binding[164] and disrupts histone-DNA interactions.[160, 166] Decompaction of chromatin by PARP-1 activity was demonstrated with purified chromatin fibers *in vitro*.[165] *In vivo,* activation of PARP-1 was found to be responsible for chromatin decondensation in *drosophila* embryos after heat shock.[167] Moreover, PARP-1-mediated poly(ADP-ribos)ylation of H1 enables the histone-to-protamine exchange in spermatids by local chromatin decondensation.[168] Similarly, upon ADP-ribosylation by PARP-1, H1 was found to be released from promoters of genes associated with memory and learning in mouse hippocampus.[169] Besides the PARylation of H1 by PARP-1 promoting the remodeling of polynucleosomes, displacement of H1 from chromatin via competitive binding of PARP-1 was reported.[159, 165] Chromatin immunoprecipitation (ChIP) analysis of breast cancer cells demonstrated a reciprocal binding of H1 and PARP-1 to chromatin, facilitating the enrichment of PAPR-1 at transcriptionally active genes.[170] Despite, PARP-1 is highly activated in response to DNA double strand breaks and PARylation promotes the recruitment of chromatin remodelers containing a macrodomain for the recognition of poly(ADP-ribose) inducing DNA repair [171]. Based on these findings, a histone shuttling model was proposed, in which displaced histones transiently bind to PAR chains subsequent nucleosome eviction. After hydrolysis of PAR chains by Poly(ADP-ribose) glycohydrolase (PARG), histones are readily available for repositioning from the local pool of stabilized histones.[166]

1.4 Tools to modify histones

To correlate a specific PTM or a pattern of PTMs with a distinct biological outcome is one of the greatest challenges in current chromatin research. As depicted above, most of the site-specific PTMs identified in linker histones, could not be linked to a specific function so far, due to a lack in specificity and availability of immunological reagents for H1. Moreover, a major obstacle has been the access to homogeneously modified histones and chromatin. Therefore, new approaches and tools have been developed to decode the histone code. Here, synthetic biology has greatly contributed to the understanding of how histone PTMs modulate chromatin structure and function by the generation of various histones carrying distinct PTMs.

1.4.1 Semisynthetic histone ubiquitylation

Previous synthesis of mono-ubiquitylated histones was limited by the size of ubiquitin as PTM, as is cannot be introduced as a single building block during peptide synthesis. Thus, a key step for the site-specific attachment of full-length Ub to histones was the synthesis of peptide-ubiquitin conjugates facilitating protein ligation-mediated generation of mono-ubiquitylated core histones.[172] First preparation of mono-ubiquitylated full-length H2B was achieved in a semi-synthetic approach in combination with expressed protein ligation (EPL).[173] Here, a synthetic H2B peptide (H2B117-125) with an A117C mutation was equipped with a photolabile protection group and an orthogonal photolytically active auxiliary. In a first auxiliary-mediated ligation with an ubiquitin *α*-thioester, an ubiquitylated H2B fragment was generated by simultaneous photolysis of the protection group. The Ub resulted from expression as intein fusion protein. In a second ligation reaction, recombinant expressed H2B(1-116) thioester was conjugated to the mono-ubiquitylated fragment and subsequent desulfurization resulted in native full-length H2B K120Ub with an overall yield of 20 %. To improve yield and accelerate the synthesis, Ub *α*-thioester with a G76A mutation was directly conjugated to Lys120 of H2B as a cysteine by native chemical ligation (NCL) omitting the auxiliary.[174] The second NCL to complete the H2B sequence and the remaining steps were very similar to the previous strategy. Finally, desulfurization resulted in the ubiquitylated H2B construct with one additional methyl group (H2B K120UbG76A). Another conjugation strategy is based on a disulfide linkage as a replacement for the isopeptide bond.[175] To achieve disulfide-directed histone ubiquitylation, a sulfhydryl group was generated in an intein-mediated transthioesterification with cysteamine at the C terminus of Ub. In this process, a K120C mutation was introduced in the H2B fragment and activated by 2,2'-dithiobis(5-nitropyridine) (DTNP). Conjugation with the Ub thiol generated the disulfide linked analogue of H2B K120Ub. Utilizing this strategy and relocation of the ubiquitin mark on H2B (K108, K116, K125) and H2A (K22) yielded various mono-ubiquitylated histones. Mono-ubiquitylation of H2A was also achieved by exploiting the strategy used to afford H2B K120UbG76A.[176] In this approach, a synthetic H2A peptide containing penicillamine at position 114 was modified with cysteine via an isopeptide bond at Lys119 and ligated to an Ub *α*-thioester. In a penicillamine-mediated ligation reaction, an expressed H2A(1-113)

thioester was conjugated to the mono-ubiquitylated fragment. Subsequent desulfurization converted the penicillamine back into valine, resulting in mono-ubiquitylated H2A at position K119, exhibiting the Ub G76A mutation. However, methods utilizing a combination of SPPS and EPL are often laborious and require sophisticated peptide chemistry. Thereby, the size of the synthetic terminal peptide carrying the PTM is limited by the scope of SPPS. Moreover, traceless EPL depends on the presence of an Ala or Cys at the ligation junction in the sequence of the precursor in order to preserve a native ligation product. Apart from that, no strategy demonstrating ubiquitylation of linker histones was presented so far.

1.4.2 Unnatural amino acids

Several PTMs in histones were sites-specifically introduced by utilizing unnatural amino acids (UAAs). The ability to genetically encode unnatural amino acids facilitated the incorporation of acetyllysine in histone H3[177]. The incorporation of N-*ε*-Boc-N-*ε*-methyl-lysine afforded mono-methylated histone H3 after TFA deprotection[178] whereas the incorporation of N-*ε*-Boc-lysine facilitated installation of dimethyl-lysine upon reductive methylation[179]. Moreover, genetic expansion with phosphoserine was reported[180] and recently used to generate H3 bearing phosphorylated serine[181]. Whereas these modified histones greatly contributed to the research of core histone acetylation, methylation and phosphorylation respectively, incorporated of UAA into H1 is still a challenge. Besides the strategy of amber codon suppression (ACS), which has been exploited for the introduction of PTMs into histones in the mentioned studies, another method termed selective pressure incorporation (SPI) was utilized in this thesis. Both strategies illustrated in the following enable the incorporation of functionalized UAAs, facilitating the modification of the target protein.

Site-specific incorporation by amber codon suppression (ACS)

This method is based on the discovery of the incorporation of the non-canonical amino acids selenocysteine (Sec)[182] and pyrrolysine (Pyl)[183]. Together with the 20 canonical amino acids they represent the 22 proteinogenic amino acids which are genetically encoded and cotranslationally incorporated during protein biosynthesis. In contrast to the canonical amino acids, Sec and Pyl are encoded by stop codons namely opal codon (UGA) and amber codon (UAG) respectively. Pyl is incorporated in *Methanosarcina* species in specific methyltransferases by utilizing a pyrrolysine-tRNA ($tRNA^{Pyl}$) which contains a complementary anticodon to suppress the binding of the release factor (RF) and translates the amber stop codon. Moreover, the corresponding pyrrolysyl-tRNA synthetase (PylRS) is required to charge the $tRNA^{Pyl}$ with pyrrolysine. In order to utilize the suppressor system for recombinant expression in a host organism, it needs to be orthogonal to the endogenous components. In detail, the exogenous aminoacyl-tRNA synthetase (aaRS) specifically aminoacylates the cognate suppressor tRNA with the corresponding (unnatural) amino acid and does not exploit any endogenous tRNAs and amino acids. Furthermore, the exogenous tRNA and (unnatural) amino acid are specific substrates for the orthogonal synthetase, but not for endogenous aaRS. Upon introduction into the host organism, the

orthogonal pair of tRNA/aaRS directs the translational incorporation of amino acid substrates in response to any amber stop codon in the mRNA (Figure 1.12). Thus, enabling site-specific incorporation of unnatural amino acids in bacteria, *Saccharomyces cerevisiae*, mammalian cells, *Caenorhabditis elegans*, *Drosophila melanogaster*, and *Arabidopsis thaliana*.[184]

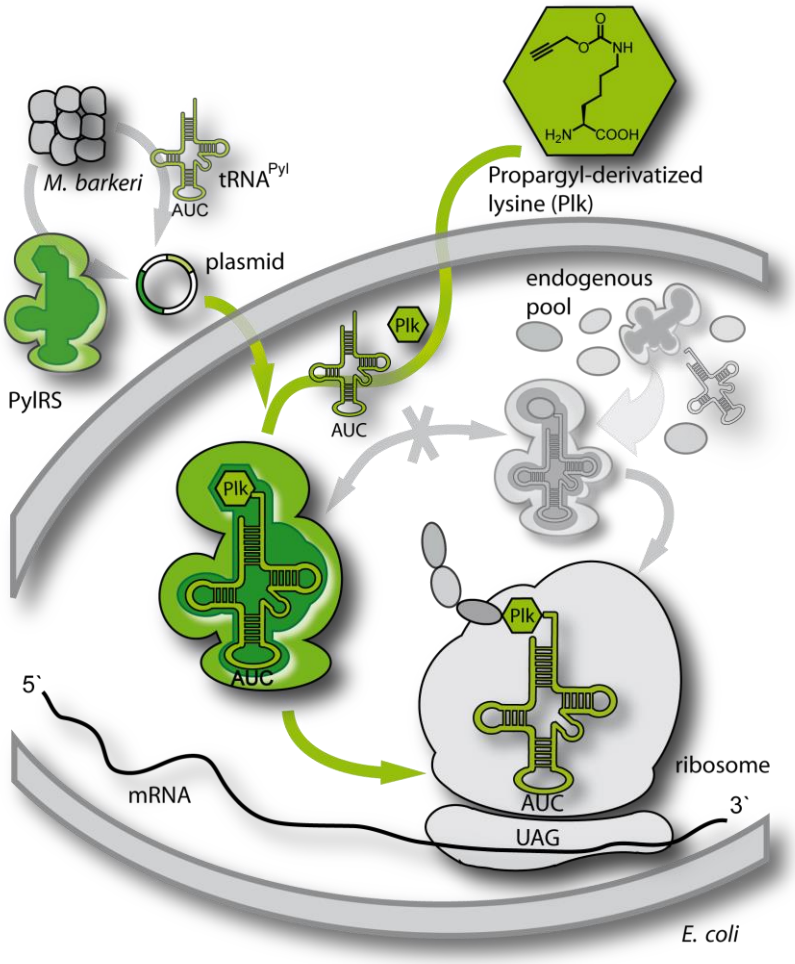

Figure 1.12 Incorporation of Plk by amber codon suppression (ACS). The propargyl-derivatized lysine Plk is incorporated instead at the site of an amber stop codon (UAG) by using the orthogonal pair PylRS/tRNA^{Pyl} from *M. barkeri*. The corresponding open reading frames are expressed from an accessory plasmid. Modified from [185].

By exploiting and engineering the substrate specificity of the orthogonal aaRS, many different UAAs containing a great diversity of functional groups are provided for the incorporation by ACS by now.[184] However, same limitation have to be considered, when this method is applied. The suppressor tRNA competes with the RF for binding at the amber stop codon and thereby with the termination of ribosomal translation, resulting in lowered yields of target protein, especially when multiple amber stop codons are suppressed. To circumvent this restriction, RF1-deficient *E. coli* strains, which have decreased competition of ACS and translational termination at the amber stop codon, were generated.[186] However, the suppression efficiency of the amber stop codon additionally depends on the sequence context in which the amber codon is introduced,[187] favoring ACS for the introduction of single point mutations.

Residue-specific incorporation by selective pressure incorporation (SPI)

Residue specific incorporation is based on the substrate tolerance of the endogenous aaRS. Endogenous aaRS are able to distinguish between particular endogenous amino acids, but not between endogenous and unnatural analogues.[188] Thus, UAAs which are electronically and structurally similar to their natural archetype - like Azidohomoalanine, an unnatural analogue of methionine - are tolerated by the native aaRS and loaded onto the native tRNA for subsequent translation, when the archetype is absent (Figure 1.13).[189, 190] To withdraw the desired canonical amino acid, auxotroph host cells were used. These cells, unable of synthesizing the desired canonical amino acid are cultured in minimal medium containing a limited amount of the canonical amino acid. After consumption, the medium is supplemented with the UAA analogue and expression is induced. Without the canonical amino acid present, the endogenous translation apparatus of the auxotroph cells utilizes the exogenous UAA for incorporation in response to the sense codon of the withdrawn canonical amino acid. Thereby, the canonical amino acids is replaced by its unnatural analogue proteome-wide.[191]

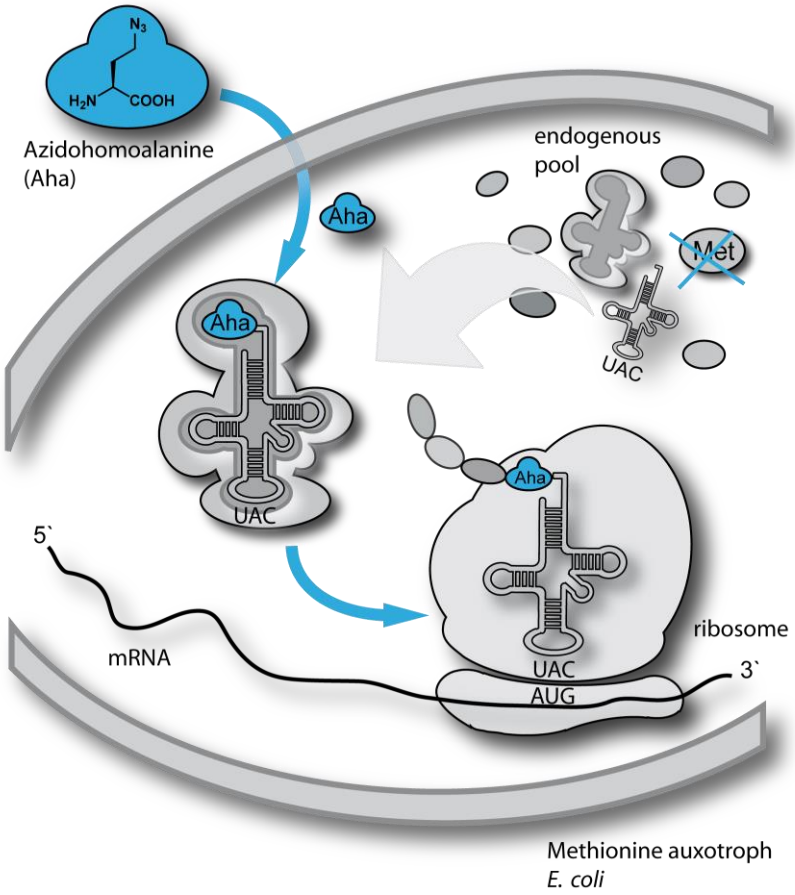

Figure 1.13 Incorporation of Azidohomoalanine (Aha) by selective pressure incorporation (SPI). The gene of interest is expressed in methionine auxotroph *E. coli* cells. Instead of methionine, the culture medium contains Aha, which is utilized by the endogenous aaRS and tRNA in thus incorporated instead of methionine into the proteome. Modified from [185].

Although this can lead to significant decrease in cell growth, the existing translational machinery allows further gene expression, resulting in yields of modified protein comparable to the wild-type.[189] In contrast to ACS, the incorporation of UAAs by SPI at multiple sites within a protein of interest is convenient and no genetic manipulation is required. However, the scope of UAAs applicable in SPI is rather limited due to the fact that UAAs need to correlate with the substrate tolerance of the endogenous aaRS.

By usage of ACS and SPI a variety of reactive functional groups can be installed into the target protein. The incorporation of the azide group and the alkyne group into proteins in the form of UAAs enables the distinct modification of the target protein in subsequent bioorthogonal reactions (e.g. click reaction).

1.4.3 Click reaction

Since its discovery in 2002,[192, 193] the Cu(I)-catalyzed azide-alkyne cycloaddition (CuAAC), has been extensively applied in many different biological studies and is now termed as “the click reaction”[194]. It is a variant of the Huisgen 1,3-dipolar cycloaddition, which was described for the first time more than 50 years ago[195]. Here, an alkyne reacts with an azide under high pressure and temperature to form a stable 1,2,3-triazole as a mixture of two regioisomers. In contrast, the Cu(I)-catalyzed variant is characterized by rapid reaction kinetics under mild conditions, excellent reliability and chemoselectivity, affording predominantly 1,4-disubstitued 1,2,3 triazoles (Figure 1.14).

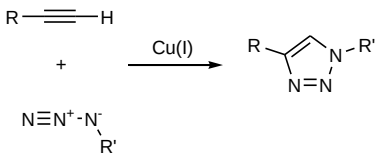

Figure 1.14 CuAAC. An alkyne reacts with and azide under physiological conditions in a Cu(I)-catalyzed cycloaddition to form a 1,4-disubstitued 1,2,3-triazole.

The CuAAC proceeds fast in aquatic solutions, and used functional groups that are stable in physiological conditions, without reacting with other functionalities present in proteins and cells. Thus, CuAAC seems ideally suited for protein modification and numerous reaction conditions have been presented[185, 196-198]. Polytriazoles such as tris-(benzyltriazolylmethyl)amine (TBTA) or tris-(hydroxypropyltriazolylmethyl)amine (THPTA) have been identified as powerful Cu(I)-stabilizing ligands enhancing the catalytic activity of Cu(I) and thereby accelerating the reaction.[199] Moreover, stabilizing Cu(I) species prevents oxidative damage of proteins under aerobic conditions.

In this thesis, the combination of ACS- and SPI-mediated incorporation of UAAs bearing an azide and an alkyne with CuAAC was applied as a tool to generate site-specifically modified linker histones.

2 Aim of this thesis

The aim of this thesis was the synthesis of site-specifically mono-ubiquitylated linker histones and the investigation of their functional properties. For the synthesis of mono-ubiquitylated linker histone H1.2 by click reaction, two unnatural amino acids, one bearing an alkyne the other bearing an azide, should be incorporated into H1.2 and Ub, respectively. The site-specific incorporation of the alkyne functionalized Plk at different positions in H1.2 should be conducted by amber codon suppression (ACS). For this purpose, the recombinant expression and the purification of H1.2 should be established and adapted for ACS. In contrast, the azide group at the C terminus in Ub should be introduced by Azidohomoalanine (Aha) via selective pressure incorporation (SPI).

Thereafter, the Plk-equipped linker histones should be modified with Ub Aha in click reactions, focusing on optimized reaction efficiency and solubility, before H1.2-Ub conjugates should be purified and further characterized. Finally, mono-ubiquitylated H1.2 should be used to assemble chromatosomes and to investigate their characteristics as acceptors for different PTMs in studies with histone modifying enzymes *in vitro* as well as within a complex biological system.

3 Results and discussion

3.1 Site-specific ubiquitylation of linker histones by click reaction

3.1.1 Introduction

So far, the generation of homogeneously mono-ubiquitylated H1, was hampered by the fact, that site-specific H1-dependent E3 ligases are not identified. Moreover, histone-modifying enzymes suffer from low enzymatic activity and target multiple residues on the target leading to high heterogeneity. Thus, an enzymatic *in vitro* synthesis of defined H1-Ub conjugates is not feasible. Furthermore, extraction of H1 from cellular samples yields histones with heterogeneous PTM patterns, which are inappropriate for systematic functional studies. In addition, (mono-)ubiquitylated histones derived from natural sources display an isopeptide bond, which is easily cleaved by DUBs in cellular extracts, limiting their scope of application.

To circumvent this limitation, mono-ubiquitylation of different acceptor proteins was successfully performed by click reactions in our group utilizing azide-functionalized ubiquitin and alkyne-functionalized acceptor proteins, resulting in a non-hydrolysable linkage. Along these lines, site-specific mono-ubiquitylation of PCNA[196], DNA polymerase beta[198] and the formation of linkage-specific Ub dimers[197] as well as Ub chains[200] was achieved, demonstrating the high potential of this versatile strategy. In order to gain access to defined and site-specifically mono-ubiquitylated linker histones, recombinant expression in *E. coli* is advantageous, providing linker histones that are devoid of PTMs, thereby representing clean templates for further modifications and studies. At the same time, it allows the incorporation of UAAs to generate a site-specifically functionalized template for subsequent mono-ubiquitylation by CuAAC.

Among the numerous ubiquitylation sites identified in H1.2 by MS analysis in proteome-wide studies, multiple sites are located at the GD (see Figure 1.10), which interacts with the nucleosome by structure specific recognition[4, 54]. However, none of the ubiquitylation sites could be linked to a specific function or related to a certain biological process so far. To investigate possible effects of mono-ubiquitylation in the GD over a wide range, modification sites at different spacial locations within the GD were chosen to be modified (Figure 3.1). Interestingly, four of these sites were found to be ubiquitylated in all three studies (see Figure 1.10).[154-156] Thus, in the context of this thesis, these acceptor sites K46, K64, K75 and K97 in H1.2 were subjected to mono-ubiquitylation by click reaction.

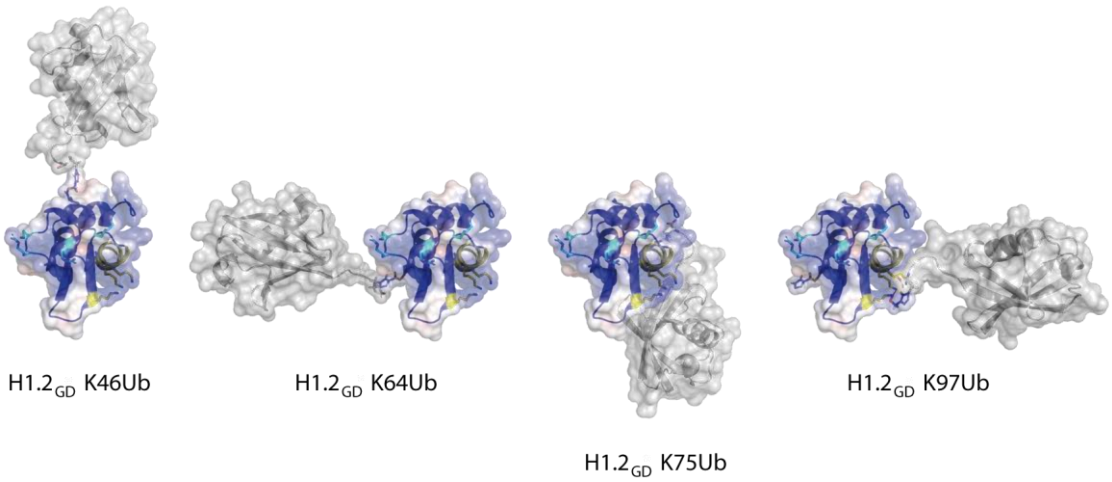

Figure 3.1 Different spatial location of Ub in H1.2-Ub conjugates. Models are shown for Ub attached at position K46, K64, K75 or K97 in the GD of H1.2 ($H1.2_{GD}$). For visualization, corresponding sites in the structure of cH1 (blue, PDB: 1HST) were replaced by Plk and the triazole linkage as well as Ub (grey, PDB: 1UBQ) G76Aha were manually modeled into the conjugate's structure. Kindly provided by Dr. Samra Ludmann.

3.1.2 Establishing the expression and purification of H1.2

In order to generate sufficient amounts of the linker histone variant H1.2 a variety of expression constructs were cloned and expression level in *E. coli* was analyzed by SDS-PAGE. Initially, the gene of wild-type H1.2 (H1.2 WT) without any tag was subcloned from the synthesized and codon optimzied construct into pET11a and transformed into *E. coli* BL21 (DE3). For identification of optimal expression conditions, cells were grown at 20 °C or 37 °C. After induction, samples of the cultures were taken at various time points (1–18 h). Due to the low recombinant expression level, H1.2 WT could not be observed when cell lysates were analyzed on Coomassie stained SDS-PAGE gels (data not shown). Therefore, H1.2 WT was enriched by perchloric acid (PCA) extraction of lysed cells prior to analysis by SDS-PAGE. As shown in Figure 3.2, highest expression levels were observed after 4 h and 18 h of expression at 37 °C. Compared to 18 h of expression, the 4 h sample contained less impurities. To further purify the PCA extracted H1.2 WT, fast protein liquid chromatography (FPLC) assisted ion exchange chromatography (IEX) was performed and elution fractions containing H1.2 WT were analyzed by SDS-PAGE (Figure 3.2). Here, significant amounts of truncated H1.2 WT were still present in all elution fractions.

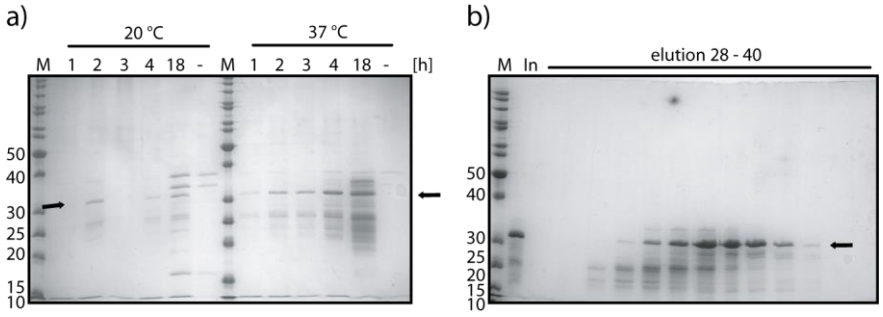

Figure 3.2 Expression and purification of untagged H1.2 WT. a) SDS-PAGE gel of PCA extracted H1.2 WT, after 1– 18 h of expression at 20 °C and 37 °C. Full-length H1.2 WT is indicated by black arrows. b) SDS-PAGE gel of elution fractions from ion exchange chromatography. M: Marker [kDa], In: Input.

To improve the purity of H1.2 WT and simplify the purification process, C-terminal affinity tags were fused to the expression construct. This strategy enables the enrichment of full-length proteins by preventing binding of truncated H1.2 during affinity based purification, what became even more important later in this work in the context of amber codon suppression (see chapter 3.1.3). Three expression constructs, modified by two different affinity tags of small size were generated by PCR. On the one hand, the *Strep*-tag which is biologically inert was added for purification under physiological conditions. For purification under denaturating conditions (urea, 6 M), a hexahistidine (His)-tag was inserted. Besides two single-tagged constructs, a double-tagged fusion protein bearing both tags was constructed (Figure 3.3a), aiming for highest purity. The C-terminal-tagged H1.2 WT constructs were cloned into the multiple cloning site of pET11a-tRNA^{Pyl}. The resulting plasmids were transformed into *E. coli* BL21(DE3). After expression, cells were lysed by sonication and inclusion bodies were isolated. The subsequent purification strategy depended on the affinity tag (Figure 3.3b). Recombinant H1.2 was extracted from inclusion bodies by treatment with 0.83 M PCA or under denaturating conditions

with 6 M urea. PCA-extracts needed to be neutralized before binding to the affinity matrix. Denatured H1.2, extracted with urea was directly applied to immobilized metal ion affinity chromatography (IMAC) but dialyzed prior to *Strep*-Tactin affinity chromatography.

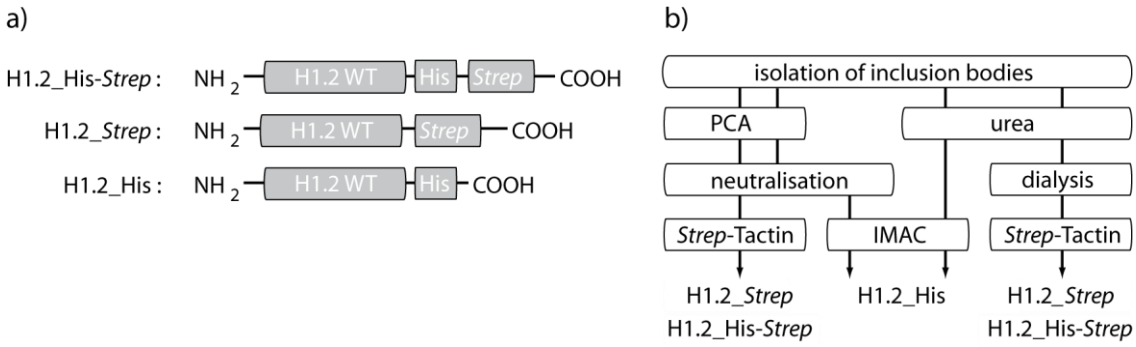

Figure 3.3 H1.2 with C-terminal affinity tags. a) Expression constructs. b) Purification strategies for *Strep*-tagged H1.2, His-tagged H1.2 and His-*Strep*-tagged H1.2 under native (PCA) and denaturating (urea) conditions.

After elution form the affinity matrix, elution fractions were analyzed by SDS-PAGE, pooled and dialyzed in water to refold H1.2 (Figure 3.4). For all constructs, treatment of inclusion bodies with PCA (Figure 3.4a, c and e), resulted in extracts containing less impurities but also decreased the yield of H1.2 (~30 % lower) compared to urea extracts (Figure 3.4b, d and f), clearly demonstrated for His-tagged H1.2; Figure 3.4e versus Figure 3.4f. Moreover, the stability of PCA extracted H1.2, in particular when combined with *Strep*-Tactin affinity chromatography was found to be impaired when H1.2 was stored at 4 °C. Initially, H1.2 constructs purified by IMAC showed a higher level of impurity compared to *Strep*-Tactin purified H1.2 caused by proteins binding unspecific to the matrix (data not shown). After optimizing the IMAC procedure by including imidazole in the binding step followed by additional washing steps with increasing imidazole concentration, His-tagged H1.2 was obtained in almost the same purity like *Strep*-tagged H1.2. Regarding the constructs, the finale yields of double-tagged H1.2 (0.35 mg l^{-1}) and *Strep*-tagged H1.2 (0.5 mg l^{-1}) were significantly lower than that of His-tagged H1.2 (5 mg l^{-1}).

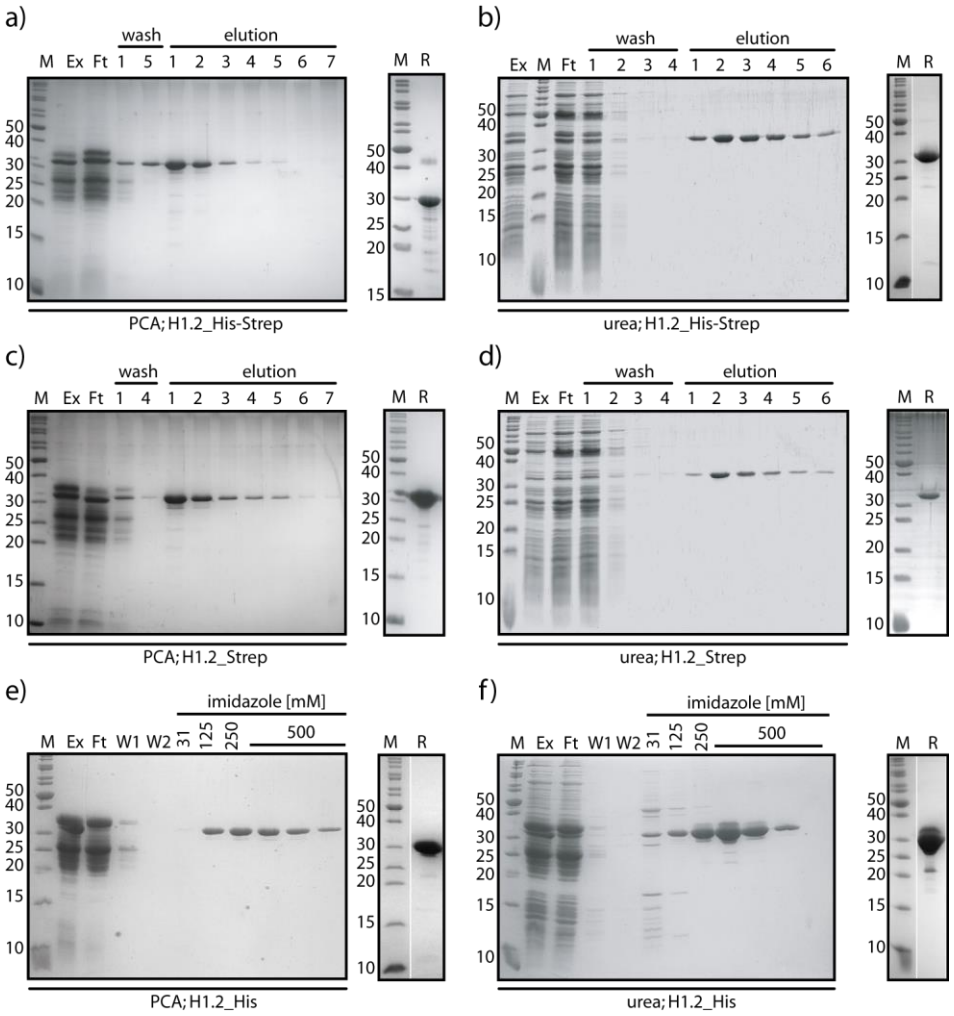

Figure 3.4 Purification of affinity-tagged H1.2 WT analyzed by SDS-PAGE. a) *Strep*-Tactin affinity chromatography of PCA extracted H1.2_His-*Strep* (left) and refolded H1.2_His-*Strep* (right). b) *Strep*-Tactin affinity chromatography of urea extracted H1.2_His-*Strep* (left) and refolded H1.2_His-*Strep* (right). c) *Strep*-Tactin affinity chromatography of PCA extracted H1.2_*Strep* (left) and refolded H1.2_*Strep* (left). d) *Strep*-Tactin affinity chromatography of urea extracted H1.2_*Strep* (left) and refolded H1.2_*Strep* (right). e) IMAC of PCA extracted H1.2_His (left) and refolded H1.2_His (right). f) IMAC of urea extracted H1.2_His (left) and refolded H1.2_His (right). M: Marker [kDa], Ex: Extract, Ft: Flow through, W: Wash fraction, R: Refolded fraction.

To analyze if all H1.2 constructs were expressed correctly and full-length protein was purified, electrospray-ionization mass spectrometry (ESI-MS) was performed (Figure 3.5a-c). It turned out, that all the determined masses correspond well to the calculated masses of the respective full-length protein.

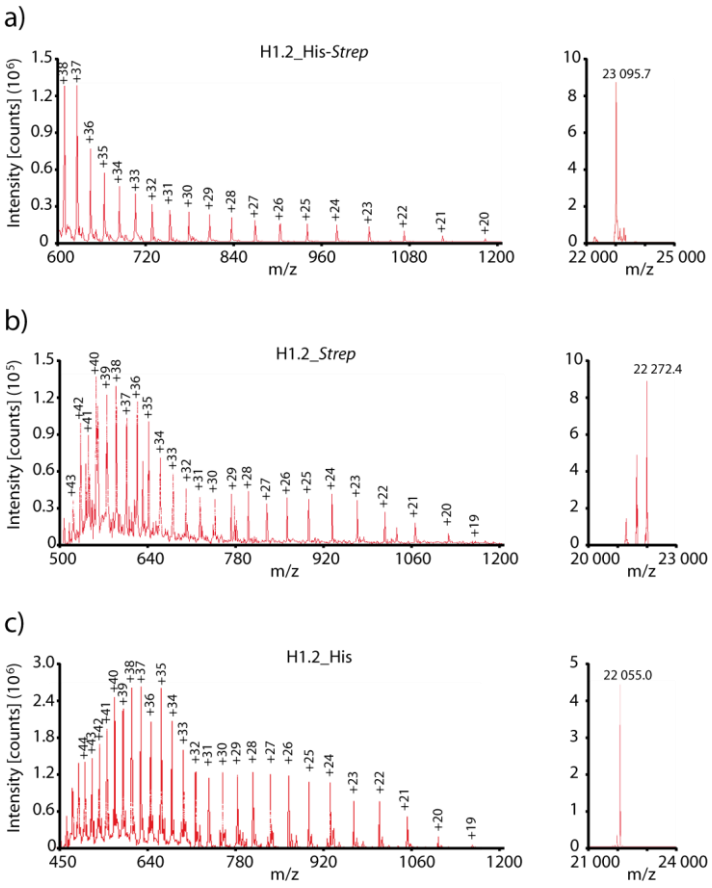

Figure 3.5 ESI-MS and deconvoluted MS-spectra of a) H1.2_His-*Strep* (calcd 23 096.6 Da), b) H1.2_*Strep* (calcd 22 273.7 Da) and c) H1.2_His (calcd 22 056.4 Da)

3.1.3 Incorporation of Plk into H1.2

To modify H1.2 with Ub G76Aha site-selectively at position K46, K64, K75 or K97 in a click reaction, acceptor sites of H1.2 had to be replaced by Plk, a propargyl-functionalized lysine derivative providing the alkyne-functionality. By using the pyrrolysyl-tRNA synthetase (PylRS)/pyrrolysine tRNA ($tRNA^{Pyl}$) pair from *Methanosarcina barkeri* for amber codon suppression (ACS) Plk can be incorporated site-specifically. Based on the findings for expression and purification of H1.2 WT, same tag and purification strategies were tested for the incorporation of Plk at position K46. To do so, the codon of K46 in the H1.2 WT sequence of His-, *Strep* and the double-tagged construct was mutated to the amber stop codon TAG. After co-transformation of the respective plasmid together with pRSFduet-1/PylRS providing the PylRS into *E. coli* BL21 (DE3), LB medium was supplemented with Plk (1.5 mM final concentration) and expression was performed. Plk-modified H1.2 was extracted by PCA or urea from inclusion bodies and purified by IMAC or *Strep*-Tactin affinity chromatography as described for H1.2 WT (Figure 3.6). In case of Plk incorporation, both *Strep*-tagged constructs showed low expression, result-

ing in very low yields (>0.1 mg l^{-1}) after affinity chromatography (Figure 3.6a-d). Similar to the results obtained for the wild-type constructs, highest yield of H1.2 K46Plk was observed for the His-tagged fusion protein (0.6–0.8 mg l^{-1}) (Figure 3.6e and f). Here, urea extraction of inclusion bodies increased yields by 60 % and resulted in a purer H1.2 K46Plk protein, compared to PCA extracted mutant.

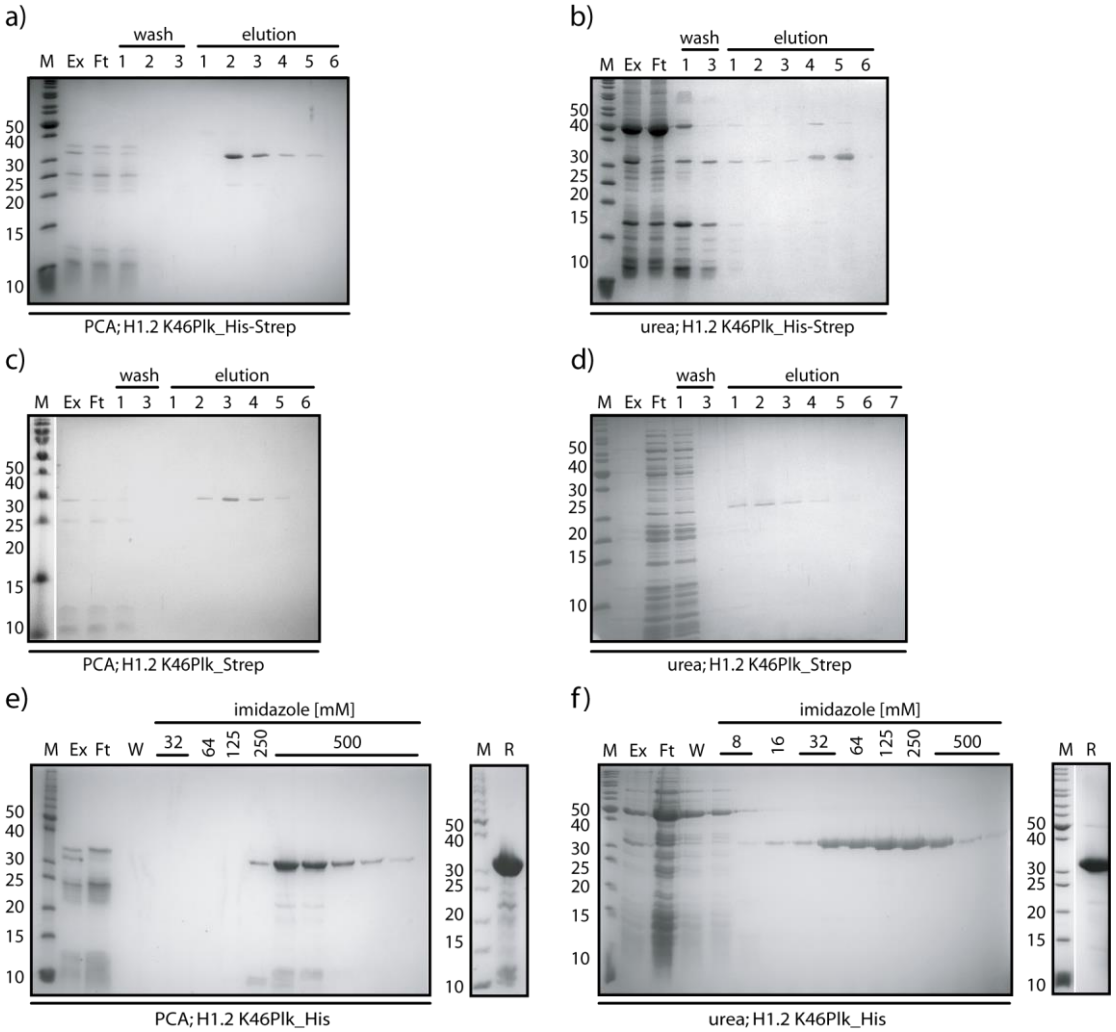

Figure 3.6 Purification of affinity-tagged H1.2 K46Plk analyzed by SDS-PAGE. a) *Strep*-Tactin affinity chromatography of PCA extracted H1.2 K46Plk_His-*Strep*. b) *Strep*-Tactin affinity chromatography of urea extracted H1.2 K46Plk_His-*Strep* (left). c) *Strep*-Tactin affinity chromatography of PCA extracted H1.2 K46Plk_*Strep*. d) *Strep*-Tactin affinity chromatography of urea extracted H1.2 K46Plk_*Strep*. e) IMAC of PCA extracted H1.2 K46Plk_His (left) and refolded H1.2 K46Plk_His (right). f) IMAC of urea extracted H1.2 K46Plk_His (left) and refolded H1.2 K46Plk_His (right). M: Marker [kDa], Ex: Extract, Ft: Flow through, W: Wash fraction, R: Refolded fraction.

Thus, pending H1.2 Plk mutants were generated as His-tagged fusion proteins and purified under denaturating conditions. In the following these His-tagged H1.2 Plk mutants were referred to as H1.2 Plk (Figure 3.7a). For this purpose, K64, K75 and K97 were separately mutated to the amber stop codon TAG in pET11a-tRNA^{Pyl}/H1.2 WT_His construct (Figure 3.7b). For expression these constructs were co-transformed with pRSFduet-1/PylRS into *E. coli* BL21(DE3). Following the established expression and purification procedure, all four Plk-equipped H1.2 mutants were obtained in high purity (Figure 3.7c) and with yields of 0.7–1.0 mg l^{-1}. Incorporation of Plk was confirmed by ESI-MS (Figure 3.7d). Differences in mass of ~82.5 Da between the wild-type and Plk mutants corresponded to the replacement of lysine by Plk.

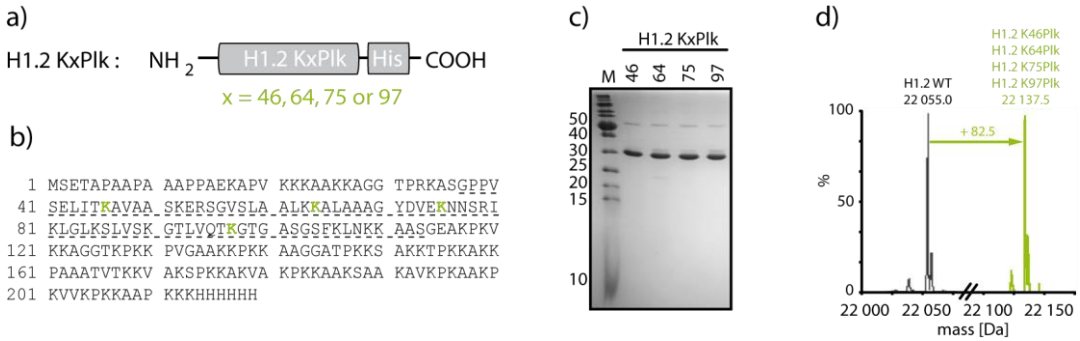

Figure 3.7 H1.2 Plk mutants. a) Construct of His-tagged fusion protein for the incorporation of Plk into H1.2. b) Amino acid sequence of H1.2 WT_His with globular domain indicated (dashed line). K46, K64, K75 and K97 (green) were replaced by Plk in ACS. c) SDS-PA gel of refolded H1.2 Plk mutants. x: position of Plk incorporation, M: Marker [kDa]. d) Deconvoluted mass spectra of H1.2 WT (22056.4 Da) and averaged H1.2 Plk mutants (calcd 22138.4 Da).

As shown in Figure 3.8a all lysines that were replaced by Plk are located at different spatial regions in the globular domain of H1.2. To investigate whether the global conformation of H1.2 is altered by the incorporation of Plk, CD spectroscopy of H1.2 WT and H1.2 Plk mutants was performed. Moreover, commercially available H1 mixture, purified from calf thymus under native conditions was included as positive control in this study, to verify prober refolding of recombinant H1.2 after purification under denaturating conditions of the recombinant H1.2 proteins (Figure 3.8b). As shown in Figure 3.8c H1.2 WT exhibited CD spectra between 190–250 nm similar to the native (n)H1, indicating correct refolding of H1.2 WT. The measured CD spectra very well correspond to the data described before characterized by a negative peak at 200 nm[201]. In case of Plk incorporation, all mutants showed very similar CD spectra were the local minima at 200 nm is diminished compared to H1.2 WT, indicating a decreased content of random coil. The slightly lower ellipticity of nH1 at 200 nm might simply reflect the micro-heterogeneous nature of the nH1 sample obviously containing a mixture of H1 variants (Figure 3.8b). However, ellipticity at 222 nm characterizing alpha helices stayed the same in all samples, excluding structural changes in the globular domain, containing three alpha helices (Figure 3.8a).

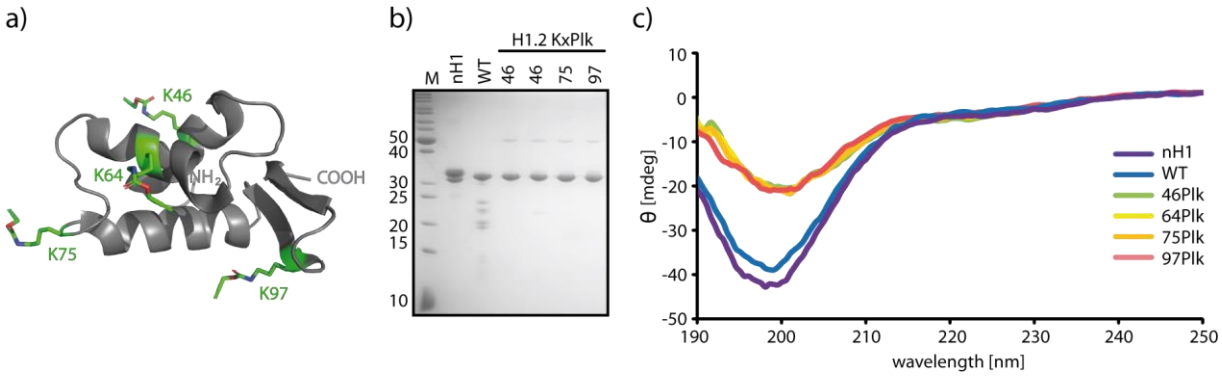

Figure 3.8 Folding analysis of H1.2 Plk mutants. a) Globular domain of cH1 (PDB: 1GHC) with indicated sites of Plk incorporation (green). Lysines were mapped to the corresponding residues in cH1. b) SDS-PA gel of samples used for CD spectroscopy: Native histone H1 mixture derived from calf thymus (nH1), refolded H1.2 WT and refolded H1.2 Plk mutants. c) CD spectra of native H1, refolded H1.2 WT and refolded H1.2 Plk mutants (11 µM in ddH_2O).

3.1.4 Click reaction with an azide-modified fluorescent dye

In order to verify the reactivity of the alkyne group in H1.2 Plk, its selective labelling in a click reaction with an azide-modified fluorescent dye (Figure 3.9a) was performed. H1.2 Plk was incubated with a 10–100 fold molar excess of sulfo-Cy5-azide, TCEP, TBTA and $CuSO_4$ under argon at room temperature for 1 hour. Samples were applied to SDS-PAGE and Cy5 was visualized in the SDS-PA gel by fluorescence detection prior to Coomassie staining. As shown in Figure 3.9b for H1.2 K46Plk, exclusively H1.2 with Plk incorporated is labelled with sulfo-Cy5-azide. While the fluorescent signal increases with the Cy5 amount added, no fluorescent signal was detected in case of H1.2 WT. This experiment also shows, that the incorporated Plk is exposed to the proteins surface being accessible for modification.

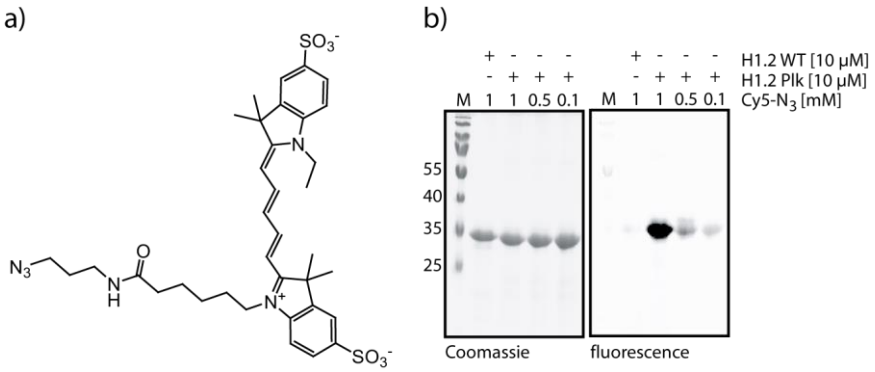

Figure 3.9 Click reaction with sulfo-Cy5-azide. a) Sulfo-Cy5-azide. b) SDS-PA gel of click reaction between H1.2 K46Plk and sulfo-Cy5-azide (Cy5-N_3) after Coomassie staining (left) and fluorescent image (right).

3.1.5 Incorporation of Aha into ubiquitin

Cloning of Ub G76M was accomplished by Daniel Schneider.

To link Ub site-selectively to H1.2 Plk by click reaction, an azide functionality had to be introduced to the C terminus of Ub. To install this bioorthogonal group, the Met analog Azidohomoalanine (Aha) was used. The incorporation of this unnatural amino acid into Ub is achieved by selective pressure incorporation (SPI). Here, the Met analogue incorporated at position 1 of Ub (note that Ub does not contain any other Met) by SPI needed to be removed to ensure site-selective conjugation via the C terminus of Ub Aha in click reactions. To achieve a single, site-specific incorporation of the azide functionality, an expression construct was used in which the N-terminal methionine codon of Ub is deleted and the C-terminal glycine codon is replaced by a methionine codon. This Ub variant was fused to the C terminus of a thrombin cleavage sequence and glutathione-S-transferase (GST) for expression and purification. Thrombin cleavage of the fusion protein resulted in Ub G76Aha, containing a short N-terminal extension (Figure 3.10a).[198]

The described Ub construct was expressed in Met auxotroph *E. coli* B834(DE3). Cells were cultured in New minimal medium (NMM) under limiting Met concentration until stationary growth was reached. The medium was then exchanged by fresh NMM supplemented with Aha and protein expression was induced with IPTG. After cell harvest, resuspension and lysis, the clarified cell lysate was applied to a GST affinity matrix, followed by washing with 1x PBS. Then, thrombin cleavage was performed and Ub G76Aha was eluted by washing with 1x PBS (Figure 3.10b). By this procedure, ~4–6 mg l^{-1} Ub G76Aha were obtained.

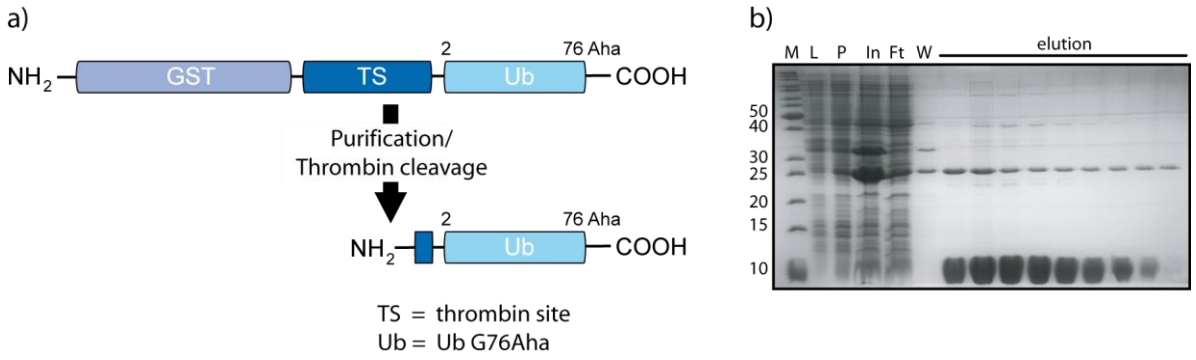

Figure 3.10 Expression of Ub as GST-fusion protein and purification of Ub G76Aha. a) Scheme of Ub G76Aha as GST fusion protein; the final purification step by thrombin cleavage yields ubiquitin with only one Aha. Modified from [185]. b) SDS-PAGE analysis of purification of Ub G76Aha. M: Marker [kDa], L: Lysed cells, P: Pellet, In: Input, Ft: Flow through, W: Wash.

To analyze if Met was quantitatively replaced by Aha and to confirm complete thrombin cleavage resulting in Ub G76Aha containing only the Aha at the C terminus (Figure 3.11a), ESI-MS of purified Ub G76Aha (Figure 3.11b) was conducted. It turned out, that the determined mass (Figure 3.11c) corresponds well to the calculated mass of the cleaved protein, verifying the incorporation and presence of a single Aha in Ub G76Aha.

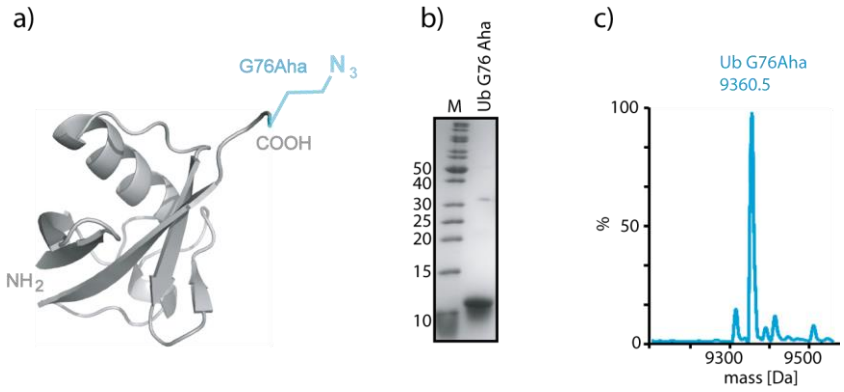

Figure 3.11 Incorporation of Aha into Ub. a) Scheme of Ub G76Aha. b) SDS-PA gel of purified Ub G76Aha. c) Deconvoluted ESI-MS spectrum of thrombin-cleaved Ub G76Aha (calcd 9630.6 Da). Adapted by permission from [198]. Copyright © 2013 Elsevier

With the Aha modified Ub and the Plk equipped histone H1.2 mutants in hand, conjugation of both functionalities in a click reaction generating site selective, mono ubiquitylated linker histone H1.2 was investigated.

3.1.6 Optimizing the reaction efficiency

After successful conjugation of H1.2 Plk by click reaction with an azide-functionalized dye (3.1.4), generation of mono-ubiquitylated H1.2 was investigated. Here, the azide-modified Ub G76Aha was used. Initial experiments, applying the reaction conditions used for Cy5-azide labeling yielded no conjugation of H1.2 Plk. Therefore, reaction parameters including Cu(I) sources, reducing agents, Cu(I) ligands and protein concentrations were varied. Finally, an up to six-fold excess of Ub G76Aha was mixed with 10 µM H1.2 (WT or K46Plk), Cu(I) complex and THPTA. After incubation under argon atmosphere for one hour on ice, samples were separated by SDS-PAGE and Coomassie stained. Here, the reaction yield remained at a maximum of ~50 %, as determined by a new band on SDS-PA gel at about 40 kDa in comparison to the unmodified H1.2 Plk with a molecular mass of ~32 kDa (Figure 3.12a). As expected, conjugation with Ub G76Aha proofed to be selective for incorporated Plk and depends on Cu(I), leaving H1.2 WT unmodified as well as H1.2 Plk in the absence of Cu(I) (Figure 3.12a). As previous studies with DNA polymerase beta suggested that the click reaction between Ub and target proteins is positively influenced by addition of SDS[185, 198], the reaction efficiency for H1.2 was tested upon addition of different surfactants. Click reactions were prepared as described above, containing 10 µM H1.2 46Plk and a six-fold excess of Ub G76Aha and samples were analyzed by SDS-PAGE (Figure 3.12b-d). Whereas no effect on click reaction efficiency was observed by addi-

tion of Triton and Tween (Figure 3.12b), n-Lauroylsarcosine (n-LS) and SDS significantly increased product formation. Concentrations of 1.0 mM n-LS or higher yielded in up to 90 % conversion of H1.2 Plk (Figure 3.12c). Almost complete conjugation of all H1.2 variants to their mono-ubiquitylated forms was achieved, when supplementing the click reaction with SDS concentrations of 0.5 mM (Figure 3.12d).

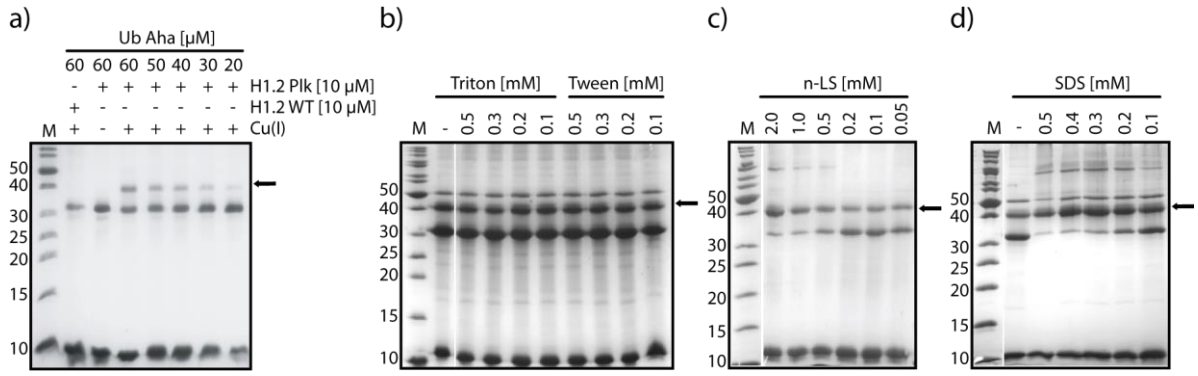

Figure 3.12 SDS-PAGE analysis of effects of surfactants on click reaction of Ub G76Aha and H1.2 Plk. a) Mono-ubiquitylation of H1.2 Plk by varying Ub G76Aha concentrations. b) Click reactions supplemented with Triton X-100 or Tween. c) Click reactions with n-Lauroylsarcosine (n-LS). d) Click reactions with SDS. M: Marker [kDa], black arrows indicate mono-ubiquitylated H1.2.

In the next step, Ub G76Aha titration in different buffer conditions was carried out to identify suitable buffers supporting minimal concentration of Ub G76Aha needed for complete conjugation of H1.2 Plk. In this context, three different buffer conditions, Tris-HCl (50 mM, pH 8.0), sodium acetate (NaOAc, 50 mM, pH 5.0) and phosphate buffered saline (PBS, 1x, pH 7.4) were investigated in click reactions carried out as described before. As shown in Figure 3.13a lowest concentration of Ub G76Aha was required in a NaOAc-buffered click reaction with 30 µM resulting in complete conjugation of H1.2 Plk. In case of Tris-HCl-buffered reaction, 60 µM Ub G76Aha led to similar results. Interestingly, without SDS supplementation of the NaOAc-buffered click reaction only minor conjugation was observed. In the presence of PBS a concentration of Ub G76Aha higher than 50 µM was needed for a quantitative conversion. However, the formation of a byproduct with a molecular mass of ~35 kDa was observed with increasing Ub G76Aha concentration. Thus, following click reactions were performed in a NaOAc-buffered solution, in order to facilitate isolation of mono-ubiquitylated H1.2 in subsequent purification and to save Ub G76Aha.

In order to reduce Cu(I)-mediated generation of reactive oxygen species (ROS),[202] the concentration of the Cu(I) complex was adjusted in a second titration step. Click reactions were prepared by adding different amounts of Cu(I) complex together with two equivalents THPTA and processed as before. The Coomassie stained gel in Figure 3.13b, indicates a minimum concentration of Cu(I) complex of 2.5 mM is required for efficient conjugation.

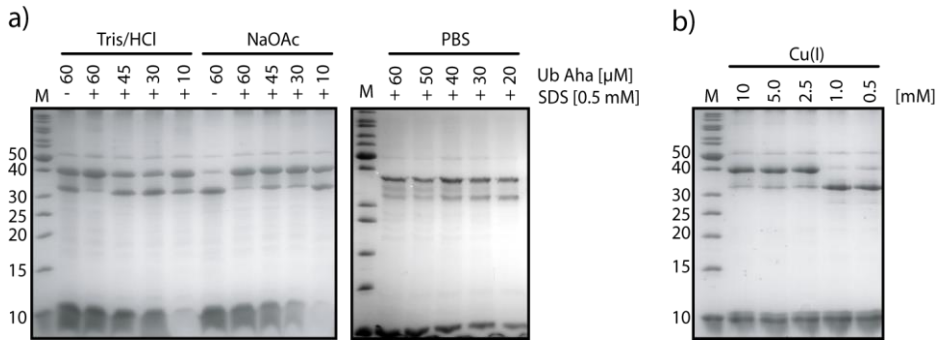

Figure 3.13 SDS-PAGE analysis of buffer and Cu(I) effects on click reaction of Ub G76Aha and H1.2 K46Plk. a) Click reactions with varying Ub G76Aha concentrations, in the presence of Tris-HCl (50 mM, pH 8.0), sodium acetate (NaOAc, 50 mM, pH 5.0) or phosphate buffered saline (PBS, 1x, pH 7.4) respectively. c) Titration of Cu(I) complex. Click reaction was performed with 10 µM H1.2K64Plk and 0.5 mM SDS. M: Marker [kDa].

Finally, the influence of the reaction temperature on H1.2 K46Plk conjugation was investigated, to prevent precipitation and degradation of H1.2 Plk caused by extensive exposure to Cu(I) complex and SDS at room temperature. Click reaction were prepared as described before and incubated at room temperature or on ice. Samples were taken at the indicated time points, immediately mixed with SDS-PAGE sample buffer and heated to 95°C to stop the conjugation reaction (Figure 3.14). For both temperatures tested, already 1 min after addition of Cu(I) complex significant conjugation of H1.2 K46Plk was observed. Depending on the protein batch, a reaction time of 30–45 minutes was sufficient for a quantitative conjugation at 0 °C.

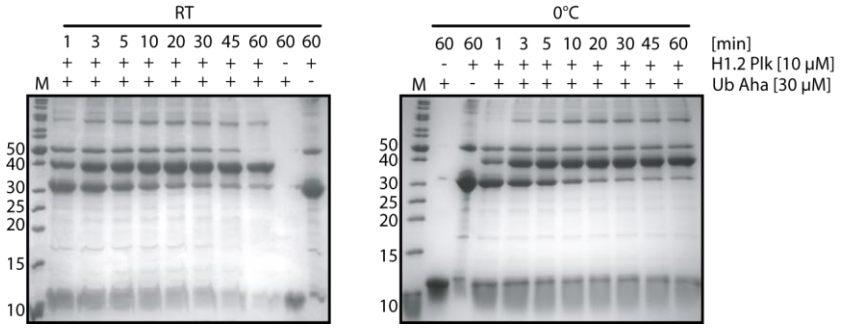

Figure 3.14 Influence of reaction time and -temperature on click reaction between Ub G76Aha and H1.2 K46Plk analyzed by SDS-PAGE. Click reaction was performed at room temperature (RT) or 0 °C for 1–60 min with 0.5 mM SDS. Signals at a molecular mass of 50 kDa are impurities derived from H1.2 K46Plk preparation. M: Marker [kDa].

After optimization of the conjugation parameters resulted in the efficient mono-ubiquitylation of H1.2 at position K46 by click reaction, this approach was expanded to the other three H1.2 Plk mutants. By applying the adjusted reaction conditions, Ub G76Aha was successfully conjugated to position K64Plk, K75Plk and K97Plk respectively in H1.2 (Figure 3.15). All Plk mutants exhibit similar properties in click reaction, reaching >95 % of conjugation after 30 min. These results are in line with previous findings, when reaction conditions were analyzed with H1.2 Plk mutants other than H1.2 K46Plk (data not shown), demonstrating the accessibility of the incorporated Plk in all examined H1.2 mutants.

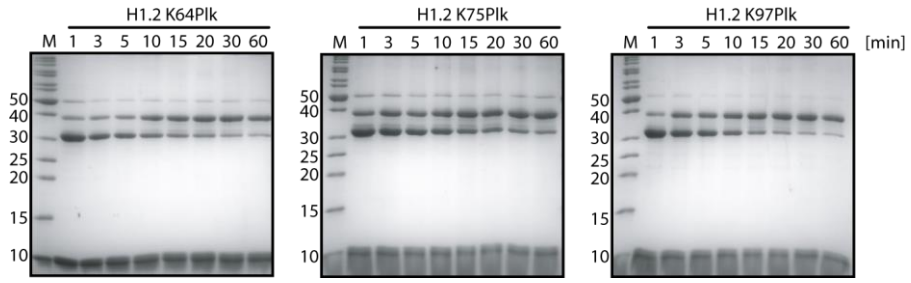

Figure 3.15 SDS-PAGE analysis of conjugating Ub G76Aha to H1.2 K64Plk, H1.2 K75Plk and H1.2 K97Plk by click reaction. Click reactions were performed with 30 µM Ub G76Aha, 10 µM H1.2 Plk and 0.5 mM SDS in 50 mM NaOAc (pH 5.0) on ice. M: Marker [kDa].

3.1.7 Optimizing the solubility

With the developed protocol for the efficient generation of site-specific mono-ubiquitylated H1.2 in hand, the produced conjugates were further analyzed. Besides an inefficient conjugation, precipitation of proteins has to be avoided in order to increase the amount of soluble proteins available for subsequent analysis and further experiments. To analyze the solubility of the produced conjugates, the reaction mixture was centrifuged before SDS-PAGE analysis, and the supernatant and the pellet were loaded separately onto the gel (Figure 3.16). It was found that reaction conditions applied so far (supplemented with 0.5 mM SDS and resulting in efficient conjugation), were hampered by low solubility of the conjugates, and accordingly characterized by high amounts of protein localized in the pellet (Figure 3.16a, lane 1). Hence, effects of surfactants on solubility of produced conjugates were reinvestigated. It was found, that with increasing concentration of SDS, the yield of mono-ubiquitylated H1.2 increased (as previously shown in Figure 3.12d), but at the same time their solubility significantly decreased. Best ratio between conjugation and precipitation was obtained at 0.25 mM SDS, resulting in efficient conjugation with high amounts of soluble conjugates in the supernatant (Figure 3.16a white rectangle). In comparison, same concentrations of n-LS yielded in an increased solubility but also in significant loss of conjugation under the evolved reaction conditions.

As consequence, the following click reactions were performed with a SDS concentration of 0.25 mM. In addition, the effects of buffers (NaOAc, PBS and Tris-HCl) on solubility of the conjugates were tested. Here, only NaOAc-buffered reactions resulted in efficient conjugation and solubility of mono-ubiquitylated H1.2 (Figure 3.16b).

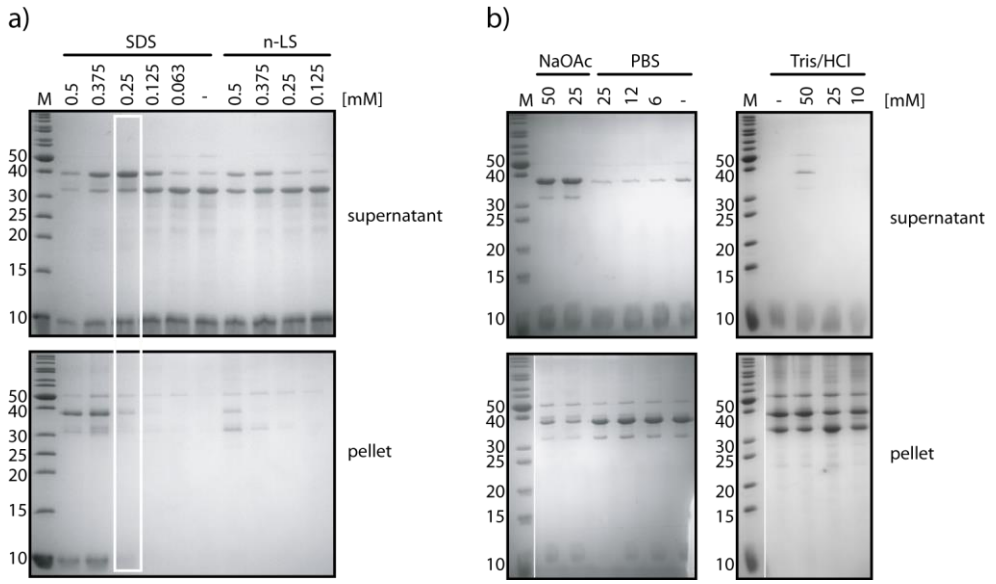

Figure 3.16 SDS-PAGE analysis of solubility of conjugates produced by click reaction. a) Influence of SDS and n-LS on protein solubility in reactions containing 10 µM H1.2 K75Plk and 50 mM NaOAc (pH 5.0). Reaction with highest yield in soluble conjugate is marked by a white rectangle. b) Influence of NaOAc, PBS and Tris-HCl on protein solubility in reactions containing 0.25 mM SDS and 10 µM H1.2 K97Plk or 10 µM H1.2 K46Plk. All click reactions were performed with 30 µM Ub G76Aha for 45 min on ice. M: Marker [kDa].

3.1.8 Upscale and purification

After successful optimization of the conjugation and the solubility of produced H1.2-Ub conjugates, click reactions had to be scaled up and purified to separate the mono-ubiquitylated H1.2 from the excess of Ub G76Aha and to remove reagents catalyzing the click reaction. During the up scaling process it was found, that the concentration of SDS could be further decreased to 0.2 mM. Finally, click reactions were performed in a total volume of 500 µl including 10 µM H1.2 Plk, 30 µM Ub G76Aha, 0.2 mM SDS, 5 mM Cu(I) complex and 10 mM THPTA in 25 mM NaOAc (pH 5.0). Mixtures were incubated for 45 min on ice and the reaction was stopped by addition of 50 mM EDTA. After centrifugation, the supernatant was diluted with ddH_2O and conjugates were purified by ultrafiltration (Figure 3.17). In this process, Ub G76Aha was completely removed and the click reaction buffer was exchanged with ddH_2O. Remarkably, no or only minor protein precipitation was observed. Finally, concentration of the conjugates was determined, adjusted to 0.5 mg ml^{-1} and 1 µg of each conjugate was subjected to SDS-PAGE analysis (Figure 3.17b). Typically, 100–150 µg of each site-specific, mono-ubiquitylated H1.2 conjugate were obtained by this procedure.

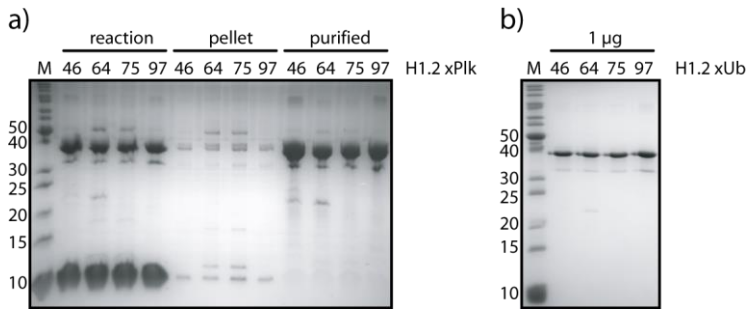

Figure 3.17 SDS-PAGE analysis of up scaled click reaction. a) Total click reaction mixture (reaction), insoluble proteins (pellet) and separated conjugates (purified), x: Site of Plk incorporation. b) 1 µg of purified mono-ubiquitylated H1.2 after buffer exchange, x: Site of mono-ubiquitylation. M: Marker [kDa]

3.1.9 Characterization of H1.2-Ub conjugates

In order to confirm site-specific conjugation of H1.2 Plk mutants with Ub G76Aha in click reactions, corresponding bands at ~40 kDa were excised from SDS-PA gel (Figure 3.17a) and further used for a tryptic in-gel digestion followed by mass spectrometry. Figure 3.18a shows the MS/MS spectrum of the triazole linked fragment of H1.2 46Ub. For all conjugates produced (H1.2 46Ub, H1.2 64Ub, H1.2 75Ub and H1.2 97Ub) the expected fragment containing the triazole linkage was confirmed by MS/MS (Figure 3.18b), demonstrating site-specific modification of H1.2 Plk by click chemistry with Ub G76Aha. So far, no ESI-MS spectra of full-length conjugates could be obtained with the applied settings.

a)

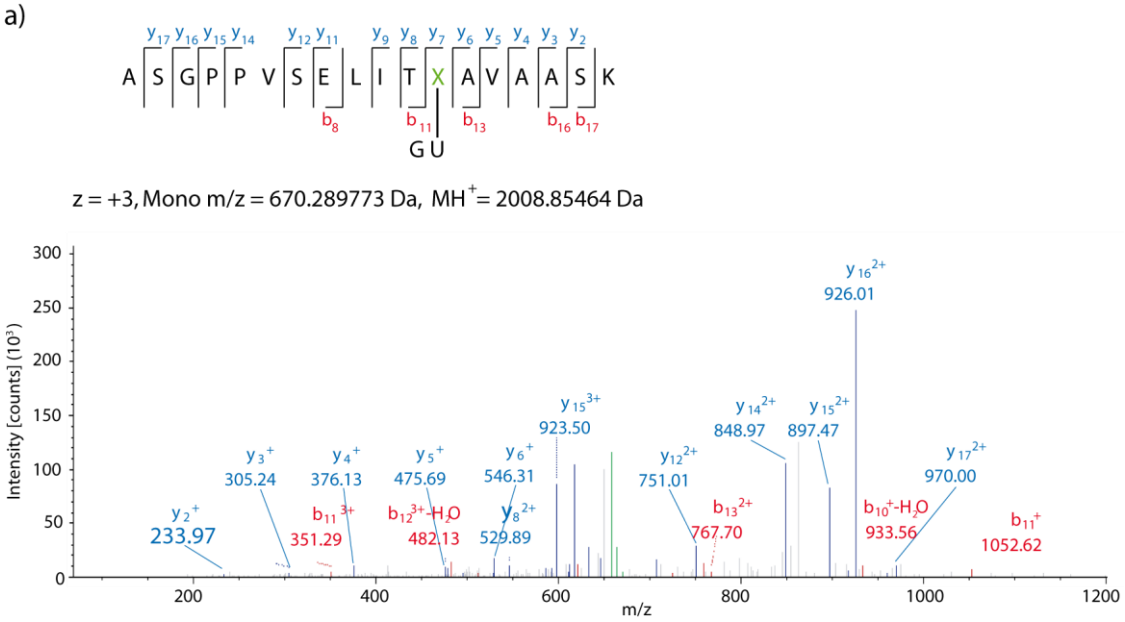

b)

conjugate	sequence coverage [%]	linkage fragment	M(calc)	M(expt)	Δ
H1.2 46Ub	45	ASGPPVSELITXAVAASK	2008.07	2008.85	-0.78
H1.2 64Ub	34	XALAAAGYDVEK	1517.76	1518.71	-0.95
		SGVSLAALKXALAAAGYDVEK	2344.25	2344.77	-0.52
H1.2 75Ub	31	ALAAAGYDVEXNNSR	1860.88	1861.91	-1.03
H1.2 97Ub	38	GTLVQTXGTGASGSFK	1820.91	1821.83	-0.92

Figure 3.18 Trypsin digestion of H1.2 Ub conjugates. a) MS/MS spectrum of trypsin digested H1.2 46Ub. All b- and y-ions marked in the peptide sequence were found in the corresponding MS/MS spectrum. b) Fragments containing respective triazole linkage were identified for each H1.2-Ub conjugate. X: Site of triazole linkage. Corresponding MS/MS spectra are attached in the appendix (7.2).

To investigate whether H1.2 ubiquitylation by click reaction affects the global conformation of the protein, CD spectroscopy of H1.2-Ub conjugates was performed (Figure 3.19). When comparing the CD spectrum of H1.2 WT treated with conditions of the click reaction with non-treated H1.2 WT, no significant alterations in folding were observed (Figure 3.19a), excluding structural changes caused by reagents of the click reaction (e.g. SDS). Interestingly, spectra of all four H1.2-Ub conjugates exhibited in addition to a diminished negative peak at 200 nm (which was already observed for Plk mutants in Figure 3.8c), a slightly increased local minimum at 222 nm (Figure 3.19b). This increased signal for alpha helical structures at 222 nm is likely attributed to the folded structure of the Ub attached, contributing to an overall less random coiled structure of H1.2-Ub conjugates compared to H1.2 WT. In contrast, CD-spectra of H1-SDS complexes exhibit a shifted minimum to ~205 nm and a characteristic maximum at 195 nm.[203]

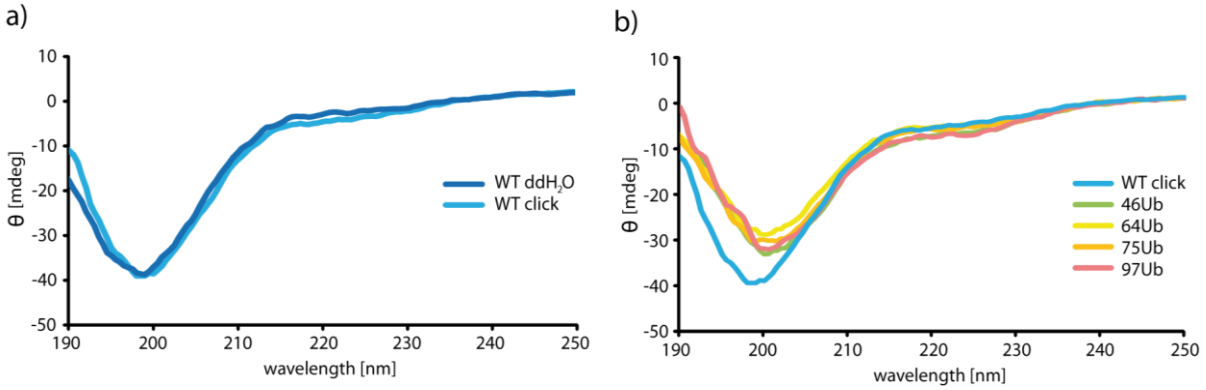

Figure 3.19 CD spectroscopy. a) CD spectra of H1.2 WT before (dark blue, ddH_2O) and after (light blue, click) incubation under click reaction conditions (17 µM in ddH_2O). b) CD spectra of mono-ubiquitylated H1.2 conjugates compared to H1.2 WT after incubation under click reaction conditions (17 µM in ddH_2O).

To further characterize H1.2-Ub conjugates, western blot analysis were performed. As shown in Figure 3.20 covalently attached Ub is still recognized by the anti-Ub antibody for all four conjugates, indicated by the signal at a molecular mass of ~37 kDa, as well as the free monomeric Ub G76Aha at ~10 kDa. Same results were obtained for H1.2. Here, both species, the mono-ubiquitylated H1.2 and the unconjugated H1.2 were successfully immunodetected. These results propose the application of all four H1.2-Ub conjugates and the H1.2 WT in comprehensive biochemical studies. As expected, the artificial triazole linkage does not interfere with the antibody recognition of Ub and H1.2 respectively.

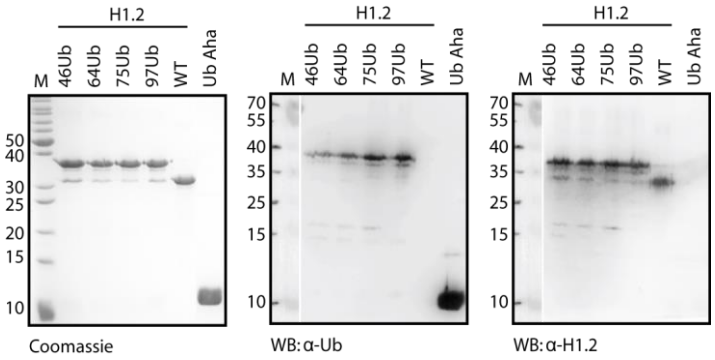

Figure 3.20 Western blot of H1.2-Ub conjugates, H1.2 WT and Ub G76Aha. Coomassie stained SDS-PA gel (left), immunodetection of ubiquitin (middle) and H1.2 (right). M: Marker [kDa].

3.1.10 Discussion and conclusion

The incorporation of Plk in the globular domain at four distinct positions of linker histone H1.2 was achieved by ACS, whereas modification of the C terminus of Ub with Aha was successfully conducted by SPI. Conjugation of both functionalized proteins in click reaction yielded site-specifically mono-ubiquitylated H1.2. Interestingly, in SDS-PAGE H1.2 is not observed at its expected molecular weight of 22 kDa, but at 32 kDa. This aberrant migration behavior of H1.2 has already been described[201] and is likely caused by the high net basic charges[204], with H1.2 consisting of 27.7 % Lys and 1.4 % Arg. The high content of Lys and Arg in H1.2 is also responsible for the generation of predominantly

small peptide fragments (most peptides consists of 5 aa or less) in trypsin digestion. These peptides exhibit low relative hydrophobicity, resulting in low retention time on reverse-phase C18 HPLC columns. These factors are likely to impair MS/MS analysis of H1.2-Ub conjugates, explaining the low sequence coverage (31–45 %) observed after in-gel-trypsin digestion (Figure 3.18b). Nevertheless, site-specific conjugation of H1.2 with Ub could eventually be verified for all four conjugates.

Compared to the preparation of H1.2 WT yielding 5 mg per liter expression culture, the incorporation of Plk by ACS significantly decreased the protein yield of H1.2 Plk mutants to 0.5–0.8 mg per liter expression culture. Thus, optimizing the expression construct and conditions proved to be indispensable in order to obtain sufficient amounts of modified protein. Remarkably, suppression efficiency of the amber stop codon turned out to be the same at all four sites, resulting in comparable yields for all Plk mutants. In contrast, suppression of an amber codon was abolished, when introduced at position two in H1.2 (data not shown). In order to adjust buffer conditions for subsequent affinity purification, inclusion body (IB) extracts were dialyzed in the respective binding buffer. In this process, protein precipitation was observed in case of H1.2 WT as well as for H1.2 Plk mutants decreasing the amount of H1.2 even before affinity chromatography. Moreover, protein precipitation and/or degradation during the final concentration step (utilizing VivaSpins for ultrafiltration) was generally observed for H1.2 when purified by *Strep*-Tactin affinity chromatography. In combination with the reduction of H1.2 expression as a result of ACS, *Strep*-tagged Plk mutants could not be obtained in quantities sufficient for further characterization by CD spectroscopy or click reactions.

In click reactions, addition of SDS and n-LS strongly increased the conjugation efficiency, whereas Tween and Triton X-100 showed no effect. Similar results were obtained when DNA polymerase beta was mono-ubiquitylated in click reactions.[205] The enhancing effect of SDS and n-LS is likely induced by their physicochemical properties.[205] In contrast to the nonionic surfactants Tween and Triton X-100, these anionic surfactants exhibit a negatively charged head and an alkane tail. Notably, non-denaturating concentrations of SDS[203, 205-207] were found to enhance the click reaction efficiency. In contrast to H1.2, mono-ubiquitylation of DNA polymerase beta by click reaction was found to favor Tris-HCl over NaOAc[185]. Click reactions with H1.2 in Tris-HCl-buffered mixtures resulted in poor solubility of the conjugates, likely caused by structural changes in H1.2. Since folding of H1 was found to be effected at a pH>7.0[208], buffering click reactions with Tris-HCl pH 8.0 presumably caused the observed protein precipitation (Figure 3.16b). Thus, adjusting the buffer conditions in click reactions according to the target protein is essential for efficient conjugation and improved solubility of the resulting conjugates.

Taken together, ACS is a practical method for the generation of alkyne-functionalized H1.2 and allows its site-specific mono-ubiquitylation. Here, utilizing click reaction proved as beneficial strategy, yielding mono-ubiquitylated H1.2, exhibiting promising biochemical characteristics for further studies.

3.2 Reconstitution of mono-ubiquitylated chromatosomes

3.2.1 Introduction

The binding mode of linker histones plays an important role in defining the higher order chromatin structure (see 1.2.1). Along these lines, PTMs of linker histones are assumed to induce altered binding modes and thereby regulate the function and structure of chromatin fibers. In order to investigate, whether specific histone PTMs (e.g. ubiquitylation) modify chromatin behavior, access to homogeneously modified nucleosomes and chromatin is essential. For these kinds of studies, chromatin extracted from natural sources is inapplicable, due to the fact that it is inherently heterogenic. Different variants of core histones and diverse PTMs contribute to the immense variety of native chromatin samples. Therefore, *in vitro* methods for the assembly of homogeneous nucleosomes consisting of defined core histones and DNA exhibiting a determined nucleosome positioning sequence (NPS) and linker DNA length have been developed. In this process, the artificial Widom 601 DNA sequence[209] is widely used for assembly and studying nucleosomes and nucleosomal arrays *in vitro*.[20, 21, 53, 58, 68] The Widom 601 sequence is a 146 bp-long strongly curved DNA that binds the histone octamer at a unique position and with high affinity. To allow specific binding and saturation of the 601 DNA with core histones (and later with linker histones) during assembly, a competitor DNA (crDNA) is added that controls the assembly and prevents oversaturation which results in aggregation and precipitation.[210] To determine whether mono-ubiquitylated H1.2 is able to bind to nucleosomes and reconstitute chromatosomes, defined nucleosomes based on the Widom 601 positioning sequence were assembled (Figure 3.21). Afterwards, binding of mono-ubiquitylated H1.2 to nucleosomes and properties of the reconstituted chromatosomes were investigated.

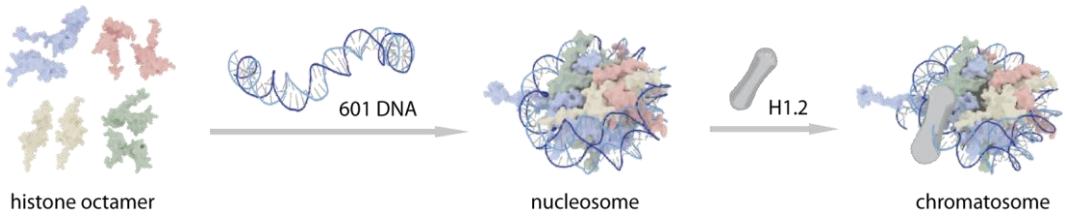

Figure 3.21 Scheme of *in vitro* nucleosome assembly with histone octamer on a Widom 601 DNA sequence and reconstitution of chromatosomes by H1.2 binding.

3.2.2 Nucleosome assembly on 601 DNA

For nucleosome assembly, a 178 bp-long nucleosome-positioning template (601 DNA) containing a centered 146 bp-long NPS from the Widom 601 DNA sequence and a 32 bp-long linker DNA was used (Figure 3.22a). This 178 bp-long 601 DNA was prepared by preparative PCR (Figure 3.22b), resulting in 1 mg 601 DNA. Before nucleosomes were reconstituted in large scale for chromatosomal studies, points of 601 DNA saturation by histone octamer in nucleosome assembly had to be identified by titration. To do so, 601 DNA was incubated with increasing amounts of histone octamer (Figure 3.22c) in the presence of crDNA in high salt buffer, followed by stepwise dialysis to reduce the salt concentration (see 6.6.2), facilitating nucleosome formation. Samples were analyzed by electrophoretic mobility shift assay (EMSA) on native-PAGE (n-PAGE) and stained with ethidium bromide (EtBr). As shown in Figure 3.22d, addition of increasing amounts of histone octamer shifts DNA signal from free 601 DNA to a new band of higher complexes in the gel, demonstrating histone octamer binding and nucleosome formation. Saturation with histone octamer was reached at a ratio of 0.6 : 1 (histone octamer : 601 DNA), indicated by the absence of free 601 DNA and appearance of a sharp band representing defined nucleosomes. Under the conditions applied, crDNA remained in the pocket of the gel. Based on this result, assembly of mono-nucleosomes was successfully scaled up (Figure 3.22e).

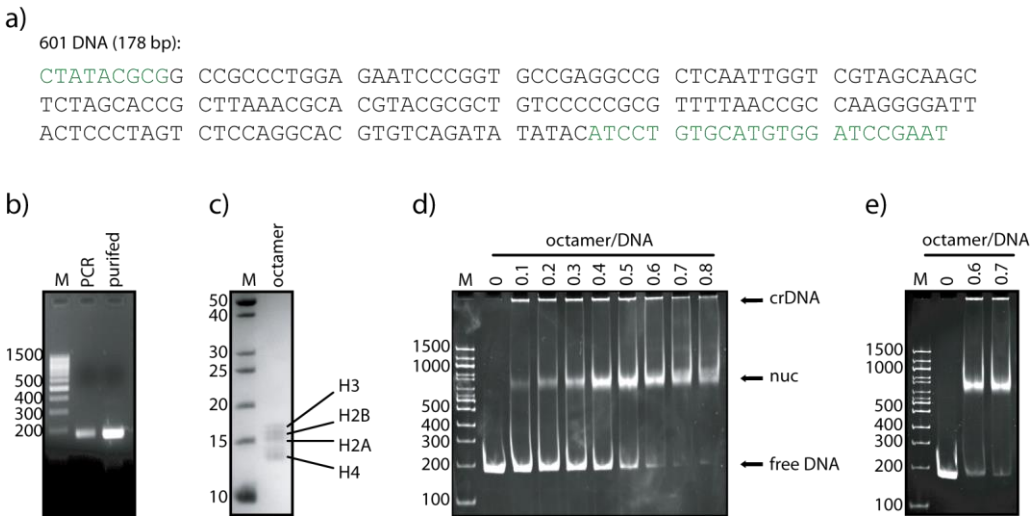

Figure 3.22 Nucleosome assembly on 601 DNA. a) Sequence of 601 DNA including the NPS (black) and the linker DNA (green). b) Agarose gel of 601 DNA. c) SDS-PAGE analysis of histone octamer. d) n-PAGE of nucleosomes, free 601 DNA, assembled nucleosomes (nuc) and competitor DNA (crDNA) are marked by arrows. e) EMSA of up scaled nucleosome assembly reactions. M: Marker [bp] in b, d and e), [kDa] in c).

3.2.3 Chromatosome reconstitution

With the mono-ubiquitylated H1.2 conjugates (see 3.1.8) in hand, defined nucleosomes were used to investigate chromatosome reconstitution. Reconstitution experiments were performed by incubation of nucleosomes with wild-type H1.2 and H1.2-Ub conjugates. Samples were analyzed by EMSA as conducted in nucleosome assembly studies. Initially, samples were analyzed by agarose gel electropho-

resis, resulting in insufficient separation of nucleosomes and chromatosomes (data not shown). Improved separation was achieved by EMSAs using n-PAGE.

At first, the behavior of the recombinant H1.2 WT in chromatosome assembly was tested, to optimize assembly conditions and to determine required concentrations of linker histone. As shown in Figure 3.23a binding of recombinant H1.2 WT to nucleosomes leads to formation of chromatosomes, indicated by higher complexes, with a decreased migration level compared to nucleosomes. In contrast, no interaction of Ub G76Aha was observed, when incubated with nucleosomes in a control experiment. Remarkable results were obtained, when H1.2-Ub conjugates were applied in chromatosome reconstitution. All four mono-ubiquitylated H1.2 conjugates were found to form chromatosomes upon incubation with nucleosomes (Figure 3.23b and c). A distinct shift of chromatosomes, caused by the additional mass of the attached Ub was observed for all four conjugates, enabling differentiation between both DNA-protein complexes present (namely nucleosomes and chromatosomes) at a ratio of 0.5 : 1 (H1.2-Ub : nuc). These results clearly demonstrate that mono-ubiquitylated H1.2 functions as nucleosome binder, independently of the site of modification. Thus, this procedure enables the generation of chromatosomes containing site-specifically modified linker histones.

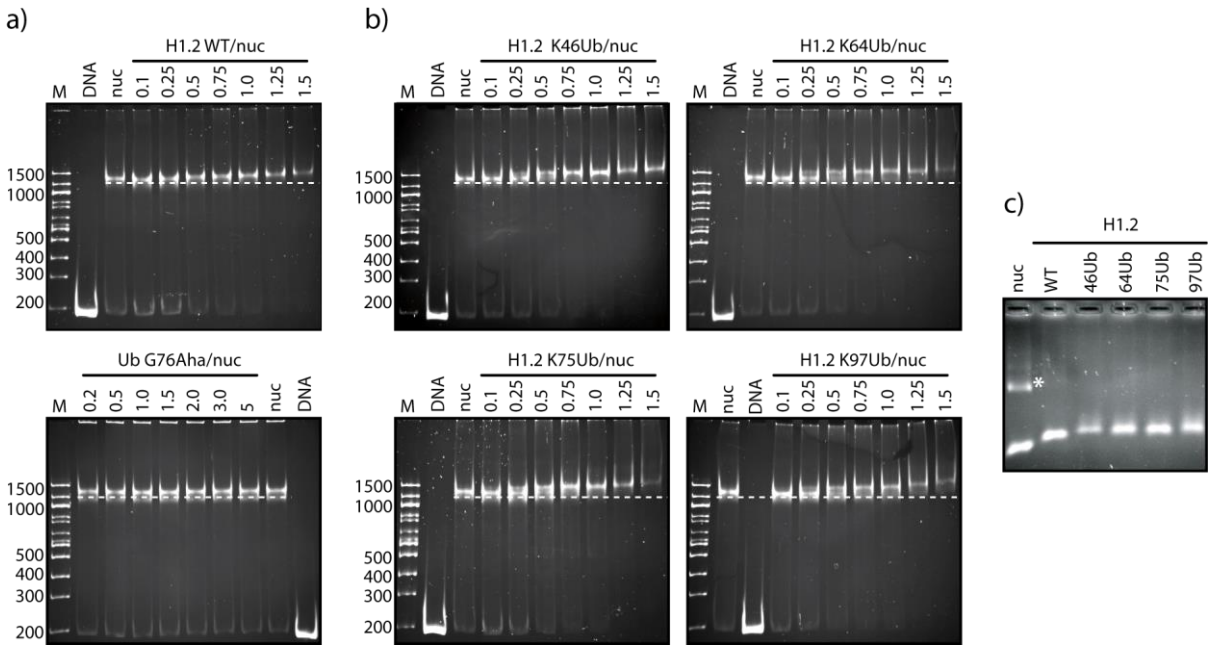

Figure 3.23 Chromatosome assembly. a) n-PAGE of H1.2 WT chromatosomes (top) and control reactions with Ub G76Aha (bottom). b) n-PAGE of chromatosomes assembled with mono-ubiquitylated H1.2. White, dashed lines indicate migration level of nucleosomes. M: Marker [bp]. c) Agarose gel of assembled chromatosomes from H1.2 WT and mono-ubiquitylated H1.2, crDNA is indicated by an asterisk.

3.2.4 Chromatosome stop assay

Numerous studies have indicated, that in chromatosomes the globular domain of linker histone H1 binds to parts of the linker DNA near the entry and exit sites of the nucleosome.[4, 48, 68] A distinctive property of the chromatosome is the protection from micrococcal nuclease (MNase) digestion of these ~20 bp of linker DNA beyond the DNA of the NCP.[3, 30, 69] To further investigate the binding of H1.2-Ub conjugates to nucleosomes and the properties of the generated mono-ubiquitylated chromatosomes, MNase digestion under limited conditions was performed. Here, MNase cuts the unprotected linker DNA first and transiently stops at the level of chromatosomes, leaving a 168 bp-long DNA fragment.[30] After removal of the remaining linker DNA – yielding the NCP containing 146 bp DNA, digestion of DNA within the nucleosome core finally takes place. Thus, the correct incorporation of linker histones into chromatosomes can be verified by the appearance of chromatosome-length DNA (168 bp) during a MNase digestion. Nucleosomes and reconstituted chromatosomes at a ratio of 1:1 (H1.2 : nucleosome) (see Figure 3.23c) were incubated with MNase for increasing time. Reactions were stopped by addition of SDS and proteins were digested. Cleaved DNA fragments were purified by ethanol precipitation and analyzed by n-PAGE and EtBr staining. Figure 3.24 shows the results from a time-dependent MNase digestion. In case of nucleosomes, the 146 bp-DNA fragment deriving from the NCP was generated within one minute and efficiently further digested to smaller fragments (Figure 3.24, top). Transient protection of linker DNA was observed for chromatosomes reconstituted with H1.2 WT, resulting in a chromatosome stop and a band at ~168 bp, consisting of the NCP and the additional ~20 bp of protected linker DNA. This result indicated proper incorporation of H1.2 WT into chromatosomes. However, after three minutes of MNase digestion, this structure was disassembled, and the linker DNA cleaved, demonstrated by the appearance of the NCP-fragment DNA in the gel. As expected, the addition of UbG76Aha had no influence on MNase digestion of H1.2 WT (Figure 3.24a, WT + Ub Aha) chromatosomes. In contrast, chromatosomes containing mono-ubiquitylated H1.2 were found to be significantly more stable during MNase digestion. With the unprotected linker DNA equally fast removed in both, WT and mono-ubiquitylated chromatosome, the DNA fragment corresponding to the NCP appeared significantly later for mono-ubiquitylated chromatosomes. Here, the 146 bp DNA fragment of the NCP was detected in the gel for the first time after five minutes of MNase digestion for all Ub-chromatosomes (Figure 3.24a). At this time point WT chromatosomes were already considerable more disassembled (Figure 3.24b). Furthermore, the 168 bp-fragment persisted as the major DNA fragment for 10 min of MNase digestion in case of all four Ub-chromatosomes (Figure 3.24a). This indicates a stronger binding of the H1.2-Ub conjugates to the nucleosome, or decreased affninity of MNase for Ub-chromatosomes, thus efficiently protecting the linker DNA from MNase digestion. Interestingly, the site of mono-ubiquitylation in H1.2 had no effect on MNase digestion.

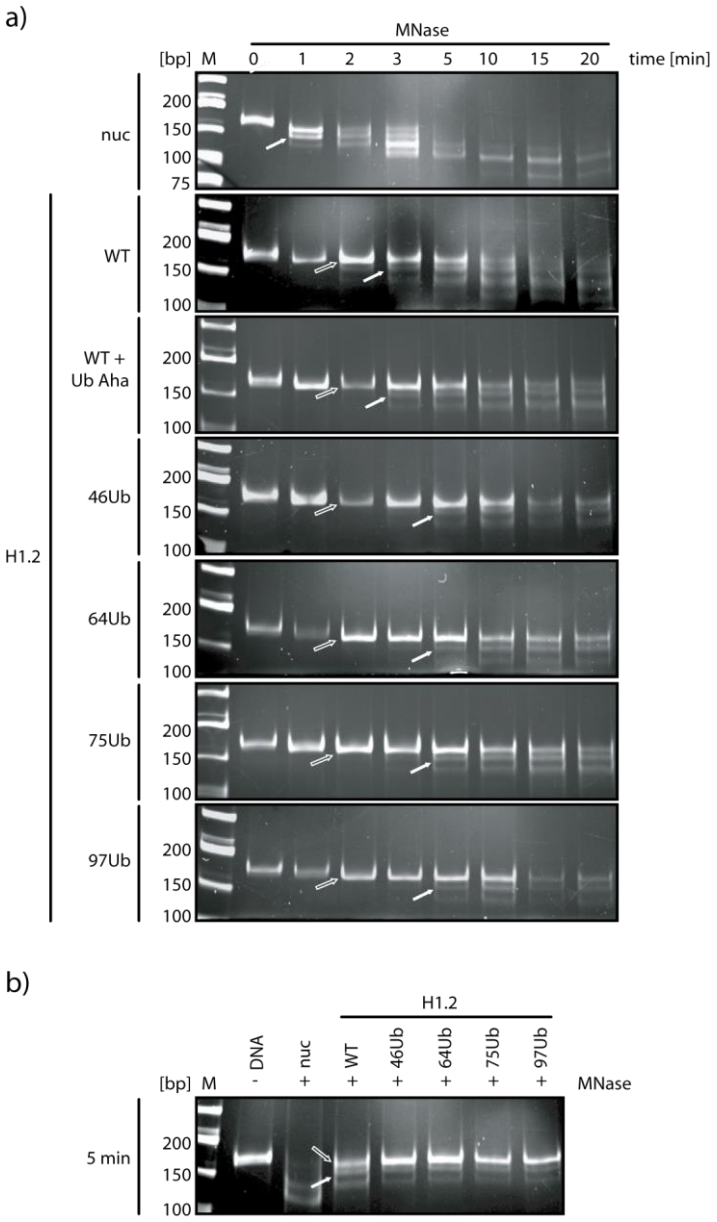

Figure 3.24 Chromatosome stop analyzed by n-PAGE. a) Time course of MNase digestion of nucleosomes (nuc), wild-type chromatosomes (WT) with free Ub G76Aha (WT + Ub Aha) and chromatosomes assembled with H1.2-Ub conjugates H1.2 K46Ub (46Ub), H1.2 K64Ub (64Ub), H1.2 K75Ub (46Ub) or H1.2 K97Ub (97Ub). b) Nucleosomes (nuc), wild-type chromatosomes (WT) and H1.2-Ub containing chromatosomes (46Ub, 64Ub, 75Ub and 97Ub) after 5 min of MNase digestion. The position of the chromatosome stop (framed arrow) and the NCP-fragment (filled arrow) are indicated. M: Marker [bp].

As the results obtained from MNase digest suggested a stronger binding of H1.2-Ub to nucleosomes than H1.2 WT, or decreased affinity of MNase for Ub-chromatosomes, the formation of chromatosomes was investigated in more detail. To quantify binding of H1.2 WT and H1.2-Ub conjugates to nucleosomes more precisely, nucleosomes were reconstituted on a ^{32}P-labelled 601 DNA template (Figure 3.25) enabling subsequent quantification of chromatosome formation. The ^{32}P-labelled template was generated by incubation of 178 bp-long 601 DNA with PNK and [γ-^{32}P]ATP. Nucleosome assembly was performed as described above. Best results were obtained at an octamer : DNA ratio of 0.65 : 1, characterized by a distinct band of the nucleosome and the absence of free 601 DNA.

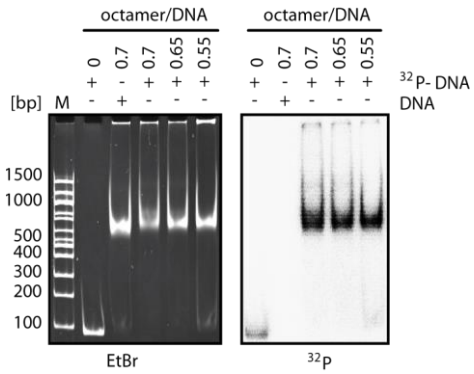

Figure 3.25 n-PAGE analysis of ^{32}P-labelled nucleosomes. Nucleosome assembly on ^{32}P-labelled or non-labelled DNA in ethidium bromide staining (EtBr, left) and corresponding autoradiogram (^{32}P, right).

Resulting ^{32}P-labelled nucleosomes were used for chromatosome reconstitution with H1.2 WT in comparison with the four H1.2-Ub conjugates, modified at position 46, 64, 75 and 97 respectively. Interestingly, chromatosomes containing ^{32}P-labelled nucleosomes showed an increased tendency to form aggregates in n-PAGE analysis. At a 1 : 1 ratio (H1.2 : nuc) >75% of Ub-chromatosomes aggregated, limiting the quantification of chromatosome formation to a H1.2 : nuc ratio of 0.8 : 1 (Figure 3.26a and b). However, within this range chromatosome assembly revealed, that there are no significant differences in binding of H1.2 WT compared to H1.2-Ub conjugates. The site of Ub attachment did not influence the binding of the mono-ubiquitylated H1.2, indicated by similar affinities for nucleosomes observed for all four H1.2-Ub conjugates.

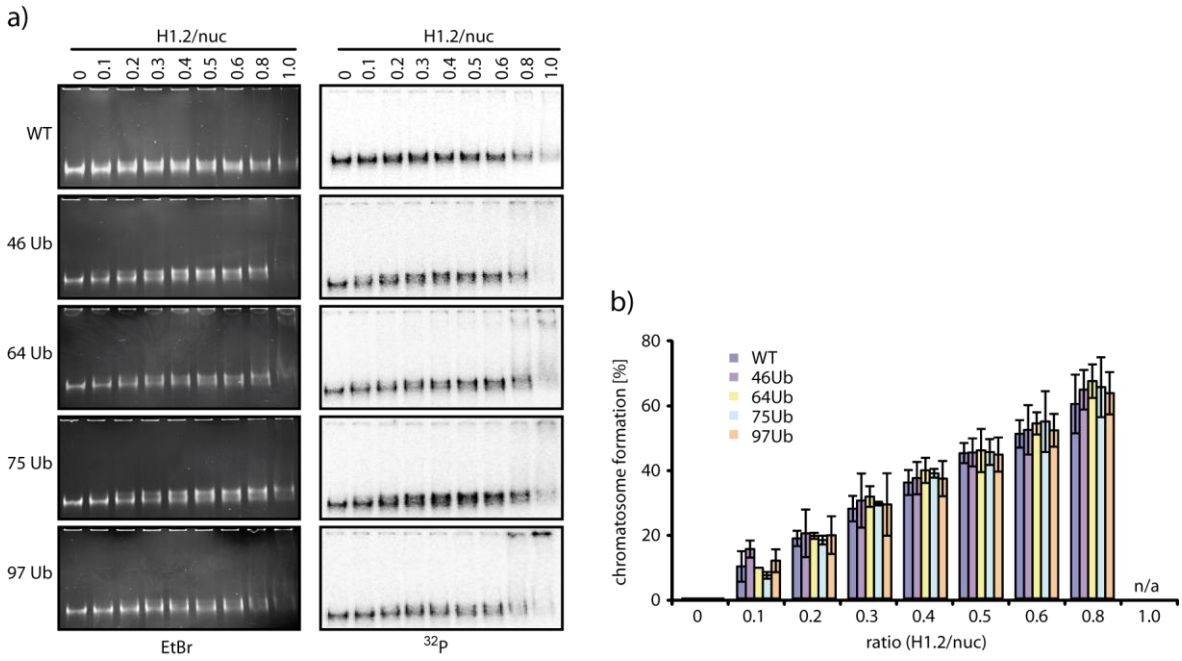

Figure 3.26 Chromatosome assembly. a) n-PAGE analysis of chromatosomes assembled with H1.2 WT and H1.2-Ub conjugates (46Ub–97Ub), ethidium bromide staining (EtBr, left) and autoradiogram (^{32}P, right). b) Quantified chromatosome formation (mean ± s.d.) at various ratios of H1.2/nuc: H1.2 WT (WT) and H1.2-Ub conjugates (46Ub–97Ub).

3.2.5 Discussion and conclusion

All four H1.2-Ub conjugates demonstrated efficient chromatosome reconstitution upon incubation with defined nucleosomes (Figure 3.23), derived from homogeneous core histone octamers and 601 DNA template (Figure 3.22). In nucleosome assembly, added histone octamers bind to the 601 DNA in preference to the weakly-binding crDNA. Without the crDNA, excess histone octamers would have bind non-specifically to the 601 nucleosome arrays causing them to aggregate and to precipitate, as observed after excessive addition of H1.2 (Figure 3.23a and b). Here, a ratio of 1.5 : 1 (H1.2 : nuc) led to aggregation of chromatosomes, as indicated by a decreased signal for chromatosomes in EtBr stained n-PA gels. Same effect was observed for nucleosomes assembled on ^{32}P-labelled DNA, exhibiting aggregation even before chromatosomes were completely assembled. Interestingly, in n-PAGE analysis, ^{32}P-labelled nucleosomes exhibited a decreased migration level, compared to non-labelled nucleosomes (Figure 3.25). However, when analyzed by agarose gel electrophoresis ^{32}P-labelled chromatosomes displayed complete binding of nucleosomes by H1.2 without aggregation (Figure 3.31). Thus, the early aggregation observed during chromatosome reconstitution on ^{32}P-labelled nucleosomes is likely an artefact attributed to the n-PAGE procedure. Nonetheless, analysis of chromatosome assembly by agarose gel based EMSAs resulted in insufficient separation of nucleosomes and chromatosomes (data not shown).

The results from Figure 3.23 and Figure 3.24 demonstrate that H1.2 WT and H1.2-Ub conjugates can recognize the nucleosomal structure of the entering and exiting linker DNAs and can provide proper organization of the 168 bp chromatosome, which is crucial for higher order chromatin structures. Remarkably, the attachment of ubiquitin within the GD of H1.2, which interacts with the nucleosome by structure specific recognition[4, 54] and is responsible for MNase protection[4, 30] did not interrupt the binding to the nucleosome (Figure 3.26), but increased MNase protection of the chromatosomal DNA compared to H1.2 WT as shown by chromatosome stop assay (Figure 3.24). This effect is likely caused by a decreased affinity of MNase towards mono-ubiquitylated chromatosomes and probably not by stronger binding of H1-2Ub conjugates to nucleosomes, since ubiquitylation was not found to influence chromatosome reconstitution (Figure 3.26).

Beyond that, all tested H1.2-Ub conjugates exhibited similar affinities for nucleosomes, independently of the Ub attachment site. These results suggest variable binding modes of H1-Ub at the nucleosome. Presumably, depending on the site of ubiquitylation within the GD, H1.2 reorients its binding mode, resulting in a conformation that allows accommodation of the attached Ub as well as binding of the GD. As demonstrated by computational studies for linker histone H5, various docking positions near the dyad axis of the nucleosome can be adopted.[67] Taken together, the results obtained support the hypothesis of flexible binding modes and versatile orientations of linker histones at sites of nucleosome interaction, further contributing to the diversity in models reported for linker histone binding.

However, so far no high resolution NMR or crystal structure of human H1.2 has been resolved neither for unbound H1.2 in solution nor in complex with a nucleosome. Therefore, crystallization trials with H1.2 WT in complex with nucleosomes containing 6 different DNA constructs, exhibiting variants in the DNA length, were conducted in cooperation with the group of C. A. Davey (Nanyang Technological

University). The obtained crystals yielded low diffraction of about 8 Å at the synchrotron and the structure could not be resolved so far.

3.3 Posttranslational modification of mono-ubiquitylated H1.2

3.3.1 Introduction

Numerous different PTMs have been identified on linker histones and H1.2 (see 1.3). Besides direct biophysical effects on chromatin structure, PTMs of histones are recognized by “reader”-proteins that interact with specific marks. Along these lines, interaction of different histone marks leading to a cross-talk of histone marks was reported.[104-107] Based on the ability of H1.2-Ub to assemble proper chromatosomes and the observed effect on MNase interaction, acceptance of the conjugates by H1.2 modifying enzymes as potential readers of mono-ubiquitylation was investigated. Thus, H1.2-Ub conjugates were examined regarding phosphorylation, which is considered the most researched PTM of histone H1. Dependent on the cell cycle context and the site of modification, H1 phosphorylation leads to both chromatin condensation and decondensation. In this process, the initiation of mitosis is triggered by the activation of the cyclin dependent kinase 1 (cdk1)/cyclin B complex in late G2 phase. This serine/threonine protein kinase comprises a catalytic subunit cdk1 and its positive regulatory subunit cyclin B. Binding of cdk1 to cyclin B is essential for activation of the kinase. (Recombinant cdk1/cyclin B is activated *in vivo* by endogenous kinases when expressed in insect cells.) During mitosis histone H1 is heavily phosphorylated by cdk1 (see Figure 1.8b).[211] Hence, H1 is widely used to evaluate the kinase activity of the cdk1/cyclin B complex. Beyond that, the DUB resistant triazole linkage in H1.2-Ub conjugates enables their application in *ex vivo* studies to investigate their properties as phosphorylation acceptor in a complex biological system. To address effects of H1.2 mono-ubiquitylation in a chromatosomal context, attention was paid to the chromatin remodeler PARP-1. PARP-1 is known to remodel chromatin structure by replacing H1 from nucleosome binding sites[159, 165, 170] and modifying H1 with PAR[168, 169].

3.3.2 Phosphorylation by cdk1/cyclin B

To investigate effects of histone ubiquitylation on phosphorylation by the cdk1/cyclin B complex, phosphorylation assays were performed. Cdk1/cyclin B was incubated with the respective H1.2-Ub conjugate in a time dependent manner. To visualize phosphorylation of the conjugate, kinase reactions were supplemented with [γ-^{32}P]ATP and samples were analyzed by SDS-PAGE followed by Coomassie staining and autoradiography (Figure 3.27). As expected, H1.2 WT is efficiently phosphorylated, as demonstrated by the autoradiogram (Figure 3.27a). To exclude an influence of the click reaction treatment on kinase activity, H1.2 WT was conducted to phosphorylation before and after incubation under click reaction conditions, resulting in equal phosphorylation levels (Figure 3.27a). Furthermore, it was shown that ubiquitin itself was no substrate for phosphorylation by the cdk1/cyclin B complex and had no effect on activity of the kinase (Figure 3.27b). Remarkably, mono-ubiquitylated H1.2 was accepted as substrate by the cdk1/cyclin B complex as well, with an increase in phosphorylation levels over time (Figure 3.27c and d). Putative differences in phosphorylation levels between conjugates were not reproducible in different replicates, accordingly no tendency regarding a favoured substrate recognition could be determined. However, the efficient modification of mono-ubiquitylated H1.2 in *in vitro* kinase assays generated the basis for studying phosphorylation in the environment of a complex biological system.

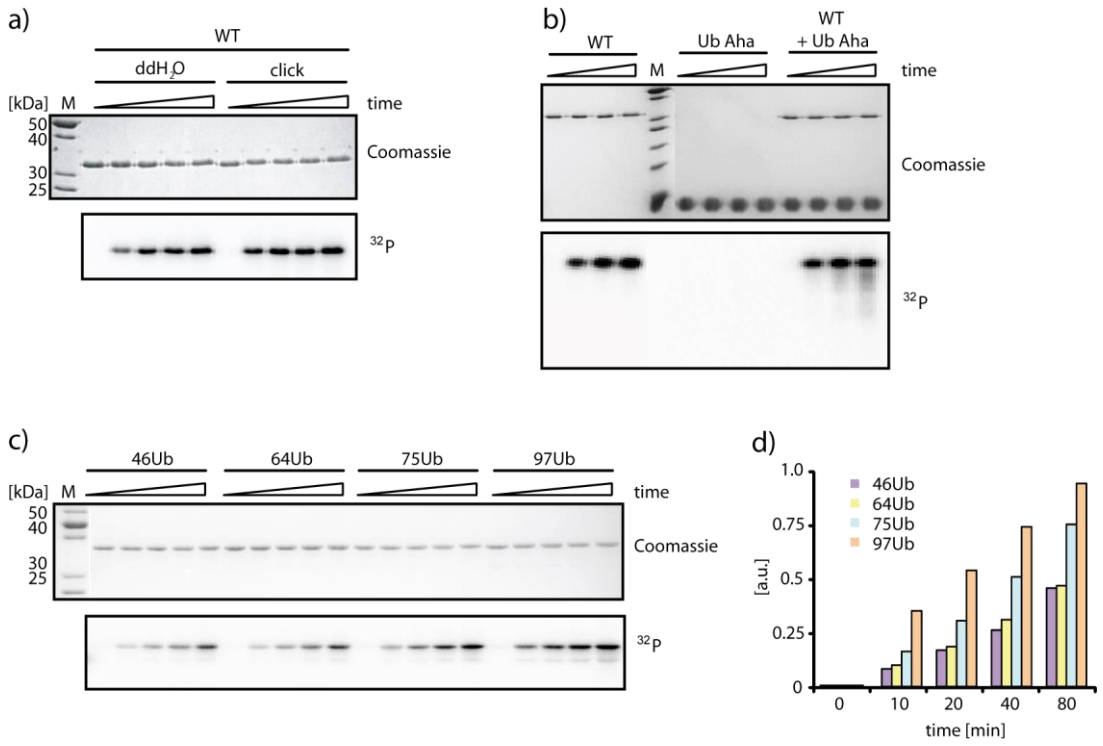

Figure 3.27 SDS-PAGE analysis of *in vitro* phosphorylation by cdk1/cyclin B. a) Phosphorylation of H1.2 WT before (ddH_2O) and after (click) incubation under click reaction conditions. b) Phosphorylation of H1.2 WT and Ub G76Aha c) Phosphorylation of mono-ubiquitylated H1.2 conjugates. Coomassie stained gels, corresponding autoradiograms are shown. M: Marker [kDa]. d) Quantified phosphorylation over time.

A distinctive property of the mono-ubiquitylation of H1.2 by click reaction is the protease-resistant linkage between H1.2 and the attached Ub. This feature enables the use of H1.2-Ub conjugates in cell extracts, generally containing de-ubiquitylating enzymes (DUBs), cleaving the isopeptide bound present after native ubiquitylation.

Phosphorylation of H1.2 WT and H1.2-Ub conjugates was analyzed in *Xenopus laevis* oocyte extracts using [γ-^{32}P]ATP to allow and visualize phosphorylation of the exogenous substrates. Samples from time-course phosphorylation were analyzed by SDS-PAGE followed by Coomassie staining and autoradiography. As shown in Figure 3.28a and b, H1.2 WT and all four H1.2-Ub conjugates were successfully phosphorylated in *Xenopus laevis* oocyte extracts. An increase of phosphorylation levels over time was observed for all exogenous substrates. Similar to the *in vitro* experiments, putative differences in phosphorylation levels between substrates could not be varified by different replicates, thus no tendency regarding a favoured substrate recognition in oocyte extracts could be determined. Although evidence for an effect of mono-ubiquitylation on cdk1/cyclin B remains elusive, *ex vivo* phosphorylation of H1.2-Ub conjugates successfully demonstrated their applicability for studying kinases in a complex biological system.

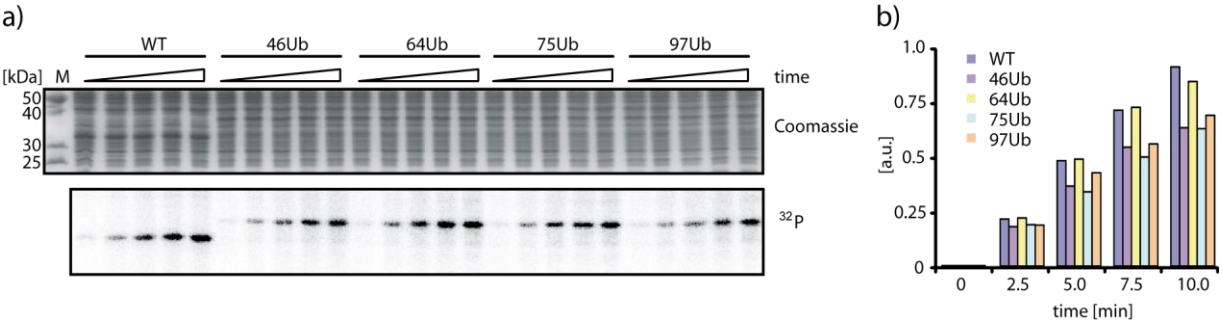

Figure 3.28 *Ex vivo* phosphorylation of H1.2-Ub conjugates. a) SDS-PA gel and corresponding autoradiogram of time-dependent phosphorylation of H1.2 WT and H1.2-Ub conjugates in *Xenopus laevis* oocyte extracts. M: Marker [kDa]. b) Quantified phosphorylation over time.

3.3.3 Chromatosome remodeling by PARP

In order to explore the binding of the linker histone to the nucleosome in the context of other histone modifications, interactions of chromatosomes with PARP-1 were investigated. Analysis of the genome-wide distribution of PARP-1 showed, that the binding of PARP-1 in chromatin is reciprocal with that of linker histone H1[170]. Therefore, the interaction of PARP-1 with DNA, nucleosomes and chromatosomes was analyzed by EMSAs. As shown in Figure 3.29a, the affinity of PARP-1 for nucleosomes is much stronger than that for naked DNA. These results are in line with reported data[160]. Interestingly, the highest affinity of PARP-1 was observed for chromatosomes. Analysis of the binding complexes supports the assumption of efficient H1.2 WT replacement in chromatosomes by PARP-1, resulting in nucleosome/PARP-1 complexes with similar migration behavior as complexes, derived from bare nucleosomes (Figure 3.29b).

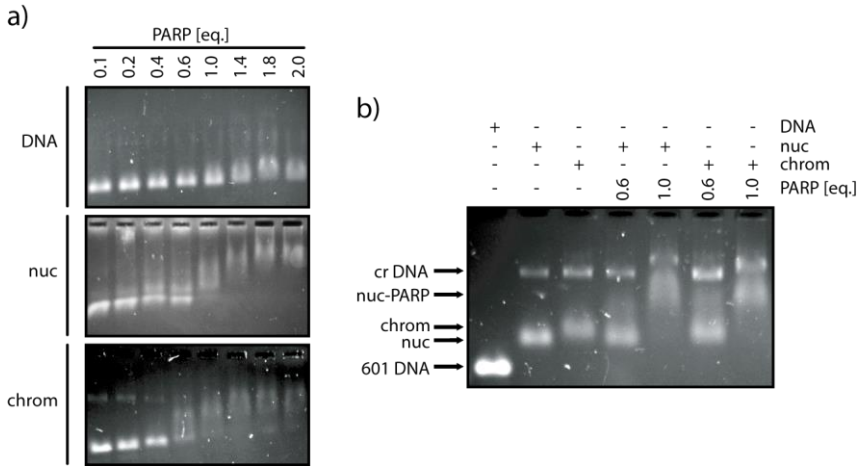

Figure 3.29 Interaction of PARP-1 with 601 DNA, nucleosomes and chromatosomes. a) Agarose gel of increasing amounts of PARP-1 incubated with 601 DNA, nucleosomes (nuc), or chromatosomes (chrom) containing H1.2 WT. b) Agarose gel of PARP-1-nucleosome complex.

To study binding of PARP-1 to nucleosomes in more detail, EMSAs of PARP-1/nucleosome binding complexes were performed (Figure 3.30a). ^{32}P-labelled nucleosomes were incubated with increasing amounts of PARP-1 and the complex formation was quantified from autoradiograms, demonstrating approximately 90 % binding of nucleosomes by PARP-1 at an equimolar ratio (Figure 3.30b).

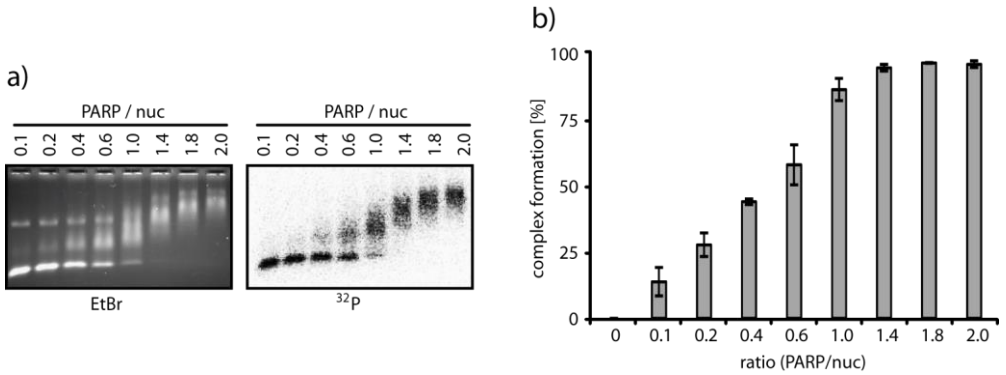

Figure 3.30 PARP binds to nucleosomes. a) Agarose gel of the formation of PARP-1/nucleosome complexes, stained with ethidium bromide and corresponding autoradiogram. b) Quantified complex formation (mean ± s.d.) at different ratios of PARP-1 : nucleosome.

To study reciprocal occupancy of H1.2 and PARP-1 in chromatosomes in more detail, ^{32}P-labelled chromatosomes, containing H1.2 WT or one of the four H1.2-Ub conjugates were assembled. Successful reconstitution of ^{32}P-labelled chromatosomes (with a 0.75 : 1 ration of H1.2 : nucleosome) was verified by agarose gel electrophoresis (Figure 3.31).

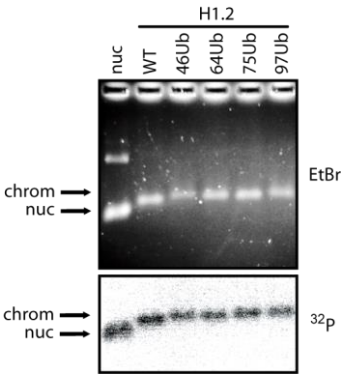

Figure 3.31 Agarose gel electrophoresis of ^{32}P-labelled chromatosomes containing wild-type H1.2 (WT) or mono-ubiquitylated H1.2 (46Ub, 64Ub, 75Ub or 97Ub). Nucleosomes (nuc) and chromatosomes are indicated in the ethidium bromide stained gel and in the autoradiogram.

In the following, ^{32}P-labelled chromatosomes containing H1.2 WT or one of the H1.2-Ub conjugates were incubated with increasing amounts of PARP-1. Samples were analyzed by ESMA utilizing agarose gel electrophoresis. The resulting gels as well as the corresponding quantification of PARP-1/nucleosome complex formation (from Figure 3.30) are shown in Figure 3.32. Incubation of all five different chromatosomes with PARP-1 resulted in efficient complex formation, confirming the strong affinity of PARP-1 for chromatosomes and nucleosomes respectively. A complete shift of chromatosomal DNA upon binding of PARP-1 was observed for WT chromatosomes as well as for mono-ubiquitylated chromatosomes. Quantification of the arising complexes indicated no considerable differences in complex formation in terms of the chromatosomal diversity used in this study (Figure 3.32b). Interestingly, when comparing these data with the results obtained from the interaction of PARP-1 with bare nucleosomes partially higher affinities of PARP-1 for chromatosomes than for bare nucleosomes were indicated (Figure 3.32c).

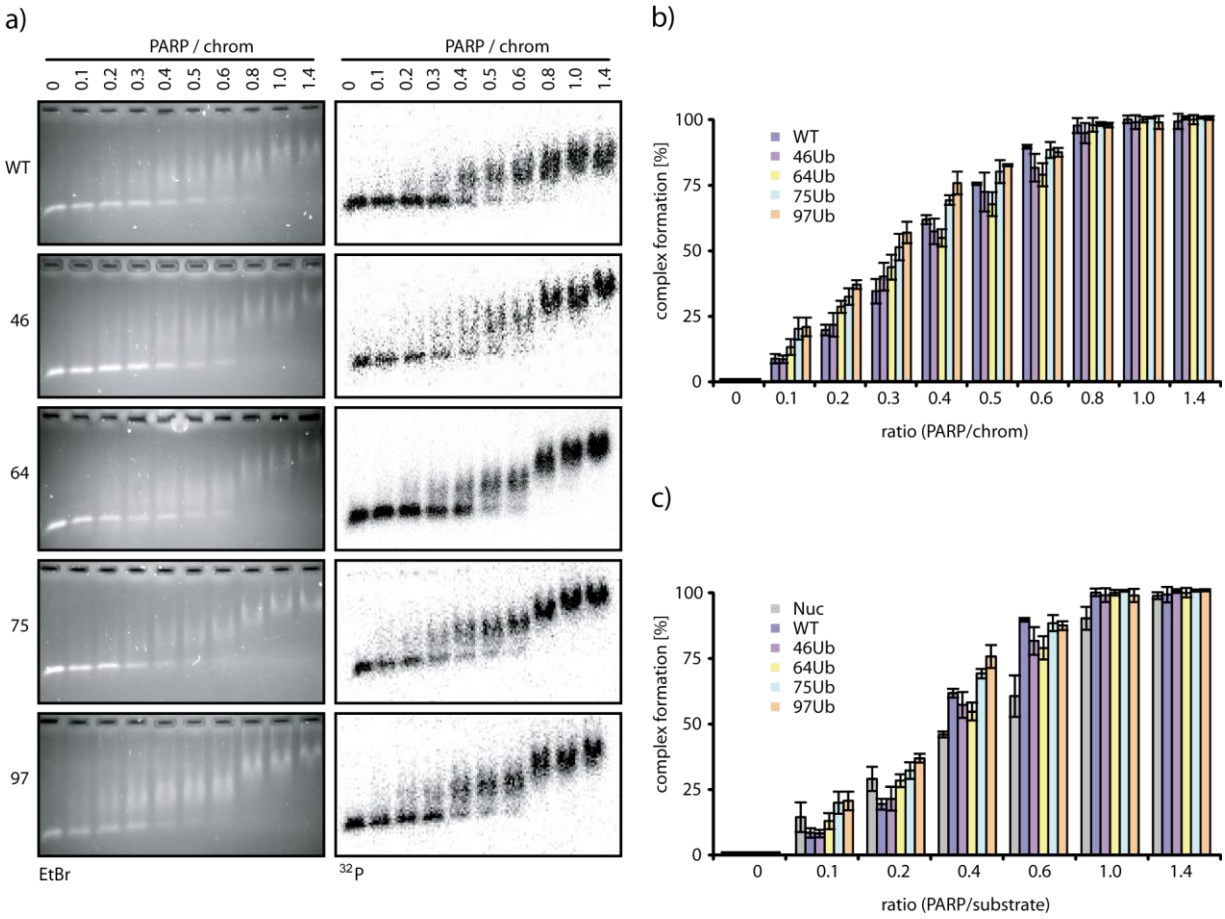

Figure 3.32 Interaction of PARP-1 with chromatosomes. a) Agarose gel electrophoresis of PARP-1/nucleosome complex formation upon interaction with chromatosomes, containing H1.2 WT, H1.2 K46Ub, H1.2 K64Ub, H1.2 K75Ub or H1.2 K97Ub, ethidium bromide staining (EtBr, left) and autoradiogram (^{32}P, right). b) Quantified PARP-1/nucleosome complex formation (mean ± s.d.) at various ratios of PARP-1 : chromatosomes. c) Comparison of quantified PARP-1 complex formation (mean ± s.d.) from Figure 3.30b and data obtained from with bare nucleosomes from Figure 2.28. b) Quantified complex formation (mean ± s.d.) at different ratios of PARP-1 : nucleosome

With the Ub modification of H1.2 within the chromatosome not affecting the interaction with PARP-1, a possible reader function for mono-ubiquitylation of H1.2 by PARP-1 in a chromatosomal context is diminished. However, in response to DNA damage linker histone H1 was reported to be the main acceptor of PAR.[212] To determine whether H1.2-Ub conjugates interact with PARP-1 when it is enzymatically active, an *in vitro* trans(ADP-ribos)ylation assay was performed. PARP-1, was incubated with H1.2 WT or H1.2-Ub conjugates, NAD^+ and a short DNA fragment, simulating DNA double strand break, to activate PARP-1. Samples were analyzed by SDS-PAGE and western blot (Figure 3.33). Efficient trans(ADP-ribos)ylation was observed for H1.2 WT as well as for all H1.2-Ub conjugates, demonstrated by smeared bands in the Coomassie stained gel, representing attached PAR polymers. Western blot with anti-PAR antibody confirmed the formation of PAR with long PAR polymers stuck in the gel pockets, indicating high activity of PARP-1 in H1.2-Ub samples. Co-localization of H1.2-Ub with PAR was shown by anti-H1.2 antibodies, verifying trans(ADP-ribos)ylation of H1.2-Ub conjugates by appearance of high molecular weight smear of comparable intensity. In constrast, intensity of H1.2

bands appear different. To investigate possible differences in PARylation efficiency of the H1.2 conjugates, kinetic studies are required.

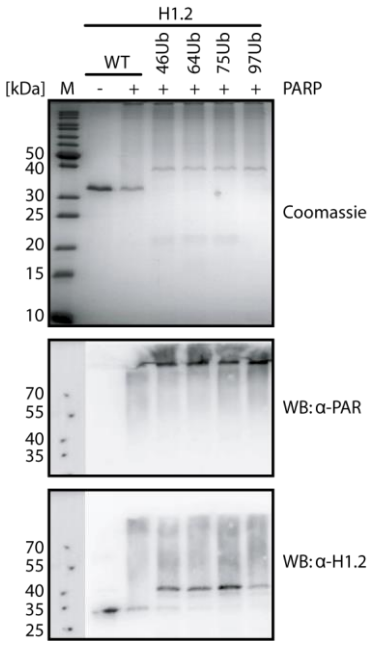

Figure 3.33 Western blot of PARylated H1.2 WT and H1.2-Ub conjugates catalyzed by PARP-1. Coomassie stained SDS-PA gel (top), immunodetection of PAR (middle) and immunodetection of H1.2 (bottom). M: Marker [kDa].

3.3.4 Discussion and conclusion

Kinase experiments demonstrated a time-dependent phosphorylation for H1.2 WT and H1.2-Ub conjugates and suggested that phosphorylation of H1.2 by cdk1/cyclin B was not significantly affected by mono-ubiquitylation. Although a possible reader function of cdk1/cyclin B for mono-ubiquitylation at the GD remains elusive, the results obtained demonstrate that H1.2-Ub conjugates serves as an acceptor for cdk1/cycling B-mediated phosphorylation and verify their function as substrate for this PTM in studies targeting kinase activity *in vitro* as well as *ex vivo*. Here, H1.2-Ub conjugates were found to be stable when incubated with *Xenopus laevis* oocyte extracts, proving its applicability for studies in complex biological systems with DUBs present.

Studies of H1.2-Ub in a chromatosomal context, focusing on the interaction of PARP-1 with nucleosomes and chromatosomes, demonstrated partially higher affinity of PARP-1 for chromatosomes compared to nucleosomes. This favoured interaction might be induced by the reported binding of H1.2 to PARP-1[97], which might attract PARP-1 to H1.2 containing chromatosomes. In contrast to the chromatosome stop assay (3.2.4), PARP-1 interaction with chromatosomes was not impaired, independently of H1.2 mono-ubiquitylation. Hence, a possible reader function for mono-ubiquitylation of H1.2 by PARP-1 in a chromatosomal context is diminished. Furthermore, the influences of mono-ubiquitylation on the enzymatic activity of PARP-1 was investigated in trans(ADP-ribos)ylation assays. Here, similar adducts of high molecular weight were detected for all four H1.2-Ub conjugates, though,

further studies are required to exclude PARP-1 as a reader for mono-ubiquitylation at the GD of H1.2. However, the results obtained clearly demonstrated acceptance of mono-ubiquitylated H1.2 as substrate for PARP-1-mediated ADP-ribosylation. Thus, mono-ubiquitylation of the N or C terminus will possibly have an influence on ADP-ribosylation, since the acceptor site for ADP-ribosylation are located in the N and C terminus[163]. Interestingly, ubiquitylation was linked to PARylation by revealing the regulation of DNA repair by Iduna, a PAR-dependent E3 ubiquitin ligase that requires PAR-binding for activation.[213] Taken together, the results suggest that mono-ubiquitylation of the GD of H1.2 might not have a major influence on chromatosome remodeling by PARP-1, although mono-ubiquitylated H1.2 interacts with PARP-1 and serves as an acceptor of ADP-ribosylation.

4 Summary and outlook

In order to generate site-specifically, alkyne-functionalized linker histone H1.2 the recombinant expression and the purification H1.2 had to be established and subsequently adapted for the incorporation of Plk by amber codon suppression (ACS). Initially, the expression and purification of untagged wild-type H1.2 was found to be hampered by its truncated forms. To improve yield of recombinant H1.2 three different expression constructs, bearing C-terminal affinity tags were generated and various purification strategies were tested. In this process, H1.2 was extracted from inclusion bodies either by perchloric acid (PCA) or with urea and was affinity purified under native or denaturating conditions. Here, PCA extraction yielded less impurities but decreased the yield of H1.2 protein compared to inclusion bodies extraction with urea. Moreover, yield of *Strep*-tagged H1.2 constructs, purified by *Strep*-Tactin affinity chromatography was found to be significantly lower than that of His-tagged H1.2, purified by immobilized metal ion affinity chromatography (IMAC). Expression and purification of full-length protein was confirmed by electrospray-ionization mass spectrometry (ESI-MS). In the next step, the incorporation of Plk at position K46 by ACS as well as the expression and purification of H1.2 K46Plk constructs was investigated. Similar to wild-type H1.2, best results for H1.2 K46Plk were obtained when expressed as His-tagged construct, extracted with urea and purified by IMAC under denaturating conditions. For all four H1.2 Plk mutants yields were found to be significantly decreased compared to their wild-type counterparts, particularly in case of *Strep*-tagged constructs. Thus, pending mutants for the incorporation of Plk at position K64, K75 and K97 respectively, were generated as His-tagged fusion proteins, purified under denaturating conditions and refolded via dialysis. The established expression and purification strategy enabled the efficient generation of Plk-equipped H1.2 mutants. Incorporation of Plk at all four sites was verified by ESI-MS and correct refolding of H1.2 Plk-mutants was confirmed by CD-spectroscopy. Moreover, first click reactions with an azide-functionalized fluorescent dye demonstrated accessibility and functionality of the incorporated alkyne group by selective labelling of the H1.2 Plk mutant.

Contrary, Aha was incorporated into Ub by selective pressure incorporation (SPI). To achieve selective functionalization of Ub at its C terminus exclusively, a modified Ub omitting the initial ATG codon was expressed as GST fusion construct. During the purification process the GST-tag, containing multiple Ahas, was removed and Ub G76Aha was obtained in milligram scale. Presence of a single modification in Ub at its C terminus was well as the quantitative replacement of Met by Aha at this site was confirmed by ESI-MS. With the Aha modified Ub and the Plk equipped histone H1.2 mutants in hand, mono-ubiquitylation of H1.2 Plk by click reaction was performed and found to be limited to a maximum conversion of ~50 %. To enhance conjugation efficiency different surfactants were tested. Whereas Triton X-100 and Tween showed no effect on click reaction, almost complete conversion was achieved by the addition of n-Lauroylsarcosine (n-LS) and SDS, respectively. The amount of Ub G76Aha needed for efficient conjugation was reduced by optimizing the buffer conditions. All Plk mutants exhibit similar properties in click reaction, reaching >95 % of conjugation after 30 min. However, reaction conditions resulting in efficient conjugation were hampered by low solubility of the conjugates. Hence,

effects of surfactants on solubility of produced conjugates were reinvestigated. Best ratio between conjugation and precipitation was obtained with SDS at a concentration of 0.25 mM. In contrast, addition of the same concentration of n-LS yielded in a significant loss of conjugation efficiency. Furthermore, only NaOAc-buffered reactions resulted in efficient conjugation and solubility of mono-ubiquitylated H1.2. After successfully up scaling the click reaction, excess of Ub G76Aha was removed by ultrafiltration and 100–150 µg of each site-specific, mono-ubiquitylated H1.2 conjugate were obtained. Site specific conjuagation of all four H1.2 Plk mutants with Ub G76Aha was verified by tryptic in-gel digestion followed by mass spectrometry. CD-spectroscopy of the purified H1.2-Ub conjugates revealed, that the global conformation of the protein is not altered by the click reaction-mediated ubiquitylation.

Based on their promising biochemical characteristics, H1.2-Ub conjugates were further investigated in functional studies. To elucidate the properties of mono-ubiquitylated H1.2 in a chromatosomal context, defined nucleosomes were assembled. As demonstrated by electrophoretic mobility shift assays (EMSAs) and MNase digestion, all four H1.2-Ub conjugates were able to recognize the structure of the nucleosome and reconstitute proper chromatosomes. Interestingly, the position of mono-ubiquitylation did not influence the behavior of the H1.2-Ub conjugates, indicating variable binding modes of H1 on the nucleosome. To further investigate the effect of a mono-ubiquitylated globular domain (GD) in H1.2 on the binding mode, nucleosomal arrays comprising multiple nucleosomes shall be assembled and used as a model system mimicking chromatin fibers. Here, EMSAs and ultracentrifugation are reasonable methods to examine the level of chromatin compaction upon binding of H1.2-Ub to the nucleosomal array. In order to expand the scope of studies, incorporation of the alkyne-functionalized Plk at other positions of H1.2, particularly in the C-terminal region shall be conducted by ACS. After modification with the azide-functionalized Ub by click reaction, these conjugates shall be utilized to investigate the role of the C terminus in the binding mode of H1.2 and its interaction with DNA at the nucleosome.

To examine the competency of mono-ubiquitylated H1.2 as acceptor for additional posttranslational modifications (PTMs) studies with the kinase complex cdk1/cyclin B were performed. In this process, a time-dependent phosphorylation of H1.2-Ub conjugates was observed in *in vitro* as well as in *ex vivo* experiments. Although a possible reader function of cdk1/cyclin B for mono-ubiquitylation at the GD remains elusive, the results clearly demonstrate the functionality of H1.2-Ub conjugates as substrate in studies targeting kinase activity. Similarly, acceptance of mono-ubiquitylated H1.2 as substrate for additional PTMs was indicated by PARP-1-mediated trans(ADP-ribos)ylation. These results demonstrate that click reaction-mediated mono-ubiquitylation of H1.2 generated conjugates which act as native-like acceptors for enzymes modifying linker histones.

Chromatosomal interaction studies suggested a partially higher affinity of PARP-1 to chromatosomes compared to bare nucleosomes and demonstrated that PARP-1 interacts with chromatosomes consisting of mono-ubiquitylated H1.2, independently of the ubiquitylation site. These results suggest that mono-ubiquitylation of the GD of H1.2 might not have a major influence on chromatosome remodeling

by PARP-1, although the H1.2-Ub conjugates interact with PARP-1 and serve as acceptors for poly(ADP-ribos)ylation as shown in trans(ADP-ribos)ylation assays.

To gain further insights into the role of mono-ubiquitylation of H1.2, sites in the vicinity of putative PTMs (for example at the terminal regions, which are known to be phosphorylated and ADP-ribosylated) shall be modified with Ub. These modifications might display marks that more efficiently influence the histone modifying enzymes, investigated in this thesis. Along these lines, other kinases targeting H1 shall be examined in terms of a reader function for mono-ubiquitylation. In this process, MS analysis will allow tracking changes in the phosphorylation pattern of H1.2-Ub conjugates in more detail, thus possibly revealing alterations in the modification of single acceptor residues. Moreover, based on the interaction studies of PARP-1 with H1.2-Ub equipped chromatosomes, phosphorylation of H1.2-Ub conjugates by cdk1/cyclin B shall be investigated in a chromatosomal context. Here, the impact of phosphorylation on chromatosome stability shall be investigated by EMSAs and changes in the modification pattern of H1.2-Ub conjugates and core histones shall be examined by MS analysis.

Finally, the DUB resistant triazole linkage allows the application of the H1.2-Ub conjugates in complex biological systems, as demonstrated by *ex vivo* phosphorylation experiments. Thus, identification of readers of mono-ubiquitylation on H1.2 in cell extracts is now feasible. Novel interaction partners will be enriched by utilizing H1.2-Ub conjugates as bait in pulldown experiments and subsequently analyzed and identified by MS.

5 Material

5.1 Reagents

Reagents for Plk synthesis	Source
Boc-Lys-OH	Iris Biotech
Dichloromethane (DCM)	Sigma-Aldrich
Diethylether (Et_2O)	Carl Roth
Ethyl acetate (EtOAc)	VWR
Hydrochloric acid	Sigma-Aldrich
Magnesium sulfate	Sigma-Aldrich
Propargyl chloroformate	Sigma-Aldrich
Sodium hydroxide	Riedel-de Haën
Tetrahydrofuran (THF)	Merck
Trifluoroacetic acid (TFA)	Merck

Reagents for molecular biology	Source
1,4-Dithiothreitol (DTT)	Carl Roth
2-Propanol	Sigma-Aldrich
Acetic acid	Carl Roth
Acetonitrile	Sigma-Aldrich
Acrylamide/Bis-acrylamide (37.5 : 1), Rotiphorese® Gel 30	Carl Roth
Agar-Agar	Carl Roth
Agarose LE	Biozym
Amino acids	Sigma-Aldrich
Ammonium acetate	Carl Roth
Ammonium chloride	Carl Roth
Ammonium hydroxide solution (33 %)	Sigma
Ammonium sulfate	Carl Roth
Ammoniumperoxodisulfat (APS)	Carl Roth
Azidohomoalanine (Aha)	Iris Biotech
Biotin	ABCR
Boric acid	VWR
Bromophenol Blue	Fluka
Calcium chloride	Merck
Carbenicillin disodium salt	Carl Roth
cOmplete His-Tag purification resin	Roche
Coomassie Roti-Blue (5x)	Carl Roth
Copper sulfate	Sigma-Aldrich
Copper(II) chloride dihydrate	Sigma-Aldrich
Coumaric acid	Riedel-de Haën
D-Glucose	Sigma-Aldrich
Dimethylsulfoxide (DMSO)	Sigma-Aldrich
Ethanol (100 %)	Sigma-Aldrich
Ethidium bromide (1 %)	Carl Roth
Ethylenediaminetetraacetic acid disodium salt (EDTA)	Carl Roth
Formamide	Carl Roth
Formic acid	Carl Roth
Glutathione Sepharose 4 fast flow (GST-beads)	GE Healthcare
Glycerol	Carl Roth
Hydrochloric acid	Sigma-Aldrich
Imidazole	Merck
Iron(II) chloride	Carl Roth

Reagents for molecular biology	Source
Isopropyl *β*-D-1-thiogalactopyranoside (IPTG)	Carl Roth
Kanamycin sulfate	Carl Roth
LB broth	Carl Roth
Luminol	Sigma Aldrich
Magnesium chloride hexahydrate	Acros Organics
Magnesium sulfate heptahydrate	Merck
Manganese(II) chloride tetrahydrate	Riedel-de Haën
Milk powder	Carl Roth
Milli-Q water	Satorius
N,N,N',N'-Tetramethylenethylendiamine (TEMED)	Carl Roth
n-Lauroylsarcosine sodium salt (n-LS)	Sigmal Aldrich
Nonidet™ P-40 Substitute	Fluka
Pefabloc® SC	Simga-Aldrich
Perchloric acid (PCA)	Riedel-de Haën
Phenylmethylsulfonylfluorid (PMSF)	Carl Roth
Polyethylenglycol (PEG)	Carl Roth
Potassium chloride	Merck
Potassium phosphate dibasic	Sigma-Aldrich
Potassium phosphate monobasic	Sigma-Aldrich
Roti®-Block	Carl Roth
Sephadex G25	GE Healthcare
SP Sepharose	GE Healthcare
Sodium acetate trihydrate	Merck
Sodium chloride	Carl Roth
Sodium dodecyl sulfate (SDS)	Carl Roth
Sodium metavanadate ($NaVO_3$)	Sigma-Aldrich
Sodium molybdate	Sigma-Aldrich
Sodium phosphate dibasic	Riedel-de Haën
Strep-Tactin® Superflow®	IBA
Strep-tag® regeneration buffer with HABA	IBA
Sulfo-Cy5-azide	S. Hacker (Marx group)
Tetrakis(acetonitrile)copper(I) tetrafluoroborate Cu(I) complex	Sigma-Aldrich
Thiamine hydrochloride	EGA-Chemie
Tris(2-carboxyethyl)phosphine (TCEP)	Carl Roth
Tris(3-hydroxypropyltriazolylmethyl)amine (THPTA)	H. Bußkamp (Marx group)
Tris(hydroxymethyl)aminomethane (Tris) Trizma base	Sigma-Aldrich
Tris[(1-benzyl-1,2,3-triazol-4-yl)methyl]amine (TBTA)	Sigma-Aldrich
Triton X-100	Carl Roth
Tryptone	Carl Roth
Tween 20	Carl Roth
Urea	VWR
Xylene cyanole	Carl Roth
Yeast extract	Carl Roth
Zinc chloride	Acros Organics
β-Glycerophosphat disodium salt hydrate	Calbiochem
β-Mercaptoethanol	Merck

5.2 Nucleotides and radiochemicals

Nucleotide / radiochemical	Source
dATP, dGTP, dCTP,dTTP	Fermentas/Roche
[γ-^{32}P]ATP	Hartmann Analytics

5.3 Primer and oligonucleotides

Primer were purchased from Metabion (Martinsried) or Sigma-Aldrich in desalted purification grade.

Name	Sequence 5' → 3'
H1.2 tag fw	GGAGATATACATATGAGCGAAACCGCACCGGCAGCAC
H1.2 C-*Strep* rev	AAGCTTGGATCCTTATTACTTTTCGAACTGCGGGTGGCTCCATTTTTTTTTCGGTGCCGCTTTCTTCGG
H1.2 C-His-*Strep* rev	AAGCTTGGATCCTTATTACTTTTCGAACTGCGGGTGGCTCCAGTGGTGATGGTGATGATGTTTTTTTTTCGG
H1.2 C-His rev	AAGCTTGGATCCTTATTAGTGGTGATGGTGATGATGTTTTTTTTTCGGTGCCGCTTTCTTCGG
H1.2 K46TAG fw	GTTAGCGAACTGATTACC**TAG**GCAGTTGCAGCAAGCAAAG
H1.2 K46TAG rev	CTTTGCTTGCTGCAACTGC**CTA**GGTAATCAGTTCGCTAAC
H1.2 K64TAG P fw	**TAG**GCACTGGCAGCAGCAGGTTATG
H1.2 K64TAG P rev	(P)-TTTCAGTGCTGCCAGGCTAACAC
H1.2 K75TAG fw	GCAGCAGGTTATGATGTGGAA**TAG**AATAATAGCCGCATTAAACTG
H1.2 K75TAG rev	CAGTTTAATGCGGCTATTATT**CTA**TTCCACATCATAACCTGCTGC
H1.2 K97TAG P fw	**TAG**GGCACCGGTGCAAGCGGTTC
H1.2 K97TAG P rev	(P)-GGTCTGAACCAG GGTGCCTTTGC
Widom (178bp) fw	CTATACGCGGCCGCCCTGG
Widom (178bp) rev	ATTCGGATCCACATGCACAGGATG
EcoRI	GGAATTCC
T7 fw	TAATACGACTCACTATAGGG

5.4 Plasmids

Name	Description	Tag(s)	Origin
pET11a/H1.2_WT	Wild-type H1.2	non	Marx group[214]
pET11a-tRNA^{Pyl}/H1.2_His	tRNA^{Pyl}, Wild-type hH1.2	C-terminal His	This thesis
pET11a-tRNA^{Pyl}/ H1.2_*Strep*	tRNA^{Pyl}, Wild-type hH1.2	C-terminal *Strep*	This thesis
pET11a-tRNA^{Pyl}/ H1.2_His-*Strep*	tRNA^{Pyl}, Wild-type hH1.2	C-terminal His C-terminal *Strep*	This thesis
pET11a-tRNA^{Pyl}/ H1.2 K46TAG_His	tRNA^{Pyl}, hH1.2 K46TAG	C-terminal His	This thesis
pET11a-tRNA^{Pyl}/ H1.2 K64TAG_His	tRNA^{Pyl}, hH1.2 K64TAG	C-terminal His	This thesis
pET11a-tRNA^{Pyl}/ H1.2 K75TAG_His	tRNA^{Pyl}, hH1.2 K75TAG	C-terminal His	This thesis
pET11a-tRNA^{Pyl}/ H1.2 K97TAG_His	tRNA^{Pyl}, hH1.2 K97TAG	C-terminal His	This thesis
pRSFduet-1/PylRS	PylRS		M. Rubini, Marx group
pET11a-tRNA^{Pyl}	tRNA^{Pyl}		Marx group[214]
pGEX 2TK_Ub G76M	Ub G76M, Thrombin site	N-terminal GST	D. Schneider, Marx group
pMA/Widom 601	208 bp Widom 601 DNA		GeneArt
pUC 18			Thermo Scientific

5.5 Enzymes and proteins

Name	Source
Phusion HF DNA polymerase	Finnzyme
DpnI	NEB
BamHI HF	NEB
NdeI	NEB
Calf intestine alkaline phosphatase (CIAP)	Fermentas
T4 DNA ligase	Fermentas
T4 polynucleotide kinase (PNK)	NEB
Micrococcal nuclease (MNase)	NEB
Proteinase K	Carl Roth
chicken histone octamer, recombinant	Abcam
native H1	Calbiochem
Cdk1/cyclin B	Meyer lab, Uni Konstanz
human PARP-1, recombinant	Enzo
DNase	Applichem
Thrombin	Biopure
Trypsin	Promega
Taq DNA polymerase	myPOLS Biotec
Bovin Serum Albumin (BSA) Standard (2 mg ml^{-1})	Thermo Scientific
Ubiquitin	Sigma-Aldrich

5.6 Antibodies

Antibody antigen	Species and Type / Conjugate	Dilution	Origin
H1.2	Rabbit, polyclonal	1 : 1000	Abcam
PAR (10H)	Mouse, monoclonal	1 : 1000	Enzo
Ub (P4G7)	Mouse, monoclonal	1 : 1000	Abcam
Anti mouse	Goat, polyclonal / HRP	1 : 5000	Dianova
Anti rabbit	Goat, polyclonal / HRP	1 : 5000	Dianova

5.7 Bacterial strains

Name	Genotype / Characteristic	Origin
E. coli XL10-Gold	endA1 supE44 recA1 thi-1 gy-rA96 relA1 lac Hte (mcrA) 183 (mcrCB-hsdSMR-mrr)173 tet^R [F' proAB $lacI^qZ$ M15 Tn10(Tet^R Amy Cam^R)]	Stratagene
E. coli BL21(DE3)	F^- *ompT* $hsdS_B$(r_B^- m_B^-) *gal dcm* λ(DE3 [lacI lacUV5-T7 gene1 ind1 sam7 nin5])	Stratagene
E. coli B834(DE3)	F^- ompT $hsdS_B$(r_B^- m_B^-) gal met dcm λ(DE3)	Novagen

5.8 Media

Medium	Composition
LB liquid medium	20 g l^{-1} LB-broth Add antibiotics at appropriate concentration: Carbenicillin 100 µg ml^{-1} Kanamycin 34 µ ml^{-1}
LB agar plates	20 g l^{-1} LB-broth 20 g l^{-1} Agar-Agar Add antibiotics at appropriate concentration: Carbenicillin 100 µg ml^{-1} Kanamycin 34 µ ml^{-1}
SOB medium	2 % (w/v) Tryptone 0.5 % (w/v) Yeast extract 10 mM NaCl 10 mM $MgCl_2$ 10 mM $MgSO_4$
SOC medium	SOB medium 20 mM glucose
TSS medium	85 % LB medium 10 % [w/v] PEG 50 mM $MgCl_2$ 5 % DMSO
New minimal medium (NMM)	7.5 mM $(NH_4)_2SO_4$ 8.5 mM NaCl 22 mM KH_2PO_4 50 mM K_2HPO_4 1 mM $MgSO_4$ 1 mg ml^{-1} $CaCl_2$ 1 mg ml^{-1} $FeCl_2$ 1 µg ml^{-1} $CuCl_2$ 1 µg ml^{-1} $MnCl_2$ 1 µg ml^{-1} $ZnCl_2$ 1 µg ml^{-1} Na_2MoO_4 50 mg ml^{-1} of each amino acid except Met 20 mM glucose 10 mg l^{-1} biotin 10 mg l^{-1} thiamine 100 mg l^{-1} carbenicillin

5.9 Buffers and solutions

5.9.1 Gel electrophoresis

Name	Composition
1x TBE buffer	40 mM Tris-HCl pH 7.5 20 mM acetic acid 1 mM EDTA
0.5x TAE buffer	45 mM Tris base 45 mM boric acid 2 mM EDTA pH 8.0
DNA loading dye (6x)	6x DNA loading dye (Thermo Scientific)
15 % SDS-PAGE separation gel	1.2 ml H_20 1.25 ml 1.5 mM Tris-HCl pH 8.8 50 µl 10 % SDS 2.5 ml Acrylamide/Bis-acrylamide 50 µl 10 % APS 5 µl TEMED
SDS-PAGE stacking gel	1.220 ml H_20 500 µl 1 M Tris-HCl pH 6.8 10 µl 10 % SDS 270 µl Acrylamide/Bis-acrylamide 20 µl 10 % APS 5 µl TEMED
10x SDS-PAGE electrophoresis buffer	250 mM Tris-HCl pH 8.9 2 M glycine 1 % [w/v] SDS
6x SDS-PAGE sample buffer	225 mM Tris-HCl pH 6.8 50 % glycerol 5 % [w/v] SDS 0.05 % [w/v] bromphenol blue 12.5 % [v/v] β-mercaptoethanol
Coomassie Roti-Blue in methanol	0.115 % Coomassie Roti-Blue 10 % acetic acid 50 % methanol
Coomassie blue staining solution	50 % Coomassie Roti-Blue in methanol 10 % acetic acid
Coomassie blue destaining solution	50 % methanol 10 % acetic acid
15 % native-PA gel	2.016 ml H_20 0.4 ml 5x TBE 2.5 ml Acrylamide/Bis-acrylamide 80 µl 10 % APS 4 µl TEMED
7.5 % native-PA gel	3.266 ml H_20 0.4 ml 5x TBE 1.25 ml Acrylamide/Bis-acrylamide 80 µl 10 % APS 4 µl TEMED
6 % native-PA gel	3.516 ml H_20 0.4 ml 5x TBE 1 ml Acrylamide/Bis-acrylamide 80 µl 10 % APS 4 µl TEMED

Name	Composition
native-PA gel staining solution	0.5x TBE 0.1 % ethidium bromide
Agarose gel staining solution	0.2x TBE 0.1 % ethidium bromide

5.9.2 Protein purification

Name	Components
Inclusion body buffer I	50 mM Tris-HCl pH 8.5 100 mM NaCl 1 mM EDTA 2 mM PMSF (added freshly) 1 % (w/v) Triton X-100
Inclusion body buffer II	50 mM Tris-HCl pH 8.5 100 mM NaCl 2 mM PMSF (added freshly) 1 mM EDTA
Urea extraction buffer	50 mM Tris-HCl pH 7.0 6 M urea 1 M NaCl 10 mM β-mercaptoethanol
Neutralization buffer	3 M Tris-HCl pH 9.5 100 mM NaCl
Strep-Tactin wash buffer	100 mM Tris-HCl pH 8.0 150 mM NaCl 1 mM EDTA
Strep-Tactin elution buffer	100 mM Tris-HCl pH 8.0 150 mM NaCl 1 mM EDTA 2.5 mM desthiobiotin
Strep-Tactin regeneration buffer	1x Strep-tag® regeneration buffer with HABA
Urea wash buffer	50 mM Tris-HCl pH 6.4 6 M urea 1 M NaCl 10 mM β-mercaptoethanol 8 mM imidazole
Urea elution buffer	50 mM Tris-HCl pH 6.4 6 M urea 1 M NaCl 10 mM β-mercaptoethanol 16–500 mM imidazole
IMAC binding buffer	50 mM Tris-HCl pH 8.0 250 mM NaCl
IMAC elution buffer	50 mM Tris-HCl pH 8.0 250 mM NaCl 8–500 mM imidazole
Ub lysis buffer	1 % (w/v) Triton X-100 in 1x PBS

5.9.3 Western blot

Name	Components
Transfer buffer	20 % methanol 20 % SDS-PAGE electrolysis buffer
1x PBS (pH 7.4)	137 mM NaCl 2.7 mM KCl 8.1 mM Na_2HPO_4 1.76 mM KH_2PO_4
PBS-T	137 mM NaCl 2.7 mM KCl 8.1 mM Na_2HPO_4 1.76 mM KH_2PO_4 0.05 % Tween
Blocking solution I	PBS-T 5 % (w/v) milk powder
Blocking solution II	1x Roti®-Block
ECL solution	100 mM Tris-HCl 225 µM coumaric acid 125 mM luminol 0.01 % H_2O_2

5.9.4 Nucleosome assembly

Name	Components
High salt buffer	10 mM Tris-HCl pH 7.6 2 M NaCl 1 mM EDTA 0.05 % (w/v) Nonidet P-40 Substitute 1 mM *β*-mercaptoethanol
20x Low salt buffer	200 Tris-HCl pH 7.6 1 M NaCl 20 mM EDTA 1 % (w/v) Nonidet P-40 Substitute 1 mM *β*-mercaptoethanol

5.9.5 Assay buffers

Name	Components
MNase storage buffer	10 mM Tris-HCl pH 7.5 50 mM NaCl 1 mM EDTA 50 % glycerol
10x MNase stop buffer	100 mM EDTA 4 % SDS
10x TE buffer	100 mM Tris-HCl pH 8.0 10 mM EDTA
hPARP-1 storage buffer	100 mM Tris-HCl pH 7.5 0.5 mM EDTA 10 % glycerol 14 mM *β*-mercaptoethanol

Name	Components
	0.5 mM PMSF
10x hPARP-1 reaction buffer	1 M Tris-HCl pH 7.8 100 mM $MgCl_2$ 10 mM DTT
5x TB buffer	250 mM Tris-HCl pH 7.5 50 µM $MgCl_2$
1x TB* buffer	50 mM Tris-HCl pH 7.5 10 µM $MgCl_2$ 5 mM β-glycerophosphat 5 mM $NaVO_3$

5.10 Standards and kits

Name	Source
GeneRuler 1 kb DNA Ladder	Thermo Scientific
Low Molecular Weight DNA Ladder	NEB
TriDye™ 100 bp DNA Ladder	NEB
PageRuler Unstained Protein Ladder	Thermo Scientific
PageRuler Prestained Protein Ladder	Thermo Scientific
High Pure Plasmid Isolation Kit	Roche
QIAprep Spin Miniprep Kit	Qiagen
QIAquick Gel Extraction Kit	Qiagen
MinElute Reaction Cleanup Kit	Qiagen
Taq 2x PCR Master Mix	myPOLS Biotec
BCA Protein Assay Kit	Pierce
Rapid DNA Ligation Kit	NEB

5.11 Disposals

Disposal	Source
96-well plate, Thermo-Fast 96, fully skirted	4titude
96-well plate, transparent U-bottom	Greiner, CellStar
Dialysis membrane (SnakeSkin dialysis tubing)	Thermo Scientific
Electroporation cuvette (GenePulser™ cuvette)	BioRad
Falkon tubes (15 ml, 50 ml)	Peske
Frit 20 µm (Isolute frits 15 ml, 20 µM)	Biotage
Paper filter	Satorius
PCR stripes	Thermo Scientific
PCR tubes (200 µl)	TreffLab
Petri dishes	Peske
Polyamide membrane filter	Satorius
Reaction tubes (1.5 ml)	Plastibrand
Reaction tubes, siliconized (0.5 ml, 1.5 ml)	Sigma-Aldrich
Reservoir 15 ml (Isolute reservoir 15 ml)	Biotage
Scalpels	Bayha
Sealing foil 96-well plate	BioRad
Sealing foil, Parafilm	Bemis
Syringe, needles	B. Braun
Syringe, sterile filters (0.2 µm 0.45 µm)	Peske
Syringes	Henke Sass Wolf
Tips	Axygen
Tips, pre-cut	StarLab
VivaSpin columns	Satorius
Whatman chromatography paper 3 mm	GE Healthcare

5.12 Equipment and software

Equipment	Source
Agarose gel racks	Fischer Scientific
Aperture for SDS-PAGE, Mini-Protean 3 System	BioRad
Autoclave, 3150 ELV	Systec
Balances, AJ150	Mettler Toledo
Balances, PG403-S	Mettler Toledo
Block heater	Stuart
CD spectrometer, J-815 spectropolarimeter	Jasco
Centrifugation tube, Nalgene Oak ridge high-speed 50 ml	Thermo Scientific
Centrifuge, 5417 C	Eppendorf
Centrifuge, 5810 R	Eppendorf
Centrifuge, mini-centrifuge “Uni-fuge”	Carl Roth
Centrifuge, Minispin®	Eppendorf
Centrifuge, biofuge primoR	Heraeus
Centrifuge, Sorvall Lynx 4000 Superspeed	Thermo Scientific
Chromas Light Version 2.1	Technelysium
Contamat, CoMo 170	S. E. A.
Electroporator, GenePulser Xcell	BioRad
FPLC-System, ÄktaPrime	GE Healtcare
Freezer -20 °C, profi line	Liebherr
Freezer -80 °C, -86 ULT Freezer	ThermoForma
Fridge 4 °C	Liebherr
Gel dryer, 583	BioRad
Image Lab Version 5.2.1	BioRad
Imager, Fluorescent image analyzer, FLA 3000	Fujifilm
Imager, Gel analyzer, ChemiDoc XRS	BioRad
Imager, Image reader LAS-3000	Fujifilm
Imager, Phosphorimager, Molecular Imager FX	BioRad
Incubator	Memmert
Magnetic stirrer, MR 3001 K	Heidolph
Mestre-Nova	Mestrelab Research
Microwave oven	Micromaxx
NMR AVANCE III 400 mHz spectrometer	Bruker
Orbital shaker incubator, Innova 44	Eppendorf
Overhead shaker, Reax 2	Heidolph
pH meter, Seven Easy	Mettler Toledo
Phosphor screen	Fuji, Kodak
Phosphor screen cassettes, BAS cassette 2 4020	Fuji, BioRad
Photometer, Biophotometer	Eppendorf
Photometer, NanoDrop Spectrophotometer (ND 1000)	PEQLAB
Pipettes	Eppendorf
Plate reader, Infinite M2000Pro	Tecan
Power supply, PowerPac 3000	BioRad
Qantity One Version 4.6.9. (basic)	BioRad
Quartz cuvettes	Hellma
Radioactivity shields	Carl Roth
Sonication device, Sonoplus HD2200, microtip Ms72	Bandelin
Speed Vac, Concentrator	Thermo Scientific
Sterile hood	HERA safe
Thermocycler	Biometra
Thermomixer comfort	Eppendorf
Tube roller	Phoenix Instruments

Equipment	Source
Vortexer, Reax 2000	Heidolph
Water bath	Memmert

6 Methods

6.1 Synthesis of Plk

The propargyl-derivatized lysine analogue Plk was synthesized according to the literature.[215] Briefly, Boc-Lys-OH was reacted with propargyl chloroformate to give Boc-protected Plk, which was deprotected by TFA to afford Plk in 53 % overall yield.

^{1}H NMR (400 MHz, D_2O): δ = 1.29 (m, 2H; CH_2), 1.46 (m, 2H; CH_2), 1.75 (m, 2H; CH_2), 2.77 (t,1H; CH), 3.04 (t, 2H; CH_2), 3.63 (t, 1H; CH), 4.55 (d, 2H, CH_2);

^{13}C NMR (100.5 MHz, D_2O): δ = 21.47, 28.38, 29.97, 40.04, 52.62, 54.22, 75.53, 78.51, 157.70, 173.85

ESI-IT-MS: m/z calcd for $C_{10}H_{16}N_2O_4$ $[M+H]^+$: 229.1, found: 229.1.

6.2 Gel electrophoresis

6.2.1 Analytical agarose gel electrophoresis

DNA fragments were separated according to their size by agarose gel electrophoresis. DNA samples were mixed with one sixth of DNA loading dye (6x) and depending on their length separated on 0.8 % or 2 % agarose gels in 0.5x TBE buffer by applying 120 V. The gels contained 0.5 µg ml^{-1} ethidium bromide for visualization of DNA under UV light by ChemiDoc XRS System.

6.2.2 Preparative agarose gel electrophoresis

DNA fragments were separated according to their size by agarose gel electrophoresis. DNA samples were mixed with one sixth of DNA loading dye (6x) and depending on their length separated on 0.8 % or 2 % agarose gels in 1x TAE buffer by applying 100 V. The gels contained 0.04 % (w/v) ethidium bromide for visualization of DNA under preparative UV light at ChemiDoc XRS. Appropriate bands were cut using a scalpel and purified with the Gel Extraction Kit.

6.2.3 SDS-PAGE

SDS-polyacrylamide gel electrophoresis (PAGE) was used to separate proteins according to their molecular weight. The used recipe based on the standard procedure including a stacking gel and a separation gel with polyacrylamide concentrations of 12 % or 15 %. Samples were mixed with one sixth of SDS-PAGE sample buffer (6x) and heated to 95 °C for 5 min to denature all proteins. Electrophoresis in SDS-PAGE electrophoresis buffer was performed for 35 min at constant 30 mA. Afterwards, the gels were stained using Coomassie blue staining solution, followed by treatment with Coomassie blue destaining solution and photographed with ChemiDoc XRS. Gels containing radioactive labelled samples were transferred onto Whatman paper, dried *in vacuo* at 80 °C for 2 h and exposed to a phosphor screen.

6.2.4 Native-PAGE

Native (n)-PAGE was used to separate small DNA fragments resulting from MNase digestion. First, a 15 % n-PA gel was prepared. After pre-running for 2 h at 90 V in 1x TBE buffer, DNA samples containing 1x DNA loading dye were separated by applying 90 V for 3.5 h in fresh buffer. Afterwards the gel was incubated in n-PA gel staining solution for 10 min. After destaining in 0.5x TBE buffer for 10 min the DNA was visualized using UV light on ChemiDoc XRS.

6.2.5 EMSA with agarose gel electrophoresis

To characterize protein-DNA complexes in solution, electrophoretic mobility shift assay (EMSA) was performed. Samples were supplemented with 20 % of glycerol and loaded onto a 1 % agarose gel in 0.2x TBE buffer. The gels were run for 60 min at 50 V in 0.2x TBE buffer. Afterwards the gel was incubated in agarose gel staining solution for 10 min. After destaining in 0.2x TBE buffer for 10 min the DNA was visualized using UV light on ChemiDoc XRS. Gels containing radioactive labelled DNA were transferred onto Whatman paper, dried *in vacuo* at room temperature overnight and exposed to a phosphor screen.

6.2.6 EMSA with n-PAGE

To characterize protein-DNA complexes in solution, EMSA was performed. First, a 6 % or 7.5 % n-PA gel was prepared. After pre-running for 1.5 h at 90 V in 0.5x TBE buffer, samples containing 20 % glycerol were separated in fresh buffer by applying 90 V for 1.5–3.5 h depending on the samples and the of the PA percentage of the gel. Afterwards the gel was incubated in n-PA gel staining solution for 10 min. After destaining in 0.5x TBE buffer for 10 min the DNA was visualized using UV light on ChemiDoc XRS. Gels containing radioactive labelled DNA were transferred onto Whatman paper, dried *in vacuo* at 80 °C for 2 h and exposed to a phosphor screen.

6.3 Molecular cloning

6.3.1 PCR

The polymerase chain reaction (PCR) was used to specifically amplify certain DNA fragments from a template plasmid. By using specific oligonucleotides (primers) specificity is obtained and sequences of the amplificate can be altered to generate new restriction sites, remove or add affinity tags. A typical PCR was set up of the following:

Component	Concentration
Template	1 ng μl^{-1}
HF-buffer	1x
dNTPs	200 µM
Primer fw	400 nM
Primer rev	400 nM
Phusion HF DNA polymerase	0.01 U μl^{-1}

The standard PCR program was as follows:

Step	Temperature	Time	
Initial denaturation	98 °C	60 sec	
Denaturation	98 °C	10 sec	
Annealing	55–75 °C	30 sec	
Elongation	72 °C	20 sec	20x
Final elongation	72 °C	10 min	

PCR products were purified by agarose gel electrophoresis (6.2.2) or MinElute Reaction Cleanup Kit.

6.3.2 QuickChange site-directed mutagenesis

Site-directed mutagenesis was performed to introduce nucleotide exchanges into a DNA sequence. According to the QuickChange Site-Directed Mutagenesis protocol (Stratagene) primers were designed with the desired mutation in the middle and to end with G or C. The mutant strand synthesis reaction was set up as indicated below:

Component	Concentration
Template	1 ng μl^{-1}
HF-buffer	1x
dNTPs	200 µM
Primer fw	400 nM
Primer rev	400 nM
Phusion HF DNA polymerase	0.01 U μl^{-1}

The cycling parameters were as follows:

Step	Temperature	Time	
Initial denaturation	98 °C	60 sec	
Denaturation	98 °C	10 sec	
Annealing	55–75 °C	30 sec	
Elongation	72 °C	4 min	18x
Final elongation	72 °C	10 min	

After amplification, the methylated, non-mutated template DNA was digested with *DpnI* for 1.5 h at 37 °C, followed by denaturation for 20 min at 80 °C. Without further purification, 3 µl of the amplification product were transformed into *E. coli* XL10-Gold.

6.3.3 Round-the-horn site-directed mutagenesis

Site-directed mutagenesis was performed to introduce nucleotide exchanges into a DNA sequence. Primers were designed with the desired mutation at the 5' end of the forward primer and a phosphorylated 5' end of the reverse primer. The PCR was set up as follows:

Component	Concentration
Template	1 ng μl^{-1}
HF-buffer	1x
dNTPs	200 µM
Primer fw	400 nM
Primer rev	400 nM
Phusion HF DNA polymerase	0.01 U μl^{-1}

The cycling parameters were as follows:

Step	Temperature	Time	
Initial denaturation	98 °C	60 sec	
Denaturation	98 °C	10 sec	
Annealing	55–75 °C	30 sec	
Elongation	72 °C	4 min	18x
Final elongation	72 °C	10 min	

After PCR, the methylated, non-mutated template DNA was digested with *DpnI* for 1.5 h at 37 °C, followed by denaturation for 20 min at 80 °C. The PCR product was purified by agarose gel electrophoresis (6.2.2) and ligated (6.3.6) before transformed into *E. coli* XL10-Gold.

6.3.4 Restriction enzyme digestion of DNA

Restriction enzymes were used according to the manufacturer's instructions to digest plasmids and PCR products. Typically, 1 ng of DNA was applied in a 40 µl reaction. Afterwards, restriction enzymes

were heat inactivated if possible and the DNA was directly dephosphorylated when required. Finally DNA fragments were purified by agarose gel electrophoresis (6.2.2).

6.3.5 Dephosphorylation of DNA

To prevent relegation during insert ligation, the 5' phosphate group of the linearized vector was removed by calf intestinal alkaline phosphates (CIAP). Immediately after restriction digestion 4.6 µl CIAP buffer and 1 µl CIAP were added and incubated for 1 h at 37 °C to dephosphorylate the vector. After inactivation for 15 min at 65 °C the vector was purified by agarose gel electrophoresis (6.2.2) to remove remaining enzymes.

6.3.6 DNA ligation

For DNA ligation 40 ng linearized and dephosphorylated vector were mixed with a 5-fold molar excess of insert and 1 µl T4 DNA in 1x ligase buffer. Ligation was performed for 15 min at room temperature in 20 µl (Rapid DNA Ligation Kit, NEB) or for 16 h at 16 °C in 10 µl (Fermentas). For transformation in *E. coli* XL10-Gold 5 µl or 3 µl ligation product were used. Control ligation reactions without insert were carried out in parallel.

6.3.7 Chemically competent cells

A 500 ml LB liquid culture was inoculated with 5 ml LB overnight culture and grown in an incubation shaker at 37 °C until an OD_{600} of 0.6–0.8 was reached. Cells were harvested by centrifugation at 4500*g* for 20 min at 4 °C and the pellet was washed in 10 ml ice-cold TSS medium on ice. Aliquots of 100 µl were frozen in liquid nitrogen and stored at -80 °C.

6.3.8 Electrocompetent cells

A 500 ml LB liquid culture was inoculated with 5 ml LB overnight culture and grown in an incubation shaker at 37 °C until an OD_{600} of 0.5–0.6 was reached. Cells were harvested by centrifugation at 4500*g* for 20 min at 4 °C and the pellet was washed twice with 500 ml ice-cold H_20 (Milli-Q) on ice. After washing the cells with 25 ml ice-cold 10 % glycerol, cells were resuspended in 5 ml ice-cold 10 % glycerol. Aliquots of 100 µl were frozen in liquid nitrogen and stored at -80 °C.

6.3.9 Transformation of chemically competent cells

For transformation, 100 µl chemically competent cells were thawed on ice and mixed with 3–5 µl of DNA sample. After incubation for 5 min on ice, cells were heat-shocked for 45 sec at 42 °C and returned on ice for another 5 min. Afterwards, cells were supplemented with 1 ml of pre-warmed (37 °C)

SOC-medium and incubated for 45 min at 37 °C on a shaker. For plating on appropriate selection LB agar plates, 100 µl cell suspension was used. For higher amounts of colonies, the residual cells were harvested by centrifugation, resuspended in 100 µl SOC medium and spread on LB agar plates.

6.3.10 Transformation of electrocompetent cells

For transformation, 100 µl electrocompetent cells were thawed on ice and mixed with 3–5 µl of DNA sample in a pre-cooled GenePulser electroporation cuvette. After treatment in a GenePulser Xcell (BioRad) with the *E. coli* program (1 mm, 1.8 kV) cells were supplemented with 1 ml pre-warmed SOC medium (37 °C) and incubated shaking for 45 min at 37 °C. For plating on appropriate selection LB agar plates, 100 µl cell suspension was used. For higher amounts of colonies, the residual cells were harvested by centrifugation, resuspended in 100 µl SOC medium and spread on LB agar plates.

6.3.11 LB agar plate culturing

Typically 100 µl of freshly transformed *E. coli* cells were plated on LB agar plates containing the appropriate antibiotic and incubated inverse overnight at 37 °C. Colonies were used to inoculate liquid cultures.

6.3.12 Plasmid isolation from liquid cultures

5 ml LB medium were inoculated with a colony from LB agar plate and incubated overnight at 37 °C. Cells were harvested by centrifugation and plasmids were isolated with QIAprep Spin Miniprep Kit according to the manual. DNA was eluted with ddH_2O.

6.3.13 Photometric measurement of DNA concentration

Concentration and purity of DNA was determined by absorption measurements at 260 nm and 280 nm. As a reference, either the respective buffer or ddH_2O was used. Absorption at 260 nm of one equals a DNA concentration of 50 µg ml^{-1}. For pure DNA solutions, the quotient of absorption 260 nm/280 nm is 1.8 or higher. Samples of 1.2 µl were applied to the NanoDrop for photometric measurements.

6.3.14 DNA sequencing

After plasmid isolation, 5 µl DNA (80–100 ng $µl^{-1}$) were mixed with 5 µl primer (5 µM) and sent to GATC Biotech for sequencing. Sequence data were analyzed by *Chromas Lite* and the online tool *SDSC Biology WorkBench* (http://www.workbench.sdsc.edu/).

6.3.15 Culture storage

For long time storage of liquid *E. coli* cultures, cells were mixed with glycerol in a ratio of 1 : 1, frozen in liquid nitrogen and stored at -80 °C.

6.4 Gene expression, cell lysate preparation and protein purification

6.4.1 Liquid cultures

Liquid cultures were incubated at 37 °C with shaking at 180 rpm if not mentioned otherwise. Overnight and test expression cultures were incubated in sterile 50-ml falcon tubes and cultures for large scale expression were handled in autoclaved 2-l Erlenmeyer flasks. For selection, appropriate antibiotics were added to the LB medium.

6.4.2 Expression of wild-type H1.2

The pET11 vector, including the gene of wild-type H1.2 (pET11a/H1.2_WT) was generated in a previous work[214] and transformed into *E. coli* BL21 (DE3) for expression.

To introduce a C-terminal His-tag, a forward primer carrying an *NdeI* restriction site and a reverse primer carrying the cDNA sequence of the His-tag followed by a *BamHI* restriction site were used in a PCR with pET11a/H1.2_WT as template. The resulting amplificate was purified by preparative agarose gel electrophoresis, digested using the restriction enzymes *NdeI* and *BamHI* and again purified by preparative agarose gel electrophoresis. The digested PCR product was cloned into pET11a-tRNA^{Pyl}, which was also cut by *NdeI* and *BamHI*. After ligation, the resulting plasmid pET11a-tRNA^{Pyl}/H1.2_His was transformed into *E. coli* BL21(DE3).

The same forward primer was used with the respective reverse primer carrying the cDNA sequence of the tag, to introduce a *Strep*-tag sequence C-terminally to the His-tag and to replace the His-tag by a *Strep*-tag. Both PCRs were performed on pET11a-tRNA^{Pyl}/H1.2_His template with the appropriate reverse primers. The resulting amplificates were separately cloned into pET11a-tRNA^{Pyl} by *NdeI* and *BamHI* restriction sites resulting in pET11a-tRNA^{Pyl}/H1.2_His-*Strep* and pET11a-tRNA^{Pyl}/H1.2_*Strep*. Finally the two plasmids were transformed into *E. coli* BL21(DE3) for expression.

Expression of all four constructs (H1.2_WT, H1.2_His, H1.2_*Strep* and H1.2_His-*Strep*) was conducted in the same way, described in the following. A 10 ml overnight culture was prepared and used to inoculate 1000 ml LB medium supplemented with 100 mg l^{-1} carbenicillin. The culture was grown to an OD_{600} of 0.6–0.8 and gene expression was induced by addition of 1 mM IPTG. After incubation for 4 h, cells were harvested by centrifugation at 4500*g* for 20 min at 4 °C. The supernatant was discarded and the pellet was stored at -20 °C.

6.4.3 Expression of H1.2 KxPlk

For analysis of Plk incorporation, the Lys46 codon of tagged H1.2 in all three pET11-tRNA^{Pyl} constructs (His, *Strep* and His-*Strep*) was mutated to the amber stop codon (TAG) by QuickChange site-

directed mutagenesis. Each resulting plasmid (pET11-tRNA^{Pyl}/H1.2 K46TAG_His, pET11-tRNA^{Pyl}/H1.2 K46TAG_*Strep* and pET11-tRNA^{Pyl}/H1.2 K46TAG_His-*Strep*) was co-transformed with pRSFduet-1/PylRS (kindly provided by M. Rubini) into *E. coli* BL21 (DE3).

For the incorporation of Plk at position Lys64, Lys75 and Lys97 respectively, single Lys codons in H1.2_His were mutated to amber stop codons by round-the-horn site-directed mutagenesis (Lys64, Lys97) or by QuickChange site-directed mutagenesis (Lys75) using the respective mutagenesis primer pairs. Finally, each expression plasmid encoding the gene of the respective His-tagged H1.2 KxPlk mutant was co-transformed with pRSFduet-1/PylRS into *E. coli* BL21(DE3).

Expression of all H1.2 KxPlk mutants (independently of the affinity tag and the site of Plk incorporation) was performed in the same way, described in the following. A 20 ml overnight culture was prepared and used to inoculate 1000 ml LB medium supplemented with 100 mg l^{-1} carbenicillin and 34 mg l^{-1} Kanamycin. The culture was grown to an OD_{600} of 0.3 and 1.5 mM Plk was added. Gene expression was induced by addition of 1 mM IPTG once OD_{600} of 0.6 was reached. After incubation for 4 h, cells were harvested by centrifugation at 4500*g* for 20 min at 4 °C. The supernatant was discarded and the pellet was stored at -20 °C.

6.4.4 Expression of Ub G76Aha

Met auxotrophic *E. coli* B834 harboring the expression construct of Ub G76Aha were used. For expression, 25 ml LB overnight culture were prepared and used to adjust the OD_{600} of 1000 ml prewarmed NMM (37 °C), supplemented with 0.04 mM Met to 0.1. The culture was incubated until stationary growth phase was reached, typically after 8 h with an OD_{600} of 1.1–1.3. Cells were harvested by centrifugation at 4500*g* for 15 min at 4 °C. The supernatant was discarded and the pelleted cells were resuspended in 1000 ml fresh and prewarmed NMM (37 °C) containing 0.5 mM Aha. After 30 min, 1 mM IPTG was added and cells were incubated for 14–16 h at 25 °C. Finally, cells were harvested by centrifugation at 4500*g* for 20 min at 4 °C. The supernatant was discarded and the pellet was stored at -20 °C.

6.4.5 Isolation of inclusion bodies

Recombinant H1.2 is expressed in E. coli as inclusion bodies. The first purification step of all H1.2 constructs comprised the isolation of inclusion bodies after expression. The following steps were carried out on ice. The cell pellet from 6.4.2 and 6.4.3 respectively, was resuspended in 40 ml inclusion body buffer I and transferred to two reaction tubes. Cells were lysed by sonication (3x 1 min, six cycles, max 20 % intensity; alternating reaction tubes) and centrifuged at 17,000*g* for 10 min at 4 °C, resulting in inclusion body-containing pellets. The supernatant was discarded and each pellet was washed once with 20 ml inclusion body buffer I and twice with 20 ml inclusion body buffer II to remove other cellular components from inclusion bodies.

6.4.6 Solubilization of inclusion bodies

After isolation, inclusion bodies were either solubilized by urea or PCA. For solubilization with 6 M urea, each pellet (derived from 500 ml expression culture) was resuspended in 15 ml urea extraction buffer and incubated for 3 h at 4 °C while rolling. After centrifugation at 21,000*g* for 15 min at 4 °C supernatants containing H1.2 were combined a new tube.

For solubilization with PCA, each pellet (derived from 500 ml expression culture) was resuspended in 8 ml 0.83 M PCA and incubated for 2 h at 4 °C while rolling. After centrifugation at 21,000*g* for 15 min at 4 °C supernatants containing H1.2 were combined in a new tube and mixed with 2.5 ml neutralization buffer.

6.4.7 Purification of untagged H1.2

Untagged H1.2_WT was purified by cation exchange chromatography. PCA extracts where dialyzed in 25 mM phosphate buffer pH 8.0 and loaded onto a 10 ml SP Sepharose column. Untagged H1.2 was eluted by linear NaCl gradient (0–1.5 M in 80 ml) and of flowrate of 0.8 ml min^{-1}. Elution fraction were analyzed by SDS-PAGE and Coomassie staining.

6.4.8 Purification of *Strep*-tagged H1.2

After solubilization of inclusion bodies, purification of H1.2_*Strep*, H1.2_His-*Strep*, H1.2 K46Plk_*Strep* and H1.2 K46Plk_His-*Strep* was performed by *Strep*-Tactin affinity chromatography. Extracts resulting from solubilization of inclusion bodies by urea and PCA (6.4.6) were dialyzed in *Strep*-Tactin wash buffer overnight at 4 °C. After centrifugation at 21,000*g* for 20 min at 4 °C, supernatant was applied to 1 ml *Strep*-Tactin affinity matrix. The matrix was washed with 5 ml *Strep*-Tactin wash buffer and proteins were eluted six times with 0.5–1 ml *Strep*-Tactin elution buffer. (For recovery, the matrix was regenerated with *Strep*-Tactin regeneration buffer). Purification was analyzed by SDS-PAGE and fractions containing the protein of interest were pooled and concentrated by ultrafiltration using VivaSpin (MWCO 10,000 kDa). After determination of the concentration by BCA assay, proteins were frozen in liquid nitrogen at stored at -20 °C.

6.4.9 Purification of His-tagged H1.2

Purification of H1.2_His and H1.2 KxPlk_His under denaturation conditions was performed with extracts resulting from solubilization of inclusion bodies by urea (6.4.6). Extracts were directly incubated with 1.5 ml cOmplete His-Tag Purification Resin in the presence of 5 mM imidazole for at least 4 h at 4 °C. After washing with 20 ml urea wash buffer, step-wise elution was carried out with urea elution buffer by increasing the imidazole concentration. Purification was analyzed by SDS-PAGE and fractions containing the protein of interest were pooled and dialyzed in H_2O (Milli-Q) overnight at 4 °C for refolding. Proteins were concentrated by ultrafiltration using VivaSpin (MWCO 10,000 kDa) and pro-

tein concentration was determined by BCA assay. Finally, aliquots were frozen in liquid nitrogen and stored at -20 °C.

Purification of H1.2_His and H1.2 KxPlk_His under native conditions was performed with extracts resulting from solubilization of inclusion bodies by PCA (6.4.6). Extracts were dialyzed in IMAC binding buffer overnight at 4 °C and incubated with 1.5 ml cOmplete His-Tag Purification Resin for at least 2 h at 4 °C. After washing with 20 ml IMAC binding buffer, step-wise elution was carried out with IMAC elution buffer by increasing the imidazole concentration. Purification was analyzed by SDS-PAGE and fractions containing the protein of interest were pooled and dialyzed in H_2O (Milli-Q) overnight at 4 °C. Proteins were concentrated by ultrafiltration using VivaSpin (MWCO 10,000 kDa) and protein concentration was determined by BCA assay. Finally, aliquots were frozen in liquid nitrogen and stored at -20 °C.

6.4.10 Purification of Ub G76Aha

Harvested cells (from 6.4.4) were resuspended in 80 ml Ub lysis buffer, mixed with 200 µg DNase and incubated for 30 min on ice. After sonication (3x 30 s, five cycles, max 20 % intensity, and alternating reaction tubes) the lysate was centrifuged at 23,000*g* for 25 min at 4 °C and the supernatant was supplemented with 1.5 ml GST-beads before incubation for 5 h at 4 °C. Beads were washed with 30 ml 1x PBS and cleavage of GST fusion protein was performed by addition of 15 U thrombin and incubation overnight at room temperature. Cleaved Ub G76Aha was eluted with 10x 200 µl 1x PBS. The concentration of Ub G76Aha was determined by BCA assay and samples were stored at 4 °C.

6.4.11 Purification of H1.2-Ub

H1.2-Ub conjugates generated by click reaction were purified by ultrafiltration. After centrifugation, the supernatant was diluted with 5 ml cooled ddH_2O (4 °C), applied to a pre-washed VivaSpin (5 ml, MWCO 30,000 kDa) and concentrated to >500 µl. Conjugates were washed three times by ultrafiltration with 5 ml ddH_2O (4 °C) to remove Ub G76Aha and click reaction reagents. Finally purity was controlled by SDS-PAGE and protein concentration was determined by BCA assay.

6.5 Protein characterization

6.5.1 Determination of protein concentration by BCA assay

Concentration of purified proteins was determined by BCA protein assay kit (Pierce) according to the manufacturer's instructions for micro assay protocol in transparent, U-bottom 96-well plates. Absorbance was measured at 562 nm with a Tecan plate reader. For determination of H1.2 concentration, H1 standard solutions were used. Concentration of Ub G76Aha was determined with Ub standards.

6.5.2 Mass spectrometry

Electrospray ionization mass spectrometry (ESI-MS) of full-length H1.2 was performed by Dr. Andreas Marquardt (Proteomics Facility, University of Konstanz). Data were analyzed using DataAnalysis (Bruker) and total protein masses were determined by deconvolution.

HPLC-ESI-MS/MS of peptide fragments, resulting from tryptic in-gel digest was performed by Dr. Andreas Marquardt (Proteomics Facility, University of Konstanz) using a Daltonics esquire 3000+ (Bruker) with an 1100 HPLC system from Agilent equipped with a Vydac MS C18 column. Data were analyzed using DataAnalysis (Bruker) and Mascot search.

ESI-MS of full-length Ub G76Aha was performed by Dr. Serge Chesnov at functional genomics center Zürich. The m/z data were deconvolved into MS-data using the MaxEnt1 Software.

6.5.3 Circular dichroism spectroscopy

Circular dichroism (CD) spectroscopy was performed on a J-815 spectropolarimeter (Jasco) with Spectra Manager software used to analyze the data. CD spectra were measured from 260–190 nm at 20 °C with 0.5 nm data intervals and were averaged from 5 scans. A quartz cuvette (1 mm light path) with 200 µl of the protein sample (11 µM or 17 µM) was used.

6.5.4 Western Blot

To identify proteins and posttranslational modifications by specific antibodies, proteins separated by SDS-PAGE (6.2.3) were transferred on a PVDF membrane (Immobilion-P, Milipore) by western blot. The transfer was carried out in a Mini-Protean 3 System (BioRad) by wet blotting in transfer buffer at 280 mA for 40 min. Afterwards, the membrane was washed with PBS-T and blocked in blocking solution I (anti-PAR, anti-H1.2) or blocking solution II (anti-Ub) overnight at 4 °C. After washing with PBS-T the primary antibody was applied in blocking solution I or PBS-T (anti-Ub) for 1 h at room temperature. Again, the membrane was washed with PBS-T and incubated with the second antibody for 1 h at room

temperature. After washing with PBS-T and PBS, the membrane was treated with ECL solution and chemiluminescence was detected by LAS-3000 Imager (Fujifilm).

6.6 Protein modification and functional studies

6.6.1 Click reaction

Click reactions with a fluorescent dye were carried out by mixing 10 µM H1.2 K46Plk with a 10–100 fold molar excess of sulfo-Cy5-azide (kindly provided by Stephan Hacker), 10 µM TBTA, 1 mM TCEP and 1 mM $CuSO_4$ in the given order. Reaction tubes were flushed with argon and incubated for 1 h at room temperature. Samples were analyzed by SDS-PAGE and fluorescence was detected by a fluorescent image analyzer FLA 3000 (Fujifilm).

Test click reactions with Ub G76Aha were carried out by mixing the following components in the given order in a final volume of 10 µl: ddH_2O, buffer as indicated, Ub G76Aha, 0.5 mM Pefabloc, H1.2 KxPlk and SDS. Applied concentrations of components are listed in the respective experiment. Reaction tubes were flushed with argon and THPTA and Cu(I) complex were added. The reaction mixtures were again flushed with argon. Indicated centrifugation was performed in a mini-centrifuge for 3 min at room temperature. Product yield and solubility was analyzed by SDS-PAGE followed by Coomassie blue staining.

Large scale click reactions were carried out in 1.5-ml reaction tubes on ice by mixing the following components in the given order and the specified final concentrations in a final volume of 500 µl: ddH_2O, 25 mM NaOAc (pH 5.0), 30 µM Ub G76Aha, 0.5 mM Pefabloc, 10 µM H1.2 KxPlk and 0.2 mM SDS. Reactions tubes were flushed with argon and 10 mM THPTA and 5 mM Cu(I) complex were added. The reaction mixtures were again flushed with argon and incubated for 45 min on ice. Reactions were stopped by addition of 50 mM EDTA and centrifuged at 15,000*g* for 5 min at 4 °C. H1.2-Ub conjugates in the supernatant were purified by ultrafiltration (6.4.11).

6.6.2 Nucleosome assembly

The strong nucleosome positioning sequences (NPS) of Widom 601 DNA was used for nucleosome assembly resulting in homogenous nucleosome repeat lengths. Nucleosomes were assembled on 178 bp 601 DNA template[216] (see 6.7.1) by stepwise dilution from 2 M NaCl. All experiments compirising nucleosomes and chromatosomes were performed in siliconized reaction tubes. Assembly was performed in a total volume of 40 µl for titration and in a volume of up to 2 ml for preparative scale in high salt buffer with the specified final concentrations: 100 ng μl^{-1} 601 DNA (with 20 % radioactive labelled 601 DNA in case of ^{32}P-labelling), 6.25 ng μl^{-1} pUC18, 200 ng μl^{-1} BSA and histone octamer as indicated in the respective experiment. After dialysis in 300 ml high salt buffer for 1 h, NaCl concentration of assembly reactions was stepwise decreased by addition of 1x low salt buffer as described in the following:

Buffer added	Volume	c(NaCl)	Time
1x Low salt buffer	500 ml	0.78 M	1 h
1x Low salt buffer	500 ml	0.5 M	1 h
1x Low salt buffer	1000 ml	0.3 M	1 h
1x Low salt buffer	1000 ml	0.23 M	1 h

Finally, nucleosomes were dialyzed in 1000 ml 1x low salt buffer overnight at 4 °C. Assembled nucleosomes were assessed by EMSA with n-PAGE and stored at 4 °C.

6.6.3 Chromatosome assembly

Chromatosome reconstitution was performed by incubation of nucleosomes with increasing amounts of H1.2_WT and H1.2-Ub conjugates in low salt buffer for 30 min at room temperature and analyzed by EMSA with n-PAGE. Preparative chromatosome reconstitution for PARP interaction studies and MNase digestion was carried out as described above with a molar ratio of 1 : 0.75 (nucleosome : H1.2) in a volume of up to 200 µl. H1.2 binding was assayed by EMSA with agarose gel electrophoresis (6.2.5) and chromatosomes were stored at 4 °C.

6.6.4 MNase digestion

For chromatosome stop assay, nucleosomes and chromatosomes were digest by MNase under limiting conditions. Typically, 50 ng μl^{-1} nucleosomes or chromatosomes were incubated with 10 gel units (GU) μl^{-1} MNase and 100 ng μl^{-1} BSA in the supplied 1x MNase reaction buffer in a total volume of 200 µl at 37 °C. Samples of 20 µl were taken after 0–20 min of digestion and reactions were stopped by 1x MNase stop buffer followed by incubation on ice for 10 min. For deproteinization, 100 ng μl^{-1} proteinase K was added and incubated for 1 h at 37 °C. Afterwards the DNA fragments were purified by EtOH precipitation as described in the following. Samples were supplemented with 0.75 M NH_4OAc followed by the addition of 85 µl EtOH (100 %) and incubated for 20 min at -20 °C. After centrifugation for at 15,000*g* for 15 min at 4 °C, the pellet was washed with 100 µl EtOH (70 %) and dried at room temperature. The DNA was resuspended in 10 µl TE buffer and analyzed by n-PAGE (6.2.4).

6.6.5 PARP-chromatosome interaction

Recombinant human (h)PARP-1 was incubated with 601 DNA, radioactive labelled nucleosomes and radioactive labelled chromatosomes respectively, for interaction studies. Typically, in a 10 µl reaction, 115 nM 601 DNA or nucleosomes or chromatosomes were mixed with increasing amounts of hPAPR-1 in 0.5x hPARP-1 storage buffer. Reactions were incubated at room temperature for 20 min. Interaction of hPARP-1 was analyzed by EMSA with agarose gel electrophoresis (6.2.5).

6.6.6 *In vitro* trans(ADP-ribos)ylation

For *in vitro* trans(ADP-ribos)ylation 150 nM hPARP-1 was mixed on ice with 3.4 µM H1.2_WT or H1.2-Ub in the presence of 14 µM *EcoRI* dsDNA and 1 mM NAD^+ in 1x hPARP-1 reaction buffer in a final volume of 10 µl. The negative control was performed without hPARP-1. After incubation for 10 min at 37 °C, reactions were stopped by the addition of 1x SDS-PAGE sample buffer. Samples were analyzed by SDS-PAGE and western blot with anti-PAR and anti-H1.2 antibody.

6.6.7 *In vitro* phosphorylation

For *in vitro* phosphorylation 3.4 µM H1.2 (and/or Ub) was mixed with 0.8 mM ATP and 160 nCi $µl^{-1}$ [γ-^{32}P]ATP in a total volume of 10 µl containing 1x TB buffer on ice. Reactions were started by the addition of 1.6 nM cdk1/cyclin B fusion protein (kindly provided from the Mayer Lab, University of Konstanz), proceeded for 0–120 min at 30 °C and stopped by the addition of 1x SDS-PAGE sample buffer. Samples were analyzed by SDS-PAGE and autoradiography.

6.6.8 *Ex vivo* phosphorylation

Ex vivo phosphorylation of H1.2 was carried out in *Xenopus laevis* oocyte extract supplemented with serine-threonine phosphatase inhibitors to retain cdk1/cyclin B activity exclusively. Thus, prior to experiments, oocyte extract was diluted 1 : 10 in 1x TB* buffer containing *β*-glycerophosphat and $NaVO_3$. Reactions of 8 µl in 1x TB buffer were prepared by mixing 3.4 µM H1.2 with 0.8 mM ATP and 160 nCi $µl^{-1}$ [γ-^{32}P]ATP on ice. Phosphorylation was initiated by the addition of 2 µl diluted oocyte extract, proceeded for 0–10 min at 20 °C and stopped by the addition of 1x SDS-PAGE sample buffer. In this process, oocyte extracts were pipetted with pre-cut tips. Samples were assessed by SDS-PAGE and autoradiography

6.7 Oligonucleotides

6.7.1 Large scale PCR of 601 DNA (178 bp)

The Widom 601 DNA containing DNA sequence was synthesized by GeneArt (Regensburg) and used to amplify a 178 bp fragment (containing the 601 positioning sequence) by PCR with the following parameters (20 reactions of 50 µl):

Component	Concentration
Template	2.7 ng μl^{-1}
HF-buffer	1x
dNTPs	500 µM
Primer fw	800 nM
Primer rev	800 nM
Phusion HF DNA polymerase	0.01 U μl^{-1}

The PCR program was as follows:

Step	Temperature	Time	
Initial denaturation	98 °C	60 sec	
Denaturation	98 °C	10 sec	
Annealing	65 °C	30 sec	
Elongation	72 °C	20 sec	25x
Final elongation	72 °C	10 min	

Resulting in 601 DNA was purified by MinElute Reaction Cleanup Kit. The amplificate was further used as template for large scale PCR with the following parameters (100 reactions of 100 µl):

Component	Concentration
Template	1 ng μl^{-1}
Primer fw	200 nM
Primer rev	200 nM
Taq 2x PCR Master Mix	1x

The PCR program was as follows:

Step	Temperature	Time	
Initial denaturation	98 °C	60 sec	
Denaturation	98 °C	10 sec	
Annealing	55–75 °C	30 sec	
Elongation	72 °C	20 sec	25x
Final elongation	72 °C	10 min	

Purification of amplificate was carried out by ethanol precipitation. Briefly, reaction mixtures were pooled in 500 µl aliquots and supplemented with 700 µl isopropanol (-20 °C). After incubation on ice for 10 min and centrifugation at 15,000*g* for 15 min at 4 °C, the supernatant was discarded, the pellet

was washed with 95 % EtOH (-20 °C) and dried at room temperature. Finally, the pellets were resolved in a total volume of 300 µl ddH_2O and DNA concentration was determined by NanoDrop.

6.7.2 Radioactive labelling of 601 DNA using [γ-^{32}P]ATP

601 DNA was radioactive labelled using [γ-^{32}P]ATP in 5' phosphorylation reactions. Labelling reactions were carried out by mixing the following components in a final volume of 20 µl: ddH_2O, 2.3 µM 601 DNA, 400 nCi µl^{-1} [γ-^{32}P]ATP and 0.4 U µl^{-1} T4 polynucleotide kinase (PNK) in the supplied 1x T4 reaction buffer. Reactions were incubated for 60 min at 37 °C and stopped by PNK inactivation for 5 min at 95 °C. The labelled 601 DNA was purified by gel filtration (Sephadex G25) and eluted in 20 µl ddH_2O.

6.7.3 Hybridization of *EcoRI*

EcoRI ssDNA was synthesized by Metabion and dissolved in 1x TE buffer, heated for 5 min at 95 °C and cooled down to room temperature within 30 min.

7 Appendix

7.1 Sequences

7.1.1 H1.2 expression constructs

E. coli optimized cDNA sequences of H1.2 expression constructs. *NdeI* restriction sites are indicated in cyan and *BamHI* sites in yellow. cDNAs of His-tags and *Strep*-tags are in purple and orange respectively. The codon of initator Met of H1.2 is in bold and sites of AAA → TAG mutation for amber codon suppression are highlighted in green. All constructs were cloned into the multiple cloning site of pET11a using *NdeI* and *BamHI* restriction sites.

H1.2 WT

…CAT**ATG**AGCGAAACCGCACCGGCAGCACCTGCTGCAGCACCTCCGGCAGAAAAAGCACCGGTTAAAAAAAAAGCAGCCAAAAAAGCCGGTGGT
ACCCCGCGTAAAGCAAGCGGTCCTCCGGTTAGCGAACTGATTACCAAAGCAGTTGCAGCAAGCAAAGAACGTAGCGGTGTTAGCCTGGCAGCAC
TGAAAAAAGCACTGGCAGCAGCAGGTTATGATGTGGAAAAAAATAATAGCCGCATTAAACTGGGCCTGAAAAGCCTGGTTAGCAAAGGCACCCT
GGTTCAGACCAAAGGCACCGGTGCAAGCGGTTCATTTAAACTGAATAAAAAAGCCGCAAGCGGTGAAGCAAAACCGAAAGTTAAAAAAGCGGGT
GGCACCAAACCGAAAAAACCGGTTGGTGCAGCAAAAAAACCGAAAAAAGCAGCCGGTGGTGCAACCCCGAAAAAAAGCGCAAAAAAAACGCCGA
AAAAAGCCAAAAAACCGGCAGCAGCAACCGTTACCAAAAAAGTTGCAAAATCTCCGAAAAAAGCGAAAGTTGCGAAACCGAAAAAGGCCGCAAA
AAGCGCAGCAAAAGCAGTTAAACCGAAAGCCGCTAAACCGAAAGTGGTTAAACCGAAGAAAGCGGCACCGAAAAAAAAATAATAAGGATCC…

H1.2_His-*Strep*

…CAT**ATG**AGCGAAACCGCACCGGCAGCACCTGCTGCAGCACCTCCGGCAGAAAAAGCACCGGTTAAAAAAAAAGCAGCCAAAAAAGCCGGTGGT
ACCCCGCGTAAAGCAAGCGGTCCTCCGGTTAGCGAACTGATTACCAAAGCAGTTGCAGCAAGCAAAGAACGTAGCGGTGTTAGCCTGGCAGCAC
TGAAAAAAGCACTGGCAGCAGCAGGTTATGATGTGGAAAAAAATAATAGCCGCATTAAACTGGGCCTGAAAAGCCTGGTTAGCAAAGGCACCCT
GGTTCAGACCAAAGGCACCGGTGCAAGCGGTTCATTTAAACTGAATAAAAAAGCCGCAAGCGGTGAAGCAAAACCGAAAGTTAAAAAAGCGGGT
GGCACCAAACCGAAAAAACCGGTTGGTGCAGCAAAAAAACCGAAAAAAGCAGCCGGTGGTGCAACCCCGAAAAAAAGCGCAAAAAAAACGCCGA
AAAAAGCCAAAAAACCGGCAGCAGCAACCGTTACCAAAAAAGTTGCAAAATCTCCGAAAAAAGCGAAAGTTGCGAAACCGAAAAAGGCCGCAAA
AAGCGCAGCAAAAGCAGTTAAACCGAAAGCCGCTAAACCGAAAGTGGTTAAACCGAAGAAAGCGGCACCGAAAAAAAAACATCATCACCATCAC
CACTGGAGCCACCCGCAGTTCGAAAAGTAATAAGGATCC…

H1.2_*Strep*

…CAT**ATG**AGCGAAACCGCACCGGCAGCACCTGCTGCAGCACCTCCGGCAGAAAAAGCACCGGTTAAAAAAAAAGCAGCCAAAAAAGCCGGTGGT
ACCCCGCGTAAAGCAAGCGGTCCTCCGGTTAGCGAACTGATTACCAAAGCAGTTGCAGCAAGCAAAGAACGTAGCGGTGTTAGCCTGGCAGCAC
TGAAAAAAGCACTGGCAGCAGCAGGTTATGATGTGGAAAAAAATAATAGCCGCATTAAACTGGGCCTGAAAAGCCTGGTTAGCAAAGGCACCCT
GGTTCAGACCAAAGGCACCGGTGCAAGCGGTTCATTTAAACTGAATAAAAAAGCCGCAAGCGGTGAAGCAAAACCGAAAGTTAAAAAAGCGGGT
GGCACCAAACCGAAAAAACCGGTTGGTGCAGCAAAAAAACCGAAAAAAGCAGCCGGTGGTGCAACCCCGAAAAAAAGCGCAAAAAAAACGCCGA
AAAAAGCCAAAAAACCGGCAGCAGCAACCGTTACCAAAAAAGTTGCAAAATCTCCGAAAAAAGCGAAAGTTGCGAAACCGAAAAAGGCCGCAAA
AAGCGCAGCAAAAGCAGTTAAACCGAAAGCCGCTAAACCGAAAGTGGTTAAACCGAAGAAAGCGGCACCGAAAAAAAAATGGAGCCACCCGCAG
TTCGAAAAGTAATAAGGATCC…

H1.2_His

…CAT**ATG**AGCGAAACCGCACCGGCAGCACCTGCTGCAGCACCTCCGGCAGAAAAAGCACCGGTTAAAAAAAAAGCAGCCAAAAAAGCCGGTGGT
ACCCCGCGTAAAGCAAGCGGTCCTCCGGTTAGCGAACTGATTACCAAAGCAGTTGCAGCAAGCAAAGAACGTAGCGGTGTTAGCCTGGCAGCAC
TGAAAAAAGCACTGGCAGCAGCAGGTTATGATGTGGAAAAAAATAATAGCCGCATTAAACTGGGCCTGAAAAGCCTGGTTAGCAAAGGCACCCT
GGTTCAGACCAAAGGCACCGGTGCAAGCGGTTCATTTAAACTGAATAAAAAAGCCGCAAGCGGTGAAGCAAAACCGAAAGTTAAAAAAGCGGGT
GGCACCAAACCGAAAAAACCGGTTGGTGCAGCAAAAAAACCGAAAAAAGCAGCCGGTGGTGCAACCCCGAAAAAAAGCGCAAAAAAAACGCCGA
AAAAAGCCAAAAAACCGGCAGCAGCAACCGTTACCAAAAAAGTTGCAAAATCTCCGAAAAAAGCGAAAGTTGCGAAACCGAAAAAGGCCGCAAA
AAGCGCAGCAAAAGCAGTTAAACCGAAAGCCGCTAAACCGAAAGTGGTTAAACCGAAGAAAGCGGCACCGAAAAAAAAACATCATCACCATCAC
CACTAATAAGGATCC…

H1.2 KxPlk

```
…CATATGAGCGAAACCGCACCGGCAGCACCTGCTGCAGCACCTCCGGCAGAAAAAGCACCGGTTAAAAAAAAAGCAGCCAAAAAAGCCGGTGGT
ACCCCGCGTAAAGCAAGCGGTCCTCCGGTTAGCGAACTGATTACCAAAGCAGTTGCAGCAAGCAAAGAACGTAGCGGTGTTAGCCTGGCAGCAC
TGAAAAAAGCACTGGCAGCAGCAGGTTATGATGTGGAAAAAAATAATAGCCGCATTAAACTGGGCCTGAAAAGCCTGGTTAGCAAAGGCACCCT
GGTTCAGACCAAAGGCACCGGTGCAAGCGGTTCATTTAAACTGAATAAAAAAGCCGCAAGCGGTGAAGCAAAACCGAAAGTTAAAAAAGCGGGT
GGCACCAAACCGAAAAAACCGGTTGGTGCAGCAAAAAAACCGAAAAAAGCAGCCGGTGGTGCAACCCCGAAAAAAAGCGCAAAAAAAACGCCGA
AAAAAGCCAAAAAACCGGCAGCAGCAACCGTTACCAAAAAAGTTGCAAAATCTCCGAAAAAAGCGAAAGTTGCGAAACCGAAAAAGGCCGCAAA
AAGCGCAGCAAAAGCAGTTAAACCGAAAGCCGCTAAACCGAAAGTGGTTAAACCGAAGAAAGCGGCACCGAAAAAAAAACATCATCACCATCAC
CACTAATAAGGATCC…
```

7.1.2 Amino acid sequences of H1.2

Sequences of human H1.2 WT and C-terminal-tagged H1.2 (see 3.1.2).The His-tag is shown in purple and the *Strep*-tag is orange. Sites of Plk incorporation are highlighted with a green background (see 3.1.3):

```
H1.2 WT             MSETAPAAPAAAPPAEKAPVKKKAAKKAGGTPRKASGPPVSELITKAVAASKERSGVSLA 60
H1.2_His-Strep      MSETAPAAPAAAPPAEKAPVKKKAAKKAGGTPRKASGPPVSELITKAVAASKERSGVSLA 60
H1.2_Strep          MSETAPAAPAAAPPAEKAPVKKKAAKKAGGTPRKASGPPVSELITKAVAASKERSGVSLA 60
H1.2_His            MSETAPAAPAAAPPAEKAPVKKKAAKKAGGTPRKASGPPVSELITKAVAASKERSGVSLA 60
H1.2 KxPlk          MSETAPAAPAAAPPAEKAPVKKKAAKKAGGTPRKASGPPVSELITKAVAASKERSGVSLA 60

H1.2 WT             ALKKALAAAGYDVEKNNSRIKLGLKSLVSKGTLVQTKGTGASGSFKLNKKAASGEAKPKV 120
H1.2_His-Strep      ALKKALAAAGYDVEKNNSRIKLGLKSLVSKGTLVQTKGTGASGSFKLNKKAASGEAKPKV 120
H1.2_Strep          ALKKALAAAGYDVEKNNSRIKLGLKSLVSKGTLVQTKGTGASGSFKLNKKAASGEAKPKV 120
H1.2_His            ALKKALAAAGYDVEKNNSRIKLGLKSLVSKGTLVQTKGTGASGSFKLNKKAASGEAKPKV 120
H1.2 KxPlk          ALKKALAAAGYDVEKNNSRIKLGLKSLVSKGTLVQTKGTGASGSFKLNKKAASGEAKPKV 120

H1.2 WT             KKAGGTKPKKPVGAAKKPKKAAGGATPKKSAKKTPKKAKKPAAATVTKKVAKSPKKAKVA 180
H1.2_His-Strep      KKAGGTKPKKPVGAAKKPKKAAGGATPKKSAKKTPKKAKKPAAATVTKKVAKSPKKAKVA 180
H1.2_Strep          KKAGGTKPKKPVGAAKKPKKAAGGATPKKSAKKTPKKAKKPAAATVTKKVAKSPKKAKVA 180
H1.2_His            KKAGGTKPKKPVGAAKKPKKAAGGATPKKSAKKTPKKAKKPAAATVTKKVAKSPKKAKVA 180
H1.2 KxPlk          KKAGGTKPKKPVGAAKKPKKAAGGATPKKSAKKTPKKAKKPAAATVTKKVAKSPKKAKVA 180

H1.2 WT             KPKKAAKSAAKAVKPKAAKPKVVKPKKAAPKKK-------------- 213
H1.2_His-Strep      KPKKAAKSAAKAVKPKAAKPKVVKPKKAAPKKKHHHHHHWSHPQFEK 227
H1.2_Strep          KPKKAAKSAAKAVKPKAAKPKVVKPKKAAPKKK------WSHPQFEK 221
H1.2_His            KPKKAAKSAAKAVKPKAAKPKVVKPKKAAPKKKHHHHHH-------- 219
H1.2 KxPlk          KPKKAAKSAAKAVKPKAAKPKVVKPKKAAPKKKHHHHHH-------- 219
```

7.1.3 Amino acid sequence of Ub G76Aha

Sequence of Ub G76Aha after thrombin cleavage (as mentioned in 3.1.5). Additional residues derived from the thrombin cleavage site are underlined. The site of Aha incorporation according to the native Ub sequence at G76M is indicated in blue:

```
                        |--> Ubiquitin
Ub G76Aha           GSRRASVGSQIFVKTLTGKTITLEVEPSDTIENVKAKIQDKEGIPPDQQRLIFAGKQLED 52
                    GRTLSDYNIQKESTLHLVLRLRGM 76
```

7.1.4 Alignment of human H1 variants

Amino acid sequence alignment was performed using T-Coffee[86]. PDB IDs and corresponding names of hH1 variants are indicated.

```
  |PDB ID|name
sp|P07305|H10_H   MTENST------SAPA-AK-P-------------------------------------------
sp|Q02539|H11_H   MSETVP------PAPA-AS----------------------------AAPEK--P---------
sp|P16403|H12_H   MSETAP------AAPA-AA----------------------------PPAEK--A---------
sp|P16402|H13_H   MSETAP------LAPT-IP----------------------------APAEK--T---------
sp|P10412|H14_H   MSETAP------AAPA-AP----------------------------APAEK--T---------
sp|P16401|H15_H   MSETAP------AETA-TP----------------------------APVEK--S---------
sp|Q92522|H1X_H   MSVELE--E---ALPV-TT--------------------------------AE--G---------
sp|P22492|H1T_H   MSETVP------AASA-SA-----GV----------------------AAMEK--L---------
sp|Q75WM6|H1FNT   MEQALT------GEAQ-SRWPRRGGSGAMAEA--------------PGPSGE--SRGHS----
sp|Q8IZA3|H1FOO   MAPGSVTSDISPSSTS-TA------------------------------GSSR--S---------
sp|P60008|HILS1   MLHAST------IWHLRSTPPRRKQWGHCDPHRILVASEVTTEITSPTPAPRAQVCGGQPWVT
cons              *

sp|P07305|H10_H   ------------------------------------------KR--------A-----K---A
sp|Q02539|H11_H   ----LAGKK----------------------AK---------KP--------AKAA--A---A
sp|P16403|H12_H   ----PVKKK----------------------AA---------KK--------A-----G---G
sp|P16402|H13_H   ----PVKKK----------------------AK---------K---------A-GA--T---A
sp|P10412|H14_H   ----PVKKK----------------------AR---------KS--------A-----G---A
sp|P16401|H15_H   ----PAKKK----------------------AT---------KK--------AAGA--G---A
sp|Q92522|H1X_H   ----MA-KK----------------------VT---------KAGGSAALSPSKKR--K---N
sp|P22492|H1T_H   ----PTKKR----------------------GR---------KP--------A-GL--I---S
sp|Q75WM6|H1FNT   ----ATQLP----------------------AE---------KT--------V-----G---G
sp|Q8IZA3|H1FOO   ----PESEK----------------------PG---------PS--------HGGVPPGGPSH
sp|P60008|HILS1   VLDPLSGHTGREAERHFATVSISAVELKYCHGWRPAGQRVPSKTA--------TG--QR---T
cons

sp|P07305|H10_H   S--KK--STDHPKYSDMIVAAIQAEKNRAGSSRQSIQK-YIKS--H-YKVGENADSQIKLSIK
sp|Q02539|H11_H   S--KK--KPAGPSVSELIVQAASSSKERGGVSLAALKK-ALAA--AGYDV-EKNNSRIKLGIK
sp|P16403|H12_H   T--PR--KASGPPVSELITKAVAASKERSGVSLAALKK-ALAA--AGYDV-EKNNSRIKLGLK
sp|P16402|H13_H   G--KR--KASGPPVSELITKAVAASKERSGVSLAALKK-ALAA--AGYDV-EKNNSRIKLGLK
sp|P10412|H14_H   A--KR--KASGPPVSELITKAVAASKERSGVSLAALKK-ALAA--AGYDV-EKNNSRIKLGLK
sp|P16401|H15_H   A--KR--KATGPPVSELITKAVAASKERNGLSLAALKK-ALAA--GGYDV-EKNNSRIKLGLK
sp|Q92522|H1X_H   S--KK--KNQPGKYSQLVVETIRRLGERNGSSLAKIYTEAKKV--PWFDQ-QNGRTYLKYSIK
sp|P22492|H1T_H   A--SR--KVPNLSVSKLITEALSVSQERVGMSLVALKK-ALAA--AGYDV-EKNNSRIKLSLK
sp|Q75WM6|H1FNT   P--SRGCSSSVLRVSQLVLQAIST---HKGLTLAALKK-ELRN--AGYEV-RRKSGRHEAP--
sp|Q8IZA3|H1FOO   SSLPV--GRRHPPVLRMVLEALQAGEQRRGTSVAAIKL-YILHKYPTVDV-LRFKYLLKQALA
sp|P60008|HILS1   C--AK--PCQKPSTSKVILRAVADKGTCKYVSLATLKK-AVST--TGYDM-ARNAYHFKRVLK
cons                          ::  :          :   :            .   .     :

sp|P07305|H10_H   RLVTTGVLK---QTKGVGASGSFRLAKSDE---------PKKSVAFKK----TKKEIKKVA--
sp|Q02539|H11_H   SLVSKGTLV---QTKGTGASGSFKLNKKAS---------SVETKPGASKV-AT--K-TKATGA
sp|P16403|H12_H   SLVSKGTLV---QTKGTGASGSFKLNKKAA---------SGEAKPKVKKAGGT--KPKKPVGA
sp|P16402|H13_H   SLVSKGTLV---QTKGTGASGSFKLNKKAA---------SGEGKPKAKKAGAA--KPRKPAGA
sp|P10412|H14_H   SLVSKGTLV---QTKGTGASGSFKLNKKAA---------SGEAKPKAKKAGAA--KAKKPAGA
sp|P16401|H15_H   SLVSKGTLV---QTKGTGASGSFKLNKKAA---------SGEAKPKAKKAGAA--KAKKPAGA
sp|Q92522|H1X_H   ALVQNDTLL---QVKGTGANGSFKLNRKKL---------EGGGERRGAPAAAT--A---PAPT
sp|P22492|H1T_H   SLVNKGILV---QTRGTGASGSFKLSKKVI---------PKSTRSKAKKSVSA--KTKKLVLS
sp|Q75WM6|H1FNT   RGQAKATLL---RVSGSDAAGYFRVWKVPK---------PRRKPGRARQEEGTRAPWRTPA--
sp|Q8IZA3|H1FOO   TGMRRGLLARPLNSKARGATGSFKLVPKHKKKIQPRKMAPATAPRRAGEAKGK--GPKKPSEA
sp|P60008|HILS1   GLVDK------------GSAGSFTLGKKQA---------SKS-KLKVKRQRQQ--RWRSGQRP
cons                           .: * * :

sp|P07305|H10_H   T--PKKASKP----KKAASKAPT--KKPKA-T---PVKKAKKKLA--------------ATP-
sp|Q02539|H11_H   SKKLKKATGA----SKKSVKTPKKAKKPAA---TR-------KSS--------------KNP-
sp|P16403|H12_H   AKKPKKAAGGATP-KKSAKKTPKKAKKPAAATVTK-------KVA--------------KSP-
sp|P16402|H13_H   AKKPKKVAGAATP-KKSIKKTPKKVKKPATAAGTK-------KVA--------------KSA-
sp|P10412|H14_H   AKKPKKATGAATP-KKSAKKTPKKAKKPAAAA-GA-------KKA--------------KSP-
sp|P16401|H15_H   T--PKKAKKAAGA-KKAVKKTPKKAKKPAAAG-VK-------KVA--------------KSP-
sp|Q92522|H1X_H   AHKAKKAAPGAAG-SRRADKKPARGQKPEQRS-H--------KKG--------------AGA-
sp|P22492|H1T_H   R--DSKS---------PKTAKTNKRAKKPRAT--TP-------KTV--------------RSG-
sp|Q75WM6|H1FNT   A--PRSSRRRRQPLRKAARKARE-VWRRNARAKAKANARARRTRR--------------ARP-
sp|Q8IZA3|H1FOO   KEDPPNVG----K-VKKAAKRPAKVQKPPPKP-GA-------ATEKARKQGGAAKDTRAQSGE
sp|P60008|HILS1   FGQHRSLLGS----KQGHKRLIK-------------------------------------------
cons                   .            :
```

```
sp|P07305|H10_H   -KKAKKPKT-VKAKP------------------------------VKAS----KPKK----AK
sp|Q02539|H11_H   -KKPK---T-VKPKKVAKSP----A-------------------KAKAV----KPKAAK--AR
sp|P16403|H12_H   -KKAK---V-AKPKKAAKSA----A---------------------KAV----KPKAAK----
sp|P16402|H13_H   -KKVK---T-PQPKKAAKSP----A-------------------KAKAP----KPKAAK--PK
sp|P10412|H14_H   -KKAK---A-AKPKKAPKSP----A-------------------KAKAV----KPKAAK--PK
sp|P16401|H15_H   -KKAK---AAAKPKKATKSP----A-------------------KPKAV----KPKAAK--PK
sp|Q92522|H1X_H   -KKDK---G-GKAKKTAAAG----G---------------------KKV----K-KAAK--PS
sp|P22492|H1T_H   -RKAK---G-AKGKQQQKSP----V-------------------KARAS----KSKLTQ----
sp|Q75WM6|H1FNT   -R-AKEPPC-ARAKEEAGATAADEG-------------------RGQAVKEDTTPRSGKDKRR
sp|Q8IZA3|H1FOO   ARKV----P-PKPDKAMRAP----SSAGGLSRKAKAKGSRSSQGDAEAY----RKTKAE--SK
sp|P60008|HILS1   -----------GVRRV-----------------------------------------AK----
cons

sp|P07305|H10_H   P-------------------------------------------------VKPKAK------
sp|Q02539|H11_H   V-------------------------------------------------TKPKTA------
sp|P16403|H12_H   ---------------------------------------------------PKVV------
sp|P16402|H13_H   S-------------------------------------------------GKPKVT------
sp|P10412|H14_H   T-------------------------------------------------AKPKAA------
sp|P16401|H15_H   AAKPKA--------------------------------------------AKPKAA------
sp|Q92522|H1X_H   ---------------------------------------------------VPKVP------
sp|P22492|H1T_H   ----------------------------------------------------HHEV------
sp|Q75WM6|H1FNT   S-------------------------------------------------SKPREE------
sp|Q8IZA3|H1FOO   SSKPTASKVKNGAASPTKKKVVAKAKAPKAGQGPNTKAAAPAKGSGSKVVPAHLSRKTEAPKG
sp|P60008|HILS1   ---------------------------------------------------CHCN------
cons

sp|P07305|H10_H   -----SSAKRA-----GKKK--
sp|Q02539|H11_H   -----KPKKAA-----PKKK--
sp|P16403|H12_H   -----KPKKAA-----PKKK--
sp|P16402|H13_H   -----KAKKAA-----PKKK--
sp|P10412|H14_H   -----KPKKAA-----AKKK--
sp|P16401|H15_H   -----KAKKAA-----AKKK--
sp|Q92522|H1X_H   -----KGR-----------K--
sp|P22492|H1T_H   -----NVRKAT-----SK-K--
sp|Q75WM6|H1FNT   -----KQEPKK----PAQRTIQ
sp|Q8IZA3|H1FOO   PRKAGLPIKASSSKVSSQRAEA
sp|P60008|HILS1   ----------------------
cons
```

7.1.5 Sequence of 601 DNA

207 bp-long DNA sequence, containing the Widom 601 NPS according to [216]. The linker DNA is highlighted in green and the amplified 178 bp-long 601 DNA fragment used for nucleosome assembly is underlined. The oligonucleotide was synthesized by GeneArt (Regensburg) and provided in the pMA vector.

…AGATATCGGA CCCTATACGC GGCCGCCCTG GAGAATCCCG GTGCCGAGGC CGCTCAATTG GTCGTAGCAA GCTCTAGCAC
CGCTTAAACG CACGTACGCG CTGTCCCCCG CGTTTTAACC GCCAAGGGGA TTACTCCCTA GTCTCCAGGC ACGTGTCAGA
TATATACATC CTGTGCATGT GGATCCGAAT TCATATTAAT TAATACT…

7.2 Mass spectrometry

7.2.1 ESI-MS spectra of H1.2 KxPlk mutants

ESI mass spectra profile (on the left) of H1.2 K46Plk, H1.2 K64Plk, H1.2 K75Plk and H1.2 K97Plk and corresponding deconvoluted mass spectra (right) according to Figure 3.7.

H1.2 K46Plk

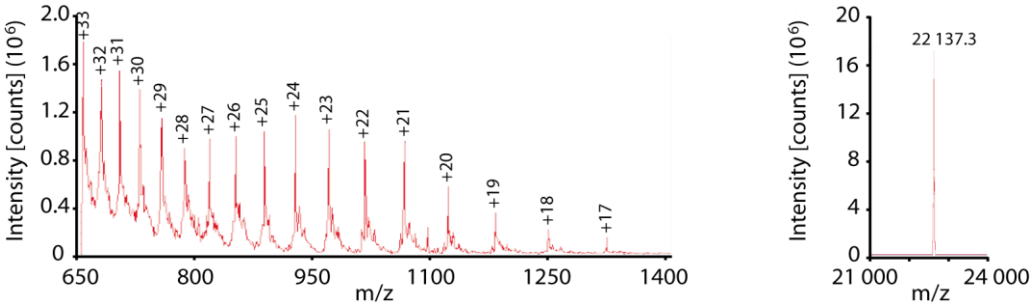

H1.2 K64Plk

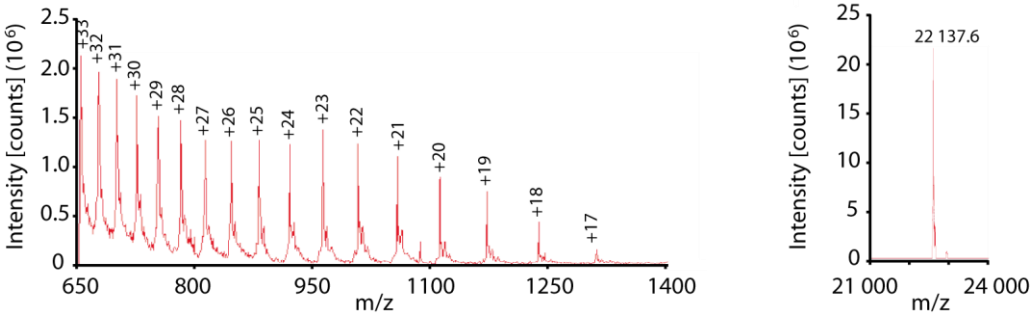

H1.2 K75Plk

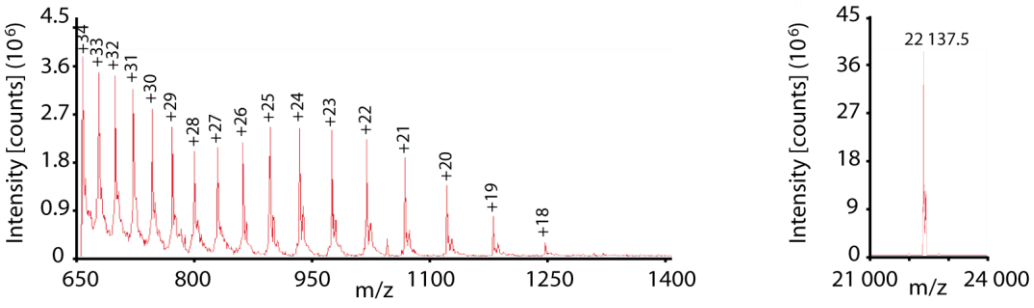

H1.2 K97Plk

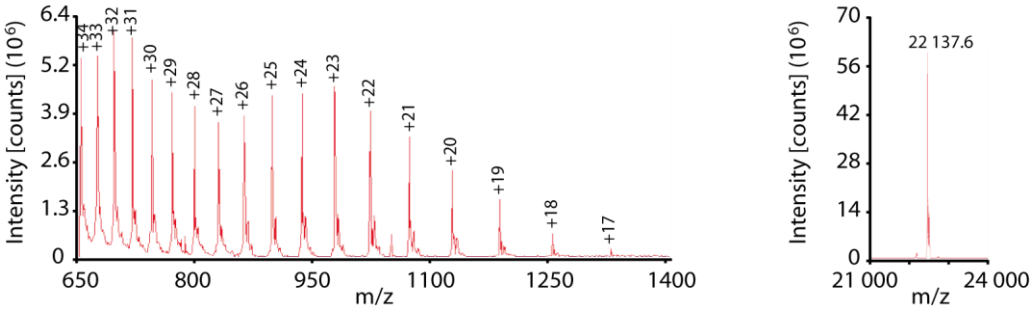

7.2.2 MS/MS spectra of H1.2-Ub conjugates

In the following, MS/MS spectra of the triazole linked fragments derived from tryptic in-gel digestion of H1.2 64Ub, H1.2 75Ub and H1.2 97Ub are shown with Plk (X) and Aha (U). MS/MS data correspond to the values listed in chapter 3.1.9.

H1.2 64Ub

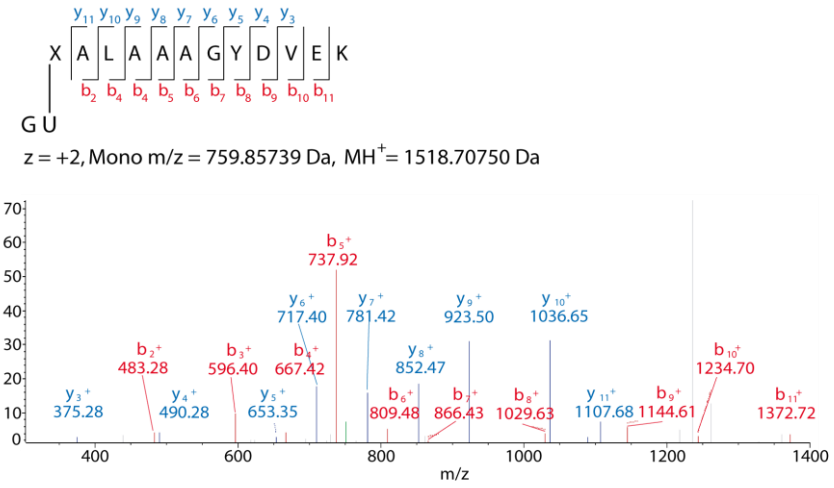

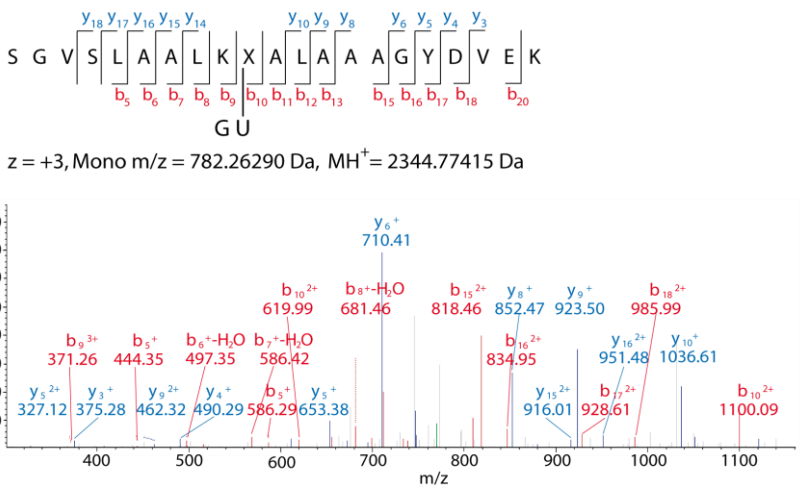

H1.2 75Ub

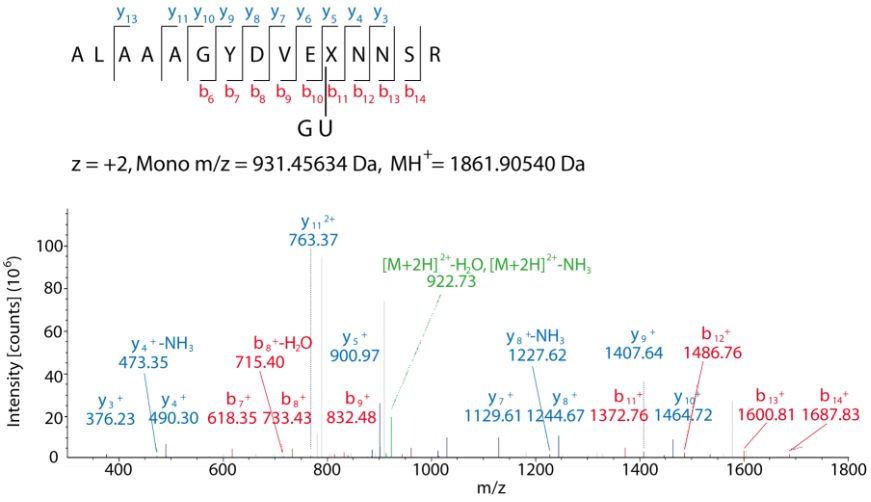

H1.2 97Ub

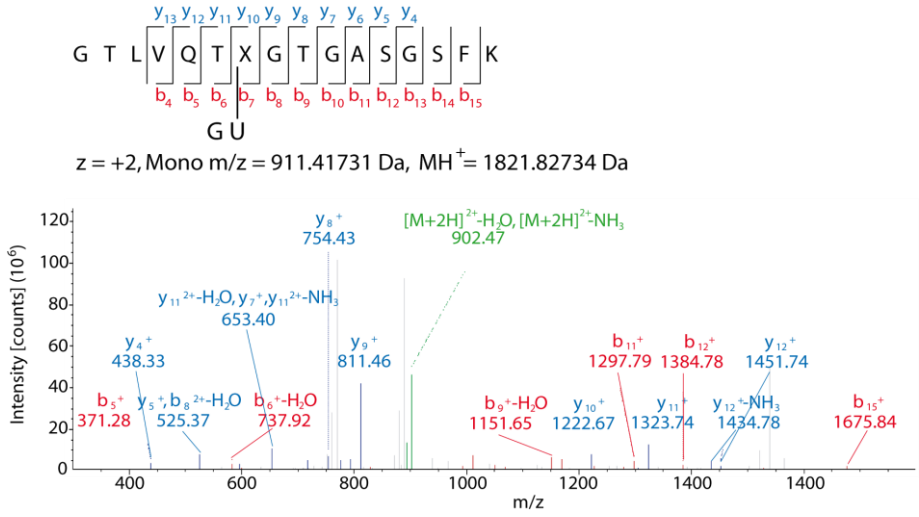

8 Abbreviations

^{32}P	phosphor 32 isotope
aa	amino acid
aaRS	aminoacyl-tRNA synthetase
ACS	amber codon suppression
ADP	adenosine diphosphate ribose
ART	ADP-ribosyltransferases
ARTD	ADP-ribosyltransferase diphtheria toxin-like
ATP	Adenosine diphosphate
Boc	*tert*-butyloxycarbonyl
bp	base pair
CD	circular dichroism
cdk	cell cycle dependent kinase
ChIP	chromatin immunoprecipitation
chrom	chromatosome
crDNA	competitor DNA
CTD	C-terminal domain
CuAAC	Cu(I)-catalyzed azide-alkyne cycloaddition
DNA	deoxyribonucleic acid / Desoxyribonukleinsäure
dNTP	2'-deoxyribonucleoside-5'-triphosphate
ds	double stranded
DTNP	2,2'-dithiobias(5-nitropyridine)
DUB	deubiquitinating enzyme
E. coli	*Escherichia coli*
e.q.	equivalent
ECL	enhanced chemiluminescence
eGFP	enhanced green fluorescent protein
EMSA	electrophoretic mobility shift assay
ESI-MS	electrospray-ionization mass spectrometry
EtBr	ethidium bromide
Fig.	figure
FPLC	fast protein liquid chromatography
FRAP	fluorescence recovery after photobleaching
fw	forward
GD	globular domain / globuläre Domäne
GST	glutathione-S-transferase
GU	gel units
HABA	2-(4'-hydroxy-benzeneazo)benzoic acid
HF	high fidelity
His-tag	hexahistidine-tag
HPLC	high performance liquid chromatography
IEX	ion exchange chromatography
IMAC	immobilized metal ion affinity chromatography
mdeg	measured in millidegrees
MNase	micrococcal nuclease
MS	mass spectrometry / Massenspektrometrie
NAD	nicotinamide adenine dinucleotide
NCL	native chemical ligation

NCP	nucleosome core particle
n-LS	n-Lauroylsarcosine
NMM	New minimal medium
NMR	nuclear magnetic resonance
nPAGE	native polyacrylamide gel electrophoresis
NPS	nucleosome positioning sequence
NRL	nucleosome repeat length
nuc	nucleosome
OD_{600}	optical density (λ=600 nm)
PAGE	polyacrylamide gel electrophoresis
PAR	poly(ADP-ribose)
PARG	poly(ADP-ribose) glycohydrolase
PARP	poly(ADP-ribose) polymerase / Poly(ADP-ribose)-Polymerase
PBS	phosphate-buffered saline
PCA	perchloric acid
PCNA	proliferating cell nuclear antigen
PCR	polymerase chain reaction
PDB	Protein Data Bank
Plk	propargyl-derivatized lysine
PTM	posttranslational modification
Pyl	pyrrolysine
PylRS	pyrrolysyl-tRNA synthetase
rev	reverse
RF	release factor
ROS	reactive oxygen species
s.d.	standard deviation
SDM	site-directed mutagenesis
SDS	sodium dodecyl sulfate
Sec	selenocysteine
SPI	selective pressure incorporation
ss	single stranded
TBTA	tris[(1-benzyl-1,2,3-triazol-4-yl)methyl]amine
TECP	tris(2-carboxyethyl)phosphine
TF	transcription factor
THPTA	tris-(hydroxypropyltriazolylmethyl)amine
tRNA	transfer ribonucleic acid
UAA	unnatural amino acid
Ub Aha	Ubiquitin G76Aha
UV	ultraviolet
WB	western blot
WHD	winged helix domain
WT	wild-type

9 References

1. Luger, K., et al., *Crystal structure of the nucleosome core particle at 2.8 A resolution.* Nature, 1997. **389**(6648): p. 251-60.
2. Carruthers, L.M., et al., *Linker histones stabilize the intrinsic salt-dependent folding of nucleosomal arrays: mechanistic ramifications for higher-order chromatin folding.* Biochemistry, 1998. **37**(42): p. 14776-87.
3. Thoma, F., T. Koller, and A. Klug, *Involvement of histone H1 in the organization of the nucleosome and of the salt-dependent superstructures of chromatin.* J Cell Biol, 1979. **83**(2 Pt 1): p. 403-27.
4. Allan, J., et al., *The structure of histone H1 and its location in chromatin.* Nature, 1980. **288**(5792): p. 675-9.
5. Ramakrishnan, V., et al., *Crystal structure of globular domain of histone H5 and its implications for nucleosome binding.* Nature, 1993. **362**(6417): p. 219-23.
6. Kouzarides, T., *Chromatin modifications and their function.* Cell, 2007. **128**(4): p. 693-705.
7. Strahl, B.D. and C.D. Allis, *The language of covalent histone modifications.* Nature, 2000. **403**(6765): p. 41-5.
8. Pachov, G.V., R.R. Gabdoulline, and R.C. Wade, *On the structure and dynamics of the complex of the nucleosome and the linker histone.* Nucleic Acids Res, 2011. **39**(12): p. 5255-63.
9. Grewal, S.I. and S. Jia, *Heterochromatin revisited.* Nat Rev Genet, 2007. **8**(1): p. 35-46.
10. Kireeva, N., et al., *Visualization of early chromosome condensation: a hierarchical folding, axial glue model of chromosome structure.* J Cell Biol, 2004. **166**(6): p. 775-85.
11. Woodcock, C.L. and R.P. Ghosh, *Chromatin higher-order structure and dynamics.* Cold Spring Harb Perspect Biol, 2010. **2**(5): p. a000596.
12. Hansen, J.C., *Conformational dynamics of the chromatin fiber in solution: determinants, mechanisms, and functions.* Annu Rev Biophys Biomol Struct, 2002. **31**: p. 361-92.
13. Szerlong, H.J. and J.C. Hansen, *Nucleosome distribution and linker DNA: connecting nuclear function to dynamic chromatin structure.* Biochem Cell Biol, 2011. **89**(1): p. 24-34.
14. Kireev, I., et al., *In vivo immunogold labeling confirms large-scale chromatin folding motifs.* Nat Methods, 2008. **5**(4): p. 311-3.
15. Konig, P., et al., *The three-dimensional structure of in vitro reconstituted Xenopus laevis chromosomes by EM tomography.* Chromosoma, 2007. **116**(4): p. 349-72.
16. Fraser, P., *Transcriptional control thrown for a loop.* Curr Opin Genet Dev, 2006. **16**(5): p. 490-5.
17. Marsden, M.P. and U.K. Laemmli, *Metaphase chromosome structure: evidence for a radial loop model.* Cell, 1979. **17**(4): p. 849-58.
18. Finch, J.T. and A. Klug, *Solenoidal model for superstructure in chromatin.* Proc Natl Acad Sci U S A, 1976. **73**(6): p. 1897-901.
19. McGhee, J.D. and G. Felsenfeld, *Nucleosome structure.* Annu Rev Biochem, 1980. **49**: p. 1115-56.
20. Robinson, P.J. and D. Rhodes, *Structure of the '30 nm' chromatin fibre: a key role for the linker histone.* Curr Opin Struct Biol, 2006. **16**(3): p. 336-43.
21. Song, F., et al., *Cryo-EM study of the chromatin fiber reveals a double helix twisted by tetranucleosomal units.* Science, 2014. **344**(6182): p. 376-80.
22. Williams, S.P., et al., *Chromatin fibers are left-handed double helices with diameter and mass per unit length that depend on linker length.* Biophys J, 1986. **49**(1): p. 233-48.
23. Woodcock, C.L., L.L. Frado, and J.B. Rattner, *The higher-order structure of chromatin: evidence for a helical ribbon arrangement.* J Cell Biol, 1984. **99**(1 Pt 1): p. 42-52.
24. McGinty, R.K. and S. Tan, *Nucleosome Structure and Function.* Chemical Reviews, 2015. **115**(6): p. 2255-2273.
25. Schlick, T., J. Hayes, and S. Grigoryev, *Toward convergence of experimental studies and theoretical modeling of the chromatin fiber.* J Biol Chem, 2012. **287**(8): p. 5183-91.
26. Grigoryev, S.A., et al., *Evidence for heteromorphic chromatin fibers from analysis of nucleosome interactions.* Proc Natl Acad Sci U S A, 2009. **106**(32): p. 13317-22.
27. Felsenfeld, G. and M. Groudine, *Controlling the double helix.* Nature, 2003. **421**(6921): p. 448-53.

28. Kornberg, R.D., *Chromatin structure: a repeating unit of histones and DNA.* Science, 1974. **184**(4139): p. 868-71.
29. Arents, G., et al., *The nucleosomal core histone octamer at 3.1 A resolution: a tripartite protein assembly and a left-handed superhelix.* Proc Natl Acad Sci U S A, 1991. **88**(22): p. 10148-52.
30. Noll, M. and R.D. Kornberg, *Action of micrococcal nuclease on chromatin and the location of histone H1.* J Mol Biol, 1977. **109**(3): p. 393-404.
31. Richmond, T.J., et al., *Structure of the nucleosome core particle at 7 A resolution.* Nature, 1984. **311**(5986): p. 532-7.
32. Simpson, R.T., *Structure of the chromatosome, a chromatin particle containing 160 base pairs of DNA and all the histones.* Biochemistry, 1978. **17**(25): p. 5524-31.
33. Whitlock, J.P., Jr. and R.T. Simpson, *Removal of histone H1 exposes a fifty base pair DNA segment between nucleosomes.* Biochemistry, 1976. **15**(15): p. 3307-14.
34. Thatcher, T.H. and M.A. Gorovsky, *Phylogenetic analysis of the core histones H2A, H2B, H3, and H4.* Nucleic Acids Res, 1994. **22**(2): p. 174-9.
35. Eickbush, T.H. and E.N. Moudrianakis, *The histone core complex: an octamer assembled by two sets of protein-protein interactions.* Biochemistry, 1978. **17**(23): p. 4955-64.
36. Kornberg, R.D. and J.O. Thomas, *Chromatin structure; oligomers of the histones.* Science, 1974. **184**(4139): p. 865-8.
37. Thomas, J.O. and R.D. Kornberg, *An octamer of histones in chromatin and free in solution.* Proc Natl Acad Sci U S A, 1975. **72**(7): p. 2626-30.
38. du Preez, L.L. and H.G. Patterton, *Secondary structures of the core histone N-terminal tails: their role in regulating chromatin structure.* Subcell Biochem, 2013. **61**: p. 37-55.
39. Zheng, C. and J.J. Hayes, *Intra- and inter-nucleosomal protein-DNA interactions of the core histone tail domains in a model system.* J Biol Chem, 2003. **278**(26): p. 24217-24.
40. Portela, A. and M. Esteller, *Epigenetic modifications and human disease.* Nat Biotechnol, 2010. **28**(10): p. 1057-68.
41. McBryant, S.J., V.H. Adams, and J.C. Hansen, *Chromatin architectural proteins.* Chromosome Res, 2006. **14**(1): p. 39-51.
42. Bates, D.L. and J.O. Thomas, *Histones H1 and H5: one or two molecules per nucleosome?* Nucleic Acids Res, 1981. **9**(22): p. 5883-94.
43. Fan, Y., et al., *H1 linker histones are essential for mouse development and affect nucleosome spacing in vivo.* Mol Cell Biol, 2003. **23**(13): p. 4559-72.
44. Fan, Y., et al., *Histone H1 depletion in mammals alters global chromatin structure but causes specific changes in gene regulation.* Cell, 2005. **123**(7): p. 1199-212.
45. VanHolde, K.E., *Chromatin*. 1989, New York: Springer Verlag.
46. Thomas, J.O., *Histone H1: location and role.* Curr Opin Cell Biol, 1999. **11**(3): p. 312-7.
47. Travers, A., *The location of the linker histone on the nucleosome.* Trends Biochem Sci, 1999. **24**(1): p. 4-7.
48. Meyer, S., et al., *From crystal and NMR structures, footprints and cryo-electron-micrographs to large and soft structures: nanoscale modeling of the nucleosomal stem.* Nucleic Acids Res, 2011. **39**(21): p. 9139-54.
49. Zhou, Y.B., et al., *Position and orientation of the globular domain of linker histone H5 on the nucleosome.* Nature, 1998. **395**(6700): p. 402-5.
50. Li, G. and P. Zhu, *Structure and organization of chromatin fiber in the nucleus.* FEBS Lett, 2015. **589**(20 Pt A): p. 2893-904.
51. Vyas, P. and D.T. Brown, *N- and C-terminal domains determine differential nucleosomal binding geometry and affinity of linker histone isotypes H1(0) and H1c.* J Biol Chem, 2012. **287**(15): p. 11778-87.
52. Allan, J., et al., *Roles of H1 domains in determining higher order chromatin structure and H1 location.* J Mol Biol, 1986. **187**(4): p. 591-601.
53. Syed, S.H., et al., *Single-base resolution mapping of H1-nucleosome interactions and 3D organization of the nucleosome.* Proc Natl Acad Sci U S A, 2010. **107**(21): p. 9620-5.
54. Crane-Robinson, C., *How do linker histones mediate differential gene expression?* Bioessays, 1999. **21**(5): p. 367-71.
55. Cerf, C., et al., *Homo- and heteronuclear two-dimensional NMR studies of the globular domain of histone H1: sequential assignment and secondary structure.* Biochemistry, 1993. **32**(42): p. 11345-51.
56. Cerf, C., et al., *Homo- and heteronuclear two-dimensional NMR studies of the globular domain of histone H1: full assignment, tertiary structure, and comparison with the globular domain of histone H5.* Biochemistry, 1994. **33**(37): p. 11079-86.

57. Krylov, D., et al., *Histones H1 and H5 interact preferentially with crossovers of double-helical DNA.* Proc Natl Acad Sci U S A, 1993. **90**(11): p. 5052-6.
58. Zhou, B.R., et al., *Structural insights into the histone H1-nucleosome complex.* Proc Natl Acad Sci U S A, 2013. **110**(48): p. 19390-5.
59. Brown, D.T., T. Izard, and T. Misteli, *Mapping the interaction surface of linker histone H1(0) with the nucleosome of native chromatin in vivo.* Nat Struct Mol Biol, 2006. **13**(3): p. 250-5.
60. Hendzel, M.J., et al., *The C-terminal domain is the primary determinant of histone H1 binding to chromatin in vivo.* J Biol Chem, 2004. **279**(19): p. 20028-34.
61. Bradbury, E.M., et al., *Studies on the role and mode of operation of the very-lysine-rich histone H1 (F1) in eukaryote chromatin. Histone H1 in chromatin and in H1 - DNA complexes.* Eur J Biochem, 1975. **57**(1): p. 97-105.
62. Lu, X. and J.C. Hansen, *Identification of specific functional subdomains within the linker histone H10 C-terminal domain.* J Biol Chem, 2004. **279**(10): p. 8701-7.
63. Caterino, T.L., H. Fang, and J.J. Hayes, *Nucleosome linker DNA contacts and induces specific folding of the intrinsically disordered H1 carboxyl-terminal domain.* Mol Cell Biol, 2011. **31**(11): p. 2341-8.
64. Hamiche, A., et al., *Linker histone-dependent DNA structure in linear mononucleosomes.* J Mol Biol, 1996. **257**(1): p. 30-42.
65. Fang, H., D.J. Clark, and J.J. Hayes, *DNA and nucleosomes direct distinct folding of a linker histone H1 C-terminal domain.* Nucleic Acids Res, 2012. **40**(4): p. 1475-84.
66. Th'ng, J.P., et al., *H1 family histones in the nucleus. Control of binding and localization by the C-terminal domain.* J Biol Chem, 2005. **280**(30): p. 27809-14.
67. Fan, L. and V.A. Roberts, *Complex of linker histone H5 with the nucleosome and its implications for chromatin packing.* Proc Natl Acad Sci U S A, 2006. **103**(22): p. 8384-9.
68. Zhou, B.R., et al., *Structural Mechanisms of Nucleosome Recognition by Linker Histones.* Mol Cell, 2015. **59**(4): p. 628-38.
69. Puigdomenech, P., et al., *Isolation of a 167 basepair chromatosome containing a partially digested histone H5.* FEBS Lett, 1983. **154**(1): p. 151-5.
70. Pruss, D., et al., *An asymmetric model for the nucleosome: a binding site for linker histones inside the DNA gyres.* Science, 1996. **274**(5287): p. 614-7.
71. An, W., et al., *Linker histone protects linker DNA on only one side of the core particle and in a sequence-dependent manner.* Proc Natl Acad Sci U S A, 1998. **95**(7): p. 3396-401.
72. Izzo, A., K. Kamieniarz, and R. Schneider, *The histone H1 family: specific members, specific functions?* Biol Chem, 2008. **389**(4): p. 333-43.
73. Happel, N., et al., *H1 subtype expression during cell proliferation and growth arrest.* Cell Cycle, 2009. **8**(14): p. 2226-32.
74. Parseghian, M.H. and B.A. Hamkalo, *A compendium of the histone H1 family of somatic subtypes: an elusive cast of characters and their characteristics.* Biochem Cell Biol, 2001. **79**(3): p. 289-304.
75. Albig, W. and D. Doenecke, *The human histone gene cluster at the D6S105 locus.* Hum Genet, 1997. **101**(3): p. 284-94.
76. Albig, W., et al., *Isolation and characterization of two human H1 histone genes within clusters of core histone genes.* Genomics, 1991. **10**(4): p. 940-8.
77. Eick, S., et al., *Human H1 histones: conserved and varied sequence elements in two H1 subtype genes.* Eur J Cell Biol, 1989. **49**(1): p. 110-5.
78. Wood, C., et al., *Post-translational modifications of the linker histone variants and their association with cell mechanisms.* FEBS J, 2009. **276**(14): p. 3685-97.
79. Zlatanova, J. and D. Doenecke, *Histone H1 zero: a major player in cell differentiation?* FASEB J, 1994. **8**(15): p. 1260-8.
80. Martianov, I., et al., *Polar nuclear localization of H1T2, a histone H1 variant, required for spermatid elongation and DNA condensation during spermiogenesis.* Proc Natl Acad Sci U S A, 2005. **102**(8): p. 2808-13.
81. Sarg, B., et al., *Testis-specific linker histone H1t is multiply phosphorylated during spermatogenesis. Identification of phosphorylation sites.* J Biol Chem, 2009. **284**(6): p. 3610-8.
82. Yan, W., et al., *HILS1 is a spermatid-specific linker histone H1-like protein implicated in chromatin remodeling during mammalian spermiogenesis.* Proc Natl Acad Sci U S A, 2003. **100**(18): p. 10546-51.
83. Tanaka, M., et al., *A mammalian oocyte-specific linker histone gene H1oo: homology with the genes for the oocyte-specific cleavage stage histone (cs-H1) of sea urchin and the B4/H1M histone of the frog.* Development, 2001. **128**(5): p. 655-64.

84. Cole, R.D., *A minireview of microheterogeneity in H1 histone and its possible significance.* Anal Biochem, 1984. **136**(1): p. 24-30.
85. Gonzalez-Romero, R. and J. Ausio, *dBigH1, a second histone H1 in Drosophila, and the consequences for histone fold nomenclature.* Epigenetics, 2014. **9**(6): p. 791-7.
86. Di Tommaso, P., et al., *T-Coffee: a web server for the multiple sequence alignment of protein and RNA sequences using structural information and homology extension.* Nucleic Acids Res, 2011. **39**(Web Server issue): p. W13-7.
87. Fan, Y., et al., *Individual somatic H1 subtypes are dispensable for mouse development even in mice lacking the H1(0) replacement subtype.* Mol Cell Biol, 2001. **21**(23): p. 7933-43.
88. Brown, D.T., B.T. Alexander, and D.B. Sittman, *Differential effect of H1 variant overexpression on cell cycle progression and gene expression.* Nucleic Acids Res, 1996. **24**(3): p. 486-93.
89. Gunjan, A., et al., *Effects of H1 histone variant overexpression on chromatin structure.* J Biol Chem, 1999. **274**(53): p. 37950-6.
90. Orrego, M., et al., *Differential affinity of mammalian histone H1 somatic subtypes for DNA and chromatin.* BMC Biol, 2007. **5**: p. 22.
91. Misteli, T., et al., *Dynamic binding of histone H1 to chromatin in living cells.* Nature, 2000. **408**(6814): p. 877-81.
92. Bhan, S., et al., *Global gene expression analysis reveals specific and redundant roles for H1 variants, H1c and H1(0), in gene expression regulation.* Gene, 2008. **414**(1-2): p. 10-8.
93. Sancho, M., et al., *Depletion of human histone H1 variants uncovers specific roles in gene expression and cell growth.* PLoS Genet, 2008. **4**(10): p. e1000227.
94. Izzo, A., et al., *The genomic landscape of the somatic linker histone subtypes H1.1 to H1.5 in human cells.* Cell Rep, 2013. **3**(6): p. 2142-54.
95. Millan-Arino, L., et al., *Mapping of six somatic linker histone H1 variants in human breast cancer cells uncovers specific features of H1.2.* Nucleic Acids Res, 2014. **42**(7): p. 4474-93.
96. Cheema, M.S. and J. Ausio, *The Structural Determinants behind the Epigenetic Role of Histone Variants.* Genes (Basel), 2015. **6**(3): p. 685-713.
97. Kim, K., et al., *Isolation and characterization of a novel H1.2 complex that acts as a repressor of p53-mediated transcription.* J Biol Chem, 2008. **283**(14): p. 9113-26.
98. Konishi, A., et al., *Involvement of histone H1.2 in apoptosis induced by DNA double-strand breaks.* Cell, 2003. **114**(6): p. 673-88.
99. Okamura, H., et al., *Histone H1.2 is translocated to mitochondria and associates with Bak in bleomycin-induced apoptotic cells.* J Cell Biochem, 2008. **103**(5): p. 1488-96.
100. Yan, N. and Y. Shi, *Histone H1.2 as a trigger for apoptosis.* Nat Struct Biol, 2003. **10**(12): p. 983-5.
101. Garg, M., et al., *The linker histone h1.2 is an intermediate in the apoptotic response to cytokine deprivation in T-effectors.* Int J Cell Biol, 2014. **2014**: p. 674753.
102. Luco, R.F., et al., *Regulation of alternative splicing by histone modifications.* Science, 2010. **327**(5968): p. 996-1000.
103. Huertas, D., R. Sendra, and P. Munoz, *Chromatin dynamics coupled to DNA repair.* Epigenetics, 2009. **4**(1): p. 31-42.
104. Wang, Z., et al., *Combinatorial patterns of histone acetylations and methylations in the human genome.* Nat Genet, 2008. **40**(7): p. 897-903.
105. Duan, Q., et al., *Phosphorylation of H3S10 blocks the access of H3K9 by specific antibodies and histone methyltransferase. Implication in regulating chromatin dynamics and epigenetic inheritance during mitosis.* J Biol Chem, 2008. **283**(48): p. 33585-90.
106. Daujat, S., et al., *HP1 binds specifically to Lys26-methylated histone H1.4, whereas simultaneous Ser27 phosphorylation blocks HP1 binding.* J Biol Chem, 2005. **280**(45): p. 38090-5.
107. Nakanishi, S., et al., *Histone H2BK123 monoubiquitination is the critical determinant for H3K4 and H3K79 trimethylation by COMPASS and Dot1.* J Cell Biol, 2009. **186**(3): p. 371-7.
108. Ernst, J. and M. Kellis, *Discovery and characterization of chromatin states for systematic annotation of the human genome.* Nat Biotechnol, 2010. **28**(8): p. 817-25.
109. Wisniewski, J.R., et al., *Mass spectrometric mapping of linker histone H1 variants reveals multiple acetylations, methylations, and phosphorylation as well as differences between cell culture and tissue.* Mol Cell Proteomics, 2007. **6**(1): p. 72-87.
110. Rothbart, S.B. and B.D. Strahl, *Interpreting the language of histone and DNA modifications.* Biochim Biophys Acta, 2014. **1839**(8): p. 627-43.
111. Kamieniarz, K., et al., *A dual role of linker histone H1.4 Lys 34 acetylation in transcriptional activation.* Genes Dev, 2012. **26**(8): p. 797-802.

112. Cheung, P., C.D. Allis, and P. Sassone-Corsi, *Signaling to chromatin through histone modifications.* Cell, 2000. **103**(2): p. 263-71.
113. Roth, S.Y. and C.D. Allis, *Chromatin condensation: does histone H1 dephosphorylation play a role?* Trends Biochem Sci, 1992. **17**(3): p. 93-8.
114. Yellajoshyula, D. and D.T. Brown, *Global modulation of chromatin dynamics mediated by dephosphorylation of linker histone H1 is necessary for erythroid differentiation.* Proc Natl Acad Sci U S A, 2006. **103**(49): p. 18568-73.
115. Harshman, S.W., et al., *Histone H1 phosphorylation in breast cancer.* J Proteome Res, 2014. **13**(5): p. 2453-67.
116. Kim, K., et al., *Functional interplay between p53 acetylation and H1.2 phosphorylation in p53-regulated transcription.* Oncogene, 2012. **31**(39): p. 4290-301.
117. Chubb, J.E. and S. Rea, *Core and linker histone modifications involved in the DNA damage response.* Subcell Biochem, 2010. **50**: p. 17-42.
118. Kysela, B., M. Chovanec, and P.A. Jeggo, *Phosphorylation of linker histones by DNA-dependent protein kinase is required for DNA ligase IV-dependent ligation in the presence of histone H1.* Proc Natl Acad Sci U S A, 2005. **102**(6): p. 1877-82.
119. Baatout, S. and H. Derradji, *About histone H1 phosphorylation during mitosis.* Cell Biochem Funct, 2006. **24**(2): p. 93-4.
120. Talasz, H., et al., *In vivo phosphorylation of histone H1 variants during the cell cycle.* Biochemistry, 1996. **35**(6): p. 1761-7.
121. Harshman, S.W., et al., *H1 histones: current perspectives and challenges.* Nucleic Acids Res, 2013. **41**(21): p. 9593-609.
122. Sarg, B., et al., *Identification of novel post-translational modifications in linker histones from chicken erythrocytes.* J Proteomics, 2015. **113**: p. 162-77.
123. Herrera, R.E., F. Chen, and R.A. Weinberg, *Increased histone H1 phosphorylation and relaxed chromatin structure in Rb-deficient fibroblasts.* Proc Natl Acad Sci U S A, 1996. **93**(21): p. 11510-5.
124. Talasz, H., et al., *In vitro binding of H1 histone subtypes to nucleosomal organized mouse mammary tumor virus long terminal repeat promotor.* J Biol Chem, 1998. **273**(48): p. 32236-43.
125. Sarg, B., et al., *Histone H1 phosphorylation occurs site-specifically during interphase and mitosis: identification of a novel phosphorylation site on histone H1.* J Biol Chem, 2006. **281**(10): p. 6573-80.
126. Green, A., et al., *Histone H1 interphase phosphorylation becomes largely established in G1 or early S phase and differs in G1 between T-lymphoblastoid cells and normal T cells.* Epigenetics Chromatin, 2011. **4**: p. 15.
127. Hohmann, P., R.A. Tobey, and L.R. Gurley, *Phosphorylation of distinct regions of f1 histone. Relationship to the cell cycle.* J Biol Chem, 1976. **251**(12): p. 3685-92.
128. Th'ng, J.P., et al., *Inhibition of histone phosphorylation by staurosporine leads to chromosome decondensation.* J Biol Chem, 1994. **269**(13): p. 9568-73.
129. Chadee, D.N., et al., *Histone H1b phosphorylation is dependent upon ongoing transcription and replication in normal and ras-transformed mouse fibroblasts.* J Biol Chem, 1997. **272**(13): p. 8113-6.
130. Alexandrow, M.G. and J.L. Hamlin, *Chromatin decondensation in S-phase involves recruitment of Cdk2 by Cdc45 and histone H1 phosphorylation.* J Cell Biol, 2005. **168**(6): p. 875-86.
131. Zheng, Y., et al., *Histone H1 phosphorylation is associated with transcription by RNA polymerases I and II.* J Cell Biol, 2010. **189**(3): p. 407-15.
132. Talasz, H., B. Sarg, and H.H. Lindner, *Site-specifically phosphorylated forms of H1.5 and H1.2 localized at distinct regions of the nucleus are related to different processes during the cell cycle.* Chromosoma, 2009. **118**(6): p. 693-709.
133. Glickman, M.H. and A. Ciechanover, *The ubiquitin-proteasome proteolytic pathway: destruction for the sake of construction.* Physiol Rev, 2002. **82**(2): p. 373-428.
134. Pinder, J.B., K.M. Attwood, and G. Dellaire, *Reading, writing, and repair: the role of ubiquitin and the ubiquitin-like proteins in DNA damage signaling and repair.* Front Genet, 2013. **4**: p. 45.
135. Zhang, Y., *Transcriptional regulation by histone ubiquitination and deubiquitination.* Genes Dev, 2003. **17**(22): p. 2733-40.
136. Scheffner, M., U. Nuber, and J.M. Huibregtse, *Protein ubiquitination involving an E1-E2-E3 enzyme ubiquitin thioester cascade.* Nature, 1995. **373**(6509): p. 81-3.

137. Reyes-Turcu, F.E., K.H. Ventii, and K.D. Wilkinson, *Regulation and cellular roles of ubiquitin-specific deubiquitinating enzymes.* Annu Rev Biochem, 2009. **78**: p. 363-97.
138. Peng, J., et al., *A proteomics approach to understanding protein ubiquitination.* Nat Biotechnol, 2003. **21**(8): p. 921-6.
139. Li, W. and Y. Ye, *Polyubiquitin chains: functions, structures, and mechanisms.* Cell Mol Life Sci, 2008. **65**(15): p. 2397-406.
140. Thrower, J.S., et al., *Recognition of the polyubiquitin proteolytic signal.* EMBO J, 2000. **19**(1): p. 94-102.
141. Hicke, L., *Protein regulation by monoubiquitin.* Nat Rev Mol Cell Biol, 2001. **2**(3): p. 195-201.
142. Kerscher, O., R. Felberbaum, and M. Hochstrasser, *Modification of proteins by ubiquitin and ubiquitin-like proteins.* Annu Rev Cell Dev Biol, 2006. **22**: p. 159-80.
143. Thorne, A.W., et al., *The structure of ubiquitinated histone H2B.* EMBO J, 1987. **6**(4): p. 1005-10.
144. Bohm, L., C. Cranerobinson, and P. Sautiere, *Proteolytic Digestion Studies of Chromatin Core-Histone Structure - Identification of a Limit Peptide of Histone H2a.* European Journal of Biochemistry, 1980. **106**(2): p. 525-530.
145. Wright, D.E., C.Y. Wang, and C.F. Kao, *Histone ubiquitylation and chromatin dynamics.* Front Biosci (Landmark Ed), 2012. **17**: p. 1051-78.
146. Goldknopf, I.L., et al., *Isolation and characterization of protein A24, a "histone-like" non-histone chromosomal protein.* J Biol Chem, 1975. **250**(18): p. 7182-7.
147. Weake, V.M. and J.L. Workman, *Histone ubiquitination: triggering gene activity.* Mol Cell, 2008. **29**(6): p. 653-63.
148. Pham, A.D. and F. Sauer, *Ubiquitin-activating/conjugating activity of TAFII250, a mediator of activation of gene expression in Drosophila.* Science, 2000. **289**(5488): p. 2357-60.
149. Wiley, E.A., C.A. Mizzen, and C.D. Allis, *Isolation and characterization of in vivo modified histones and an activity gel assay for identification of histone acetyltransferases.* Methods Cell Biol, 2000. **62**: p. 379-94.
150. Solow, S., et al., *Taf(II) 250 phosphorylates human transcription factor IIA on serine residues important for TBP binding and transcription activity.* J Biol Chem, 2001. **276**(19): p. 15886-92.
151. Lesner, A., et al., *Monoubiquitinated histone H1B is required for antiviral protection in CD4(+)T cells resistant to HIV-1.* Biochemistry, 2004. **43**(51): p. 16203-11.
152. Liu, C., et al., *RNF168 forms a functional complex with RAD6 during the DNA damage response.* J Cell Sci, 2013. **126**(Pt 9): p. 2042-51.
153. Thorslund, T., et al., *Histone H1 couples initiation and amplification of ubiquitin signalling after DNA damage.* Nature, 2015. **advance online publication**.
154. Danielsen, J.M., et al., *Mass spectrometric analysis of lysine ubiquitylation reveals promiscuity at site level.* Mol Cell Proteomics, 2011. **10**(3): p. M110 003590.
155. Wagner, S.A., et al., *A proteome-wide, quantitative survey of in vivo ubiquitylation sites reveals widespread regulatory roles.* Mol Cell Proteomics, 2011. **10**(10): p. M111 013284.
156. Kim, W., et al., *Systematic and quantitative assessment of the ubiquitin-modified proteome.* Mol Cell, 2011. **44**(2): p. 325-40.
157. Gibson, B.A. and W.L. Kraus, *New insights into the molecular and cellular functions of poly(ADP-ribose) and PARPs.* Nat Rev Mol Cell Biol, 2012. **13**(7): p. 411-24.
158. Burkle, A., *Physiology and pathophysiology of poly(ADP-ribosyl)ation.* Bioessays, 2001. **23**(9): p. 795-806.
159. Kim, M.Y., et al., *NAD+-dependent modulation of chromatin structure and transcription by nucleosome binding properties of PARP-1.* Cell, 2004. **119**(6): p. 803-14.
160. Martinez-Zamudio, R. and H.C. Ha, *Histone ADP-ribosylation facilitates gene transcription by directly remodeling nucleosomes.* Mol Cell Biol, 2012. **32**(13): p. 2490-502.
161. Adamietz, P. and A. Rudolph, *ADP-ribosylation of nuclear proteins in vivo. Identification of histone H2B as a major acceptor for mono- and poly(ADP-ribose) in dimethyl sulfate-treated hepatoma AH 7974 cells.* J Biol Chem, 1984. **259**(11): p. 6841-6.
162. Ogata, N., et al., *Poly(ADP-ribose) synthetase, a main acceptor of poly(ADP-ribose) in isolated nuclei.* J Biol Chem, 1981. **256**(9): p. 4135-7.
163. Ogata, N., et al., *ADP-ribosylation of histone H1. Identification of glutamic acid residues 2, 14, and the COOH-terminal lysine residue as modification sites.* J Biol Chem, 1980. **255**(16): p. 7616-20.
164. D'Amours, D., et al., *Poly(ADP-ribosyl)ation reactions in the regulation of nuclear functions.* Biochem J, 1999. **342 (Pt 2)**: p. 249-68.
165. Poirier, G.G., et al., *Poly(ADP-ribosyl)ation of polynucleosomes causes relaxation of chromatin structure.* Proc Natl Acad Sci U S A, 1982. **79**(11): p. 3423-7.

166. Realini, C.A. and F.R. Althaus, *Histone shuttling by poly(ADP-ribosylation).* J Biol Chem, 1992. **267**(26): p. 18858-65.
167. Tulin, A. and A. Spradling, *Chromatin loosening by poly(ADP)-ribose polymerase (PARP) at Drosophila puff loci.* Science, 2003. **299**(5606): p. 560-2.
168. Meyer-Ficca, M.L., et al., *Poly(ADP-ribosyl)ation during chromatin remodeling steps in rat spermiogenesis.* Chromosoma, 2005. **114**(1): p. 67-74.
169. Fontan-Lozano, A., et al., *Histone H1 poly[ADP]-ribosylation regulates the chromatin alterations required for learning consolidation.* J Neurosci, 2010. **30**(40): p. 13305-13.
170. Krishnakumar, R., et al., *Reciprocal binding of PARP-1 and histone H1 at promoters specifies transcriptional outcomes.* Science, 2008. **319**(5864): p. 819-21.
171. Gottschalk, A.J., et al., *Poly(ADP-ribosyl)ation directs recruitment and activation of an ATP-dependent chromatin remodeler.* Proc Natl Acad Sci U S A, 2009. **106**(33): p. 13770-4.
172. Chatterjee, C., et al., *Auxiliary-mediated site-specific peptide ubiquitylation.* Angew Chem Int Ed Engl, 2007. **46**(16): p. 2814-8.
173. McGinty, R.K., et al., *Chemically ubiquitylated histone H2B stimulates hDot1L-mediated intranucleosomal methylation.* Nature, 2008. **453**(7196): p. 812-6.
174. McGinty, R.K., et al., *Structure-activity analysis of semisynthetic nucleosomes: mechanistic insights into the stimulation of Dot1L by ubiquitylated histone H2B.* ACS Chem Biol, 2009. **4**(11): p. 958-68.
175. Chatterjee, C., et al., *Disulfide-directed histone ubiquitylation reveals plasticity in hDot1L activation.* Nat Chem Biol, 2010. **6**(4): p. 267-9.
176. Fierz, B., et al., *Stability of nucleosomes containing homogenously ubiquitylated H2A and H2B prepared using semisynthesis.* J Am Chem Soc, 2012. **134**(48): p. 19548-51.
177. Neumann, H., et al., *A method for genetically installing site-specific acetylation in recombinant histones defines the effects of H3 K56 acetylation.* Mol Cell, 2009. **36**(1): p. 153-63.
178. Nguyen, D.P., et al., *Genetically encoding N(epsilon)-methyl-L-lysine in recombinant histones.* J Am Chem Soc, 2009. **131**(40): p. 14194-5.
179. Nguyen, D.P., et al., *Genetically directing varepsilon-N, N-dimethyl-L-lysine in recombinant histones.* Chem Biol, 2010. **17**(10): p. 1072-6.
180. Park, H.S., et al., *Expanding the genetic code of Escherichia coli with phosphoserine.* Science, 2011. **333**(6046): p. 1151-4.
181. Lee, S., et al., *A facile strategy for selective incorporation of phosphoserine into histones.* Angew Chem Int Ed Engl, 2013. **52**(22): p. 5771-5.
182. Stadtman, T.C., *Selenium biochemistry.* Science, 1974. **183**(4128): p. 915-22.
183. Srinivasan, G., C.M. James, and J.A. Krzycki, *Pyrrolysine encoded by UAG in Archaea: charging of a UAG-decoding specialized tRNA.* Science, 2002. **296**(5572): p. 1459-62.
184. Lang, K. and J.W. Chin, *Cellular incorporation of unnatural amino acids and bioorthogonal labeling of proteins.* Chem Rev, 2014. **114**(9): p. 4764-806.
185. Rosner, D., et al., *Click chemistry for targeted protein ubiquitylation and ubiquitin chain formation.* Nat Protoc, 2015. **10**(10): p. 1594-611.
186. Johnson, D.B., et al., *RF1 knockout allows ribosomal incorporation of unnatural amino acids at multiple sites.* Nat Chem Biol, 2011. **7**(11): p. 779-86.
187. Pott, M., M.J. Schmidt, and D. Summerer, *Evolved sequence contexts for highly efficient amber suppression with noncanonical amino acids.* ACS Chem Biol, 2014. **9**(12): p. 2815-22.
188. Budisa, N., et al., *Toward the experimental codon reassignment in vivo: protein building with an expanded amino acid repertoire.* FASEB J, 1999. **13**(1): p. 41-51.
189. Budisa, N., et al., *High-level biosynthetic substitution of methionine in proteins by its analogs 2-aminohexanoic acid, selenomethionine, telluromethionine and ethionine in Escherichia coli.* Eur J Biochem, 1995. **230**(2): p. 788-96.
190. Johnson, J.A., et al., *Residue-specific incorporation of non-canonical amino acids into proteins: recent developments and applications.* Curr Opin Chem Biol, 2010. **14**(6): p. 774-80.
191. Link, A.J., M.L. Mock, and D.A. Tirrell, *Non-canonical amino acids in protein engineering.* Curr Opin Biotechnol, 2003. **14**(6): p. 603-9.
192. Rostovtsev, V.V., et al., *A stepwise huisgen cycloaddition process: copper(I)-catalyzed regioselective "ligation" of azides and terminal alkynes.* Angew Chem Int Ed Engl, 2002. **41**(14): p. 2596-9.
193. Tornoe, C.W., C. Christensen, and M. Meldal, *Peptidotriazoles on solid phase: [1,2,3]-triazoles by regiospecific copper(i)-catalyzed 1,3-dipolar cycloadditions of terminal alkynes to azides.* J Org Chem, 2002. **67**(9): p. 3057-64.
194. Kolb, H.C., M.G. Finn, and K.B. Sharpless, *Click Chemistry: Diverse Chemical Function from a Few Good Reactions.* Angew Chem Int Ed Engl, 2001. **40**(11): p. 2004-2021.

195. Huisgen, R., *Kinetics and mechanism of 1,3-dipolar cycloadditions.* Angew Chem Int Ed Engl, 1963. **2**: p. 633-645.
196. Eger, S., et al., *Generation of a mono-ubiquitinated PCNA mimic by click chemistry.* Chembiochem, 2011. **12**(18): p. 2807-12.
197. Eger, S., et al., *Synthesis of defined ubiquitin dimers.* J Am Chem Soc, 2010. **132**(46): p. 16337-9.
198. Schneider, D., et al., *Improving bioorthogonal protein ubiquitylation by click reaction.* Bioorg Med Chem, 2013. **21**(12): p. 3430-5.
199. Chan, T.R., et al., *Polytriazoles as copper(I)-stabilizing ligands in catalysis.* Org Lett, 2004. **6**(17): p. 2853-5.
200. Schneider, T., et al., *Dissecting ubiquitin signaling with linkage-defined and protease resistant ubiquitin chains.* Angew Chem Int Ed Engl, 2014. **53**(47): p. 12925-9.
201. Han, J., et al., *The potent inhibitory activity of histone H1.2 C-terminal fragments on furin.* FEBS J, 2006. **273**(19): p. 4459-69.
202. Hong, V., et al., *Labeling live cells by copper-catalyzed alkyne--azide click chemistry.* Bioconjug Chem, 2010. **21**(10): p. 1912-6.
203. Bathaie, S.Z., et al., *A mechanistic study of the histone H1-DNA complex dissociation by sodium dodecyl sulfate.* Colloids and Surfaces B: Biointerfaces, 2003. **28**(1): p. 17-25.
204. Weber, K., J.R. Pringle, and M. Osborn, *Measurement of molecular weights by electrophoresis on SDS-acrylamide gel.* Methods Enzymol, 1972. **26**: p. 3-27.
205. Schneider, D., et al., *Anionic surfactants enhance click reaction-mediated protein conjugation with ubiquitin.* Bioorg Med Chem, 2016. **24**(5): p. 995-1001.
206. Shaw, B.F., et al., *Complexes of native ubiquitin and dodecyl sulfate illustrate the nature of hydrophobic and electrostatic interactions in the binding of proteins and surfactants.* J Am Chem Soc, 2011. **133**(44): p. 17681-95.
207. Shaw, B.F., G.F. Schneider, and G.M. Whitesides, *Effect of surfactant hydrophobicity on the pathway for unfolding of ubiquitin.* J Am Chem Soc, 2012. **134**(45): p. 18739-45.
208. Barbero, J.L., et al., *Structural studies on histones H1. Circular dichroism and difference spectroscopy of the histones H1 and their trypsin-resistant cores from calf thymus and from the fruit fly Ceratitis capitata.* Biochemistry, 1980. **19**(17): p. 4080-7.
209. Thastrom, A., L.M. Bingham, and J. Widom, *Nucleosomal locations of dominant DNA sequence motifs for histone-DNA interactions and nucleosome positioning.* J Mol Biol, 2004. **338**(4): p. 695-709.
210. Huynh, V.A., P.J. Robinson, and D. Rhodes, *A method for the in vitro reconstitution of a defined "30 nm" chromatin fibre containing stoichiometric amounts of the linker histone.* J Mol Biol, 2005. **345**(5): p. 957-68.
211. Swank, R.A., et al., *Four distinct cyclin-dependent kinases phosphorylate histone H1 at all of its growth-related phosphorylation sites.* Biochemistry, 1997. **36**(45): p. 13761-8.
212. Kreimeyer, A., et al., *DNA repair-associated ADP-ribosylation in vivo. Modification of histone H1 differs from that of the principal acceptor proteins.* J Biol Chem, 1984. **259**(2): p. 890-6.
213. Kang, H.C., et al., *Iduna is a poly(ADP-ribose) (PAR)-dependent E3 ubiquitin ligase that regulates DNA damage.* Proc Natl Acad Sci U S A, 2011. **108**(34): p. 14103-8.
214. Rösner, D., *Synthese von Mono-ADP-ribosyliertem Histon H1.2.* Master Thesis, 2010.
215. Nguyen, D.P., et al., *Genetic encoding and labeling of aliphatic azides and alkynes in recombinant proteins via a pyrrolysyl-tRNA Synthetase/tRNA(CUA) pair and click chemistry.* J Am Chem Soc, 2009. **131**(25): p. 8720-1.
216. Nikitina, T., et al., *MeCP2-chromatin interactions include the formation of chromatosome-like structures and are altered in mutations causing Rett syndrome.* J Biol Chem, 2007. **282**(38): p. 28237-45.